2021

Beyond Apoptosis: Insight into the Complex Intracellular Networks that Govern Cell Fate

Hayley Neal Widden
University of Alabama at Birmingham

BEYOND APOPTOSIS: INSIGHT INTO THE COMPLEX INTRACELLULAR NETWORKS THAT GOVERN CELL FATE

by

HAYLEY N. WIDDEN

WILLIAM PLACZEK, CHAIR
DOUGLAS HURST
NATALIA KEDISHVILI
JOHN PARANT
LALITA SHEVDE-SAMANT

A DISSERTATION

Submitted to the graduate faculty of The University of Alabama at Birmingham, in partial fulfillment of the requirements for the degree of
Doctor of Philosophy

BIRMINGHAM, ALABAMA

2021

BEYOND APOPTOSIS: INSIGHT INTO THE COMPLEX INTRACELLULAR NETWORKS THAT GOVERN CELL FATE

HAYLEY N. WIDDEN

BIOCHEMISTRY AND MOLECULAR GENETICS

ABSTRACT

The determination of cell fate is a dynamic process regulated by hundreds of proteins that converge into complex cell signaling pathways. Upon irreparable intracellular stress, a cell undergoes programmed cell death, a process known as intrinsic apoptosis. Apoptosis is regulated by the Bcl-2 family, a class of proteins that act either as pro-survival or pro-death signaling molecules. Due to the oncogenic upregulation of prosurvival Bcl-2 family proteins across human cancer cell types, a novel class of small molecule inhibitors called 'BH3-mimetics' have emerged as promising anti-cancer therapeutics currently under clinical investigation. Here, we highlight the crosstalk between anti-apoptotic Bcl-2 family member, MCL1, and how it interacts with complex cellular circuits to modulate cell survival. Furthermore, we present a novel proteinprotein interaction between MCL1 and tumor suppressor p73, characterizing a novel role of MCL1 in modulating transcriptional regulation. Importantly, there is significant crosstalk between MCL1 and the DNA damage response pathway that extends beyond p73 regulation, providing an opportunity for targeted combination therapy with emerging MCL1 inhibitors. As we transition into an era of Precision Medicine, this work will provide a foundation for applying MCL1 inhibitors to current standard of care in combination with cytotoxic therapy, radiation therapy, or other targeted therapeutics.

Keywords: Apoptosis, BH3-mimetics, MCL1, p73, Epigenetics, SET/MLL Histone Methyltransferase

DEDICATION

This work is dedicated to my angels in Heaven.

Jo-Anne Lawson
James Neal
Deirdre Collins

“So much of me
Is made of what I learned from you
You’ll be with me
Like a handprint on my heart”

ACKNOWLEDGMENTS

I want to acknowledge the following individuals as this work would have not been possible without them:

First and foremost, my husband Nick Greco, who has been my biggest supporter and shoulder to lean on through the darkest times. I couldn't have done it without your love and support, and the constant reminder to 'always make time to dance'. Thank you always, and I owe this achievement to you. I love you and can't wait for our next adventure. Green light.

To my mother, Lora Neal. You have heard all about the drama, good science days, and graduate school hardships. You have talked me through tears on more occasions than I can count. Without your words of encouragement, I don't know if I would have made it. I cannot thank you enough for the endless pep talks and post-work phone calls. They truly made every day a little brighter. Without the lifetime of opportunity you have given me, I could not have accomplished this today.

To my mentor, Dr. William Placzek, for all of your mentorship and guidance over the past five years. None of this would be possible without you and for that, I am thankful.

To the Placzek lab members, past and present. You all have been instrumental to my development as a person, a mentor, and a scientist. Tessa, you have been there through it all and I look forward to your continued success in the lab for years to come. Christine, you have been solely responsible for absorbing all my complaints, frustration, and chaos over the years and I don't know how I could have done it without your support. You are going to be a rockstar physician-scientist and maybe one day, we'll be collaborating again in the future. And Lexi, my last true rotation student and the one who I believe will follow right along my path. Just remember, when times get tough, you can do it. I'll be cheering you on always and will only be a text away when you can't find the buried primer in the frost of the freezer.

To my committee members, Dr. Douglas Hurst, Dr. Natalia Kedishvili, Dr. John Parant, and Dr. Lalita Samant. Thank you for providing guidance, support, and a regular rigorous line of questioning that trained me to be a critical and confident scientist. I admire your tenacity and am thankful you instilled that in me.

To our family here in Birmingham, "The Jabroni Squad". You all have been the best support system here in Alabama and I can't thank you enough for giving me something to look forward to after-hours. This period of my life wouldn't have been the same without each and every one of you and you truly have become family.

Last, but certainly not least, to my friends and family in Virginia, especially Erin Fleming, my Aunt Leslie, and my in-laws, Steven and Laurie Greco. Thank you for your unwavering support and patience through this process. It's not easy being far from home, but you all made sure I felt your presence from afar. I love you all.

TABLE OF CONTENTS

Page

LIST OF TABLES

Table *Page*

MCL1 BINDS AND NEGATIVELY REGULATES THE TRANSCRIPTIONAL FUNCTION OF TUMOR SUPPRESSOR P73

SRI-41155 INHIBITS HISTONE 3, LYSINE 4 METHYLATION AND MLL-REARRANGED LEUKEMIC PROLIFERATION

LIST OF FIGURES

Figures *Page*

INTRODUCTION

THE MULTIPLE MECHANISMS OF MCL1 IN THE REGULATION OF CELL FATE

MCL1 BINDS AND NEGATIVELY REGULATES THE TRANSCRIPTIONAL FUNCTION OF TUMOR SUPPRESSOR P73

SRI-41155 INHIBITS HISTONE 3, LYSINE 4 METHYLATION AND MLL-REARRANGED LEUKEMIC PROLIFERATION

LIST OF ABBREVIATIONS

53BP1	p53-Binding Protein 1
ADME	Absorption, Distribution, Metabolism, and Excretion
ALL	Acute Lymphoblastic Leukemia
AMBRA1	Activating Molecule in Beclin-1 Regulated Autophagy protein-1
ASH2L	Absent, Small, or Homeotic 2-Like protein
AUC	Area Under the Curve
BAK	Bcl-2 homologous Antagonist/Killer
BAX	Bcl-2 Associated X
Bcl-2	B-cell lymphoma-2
BCLxL	B-cell Lymphoma-extra large
BH3	Bcl-2 Homology-3
BLAST	Basic Local Alignment Search Tool
BRCA1	Breast Cancer gene-1
Ca^{2+}	Calcium Ions
CDCA7	Cell Division Cycle-Associated protein 7
CDK	Cyclin Dependent Kinase
CHK1	Checkpoint Kinase-1
CIP/KIP	Cyclin Interacting Protein/Kinase Inhibitory Protein
CLPs	Common Lymphoid Progenitor cells
CMPs	Common Myeloid Progenitor cells

CNS	Central Nervous System
CSP	Chemical Shift Perturbation
CSP	Cisplatin
CTV	CellTrace Violet
DBD	DNA Binding Domain
DDR	DNA Damage Response
DMF	Dimethylformamide
DMSO	Dimethyl Sulfoxide
DNp73	N-terminal truncated isoform of p73 (Delta N-p73)
DP thymocytes	Double Positive $CD4^+/CD8^+$ thymocytes
DRP-1	Dynamin-Related Protein-1
DSB	Double Stand Break
FAO	Fatty Acid E-Oxidation
FBS	Fetal Bovine Serum
FBW7	F-Box and WD repeat domain-containing-7
FITC/F-	Fluorescein Isothiocyanate
FPA	Florescence Polarization Assay
G1/G2 phase	Gap 1 or Gap 2 phase
GADD45	Growth Arrest and DNA Damage-inducible gene-45
GAPDH	Glyveraldehyde 3-Phosphate Dehydrogenase
GMPs	Granulocyte Monocyte Progenitor cells
H3K4me#	Histone 3, Lysine 4 with 1, 2, or 3 methyl groups

HLM/MLM	Human or Mouse Liver Microsomes
HMT/KMT	Histone or Lysine Methyltransferase
HR	Homologous Recombination
HSCs	Hematopoietic Stem Cells
HSQC	Heteronuclear Single Quantum Coherence
HUWE1/MULE	HECT domain-containing Ubiquitin E3/MCL1 Ubiquitin Ligase E3
IC50	Inhibitory Concentration at 50%
ID	Inhibitors of Differentiation
IND	Investigational New Drug
INK4	Inhibitors of CDK4
IP	Immunoprecipitation
IP3R	Inositol Triphosphate Receptor
IR	Ionizing Radiation
K_D	Dissociation constant
LMPPs	Lympho-Myeloid Progenitor cells
M phase	Mitosis
MAMs	Mitochondrial-Associated Membranes
MCL1	Myeloid Cell Leukemia-1
MCM3	MiniChromosone Maintinance-3
MIM	Mitochondrial Inner Matrix
MLL	Mixed Lineage Leukemia
MOMP	Mitochondrial Outer Membrane Permeabilization
MPECs	Memory Precursors Cells

MPPs	Multi-Potent Progenitor cells
MRN Complex	Meiotic recombination-11 (MRE11), RAD50, and Nijmegan Breakage Syndrome protein-1 (NBS1) protein Complex
mTORC	Mechanistic/Mammalian Target of Rapamycin Complex-1
MW	Molecular Weight
NDA	New Drug Application
NHEJ	Non-Homologous End Joining
NK cells	Natural Killer cells
NMR	Nuclear Magnetic Resonance
NPCs	Neural Progenitor Cells
NSCs	Neural Stem Cells
OMM	Outer Mitochondrial Membrane
p.p.m.	parts per million
PARP	Poly Adenosine diphosphate Ribose Polymerase
PCNA	Proliferating Cell Nuclear Antigen
PD	Pharmacodynamics
PINK1	PTEN-Induced Kinase-1
PK	Pharmacokinetics
PSA	Polar Surface Area
PUMA	P53 Upregulated Modulator of Apoptosis
Rb	Retinoblastoma
RBBP5	RB Binding Protein 5
rBH3	Reverse Bcl-2 Homology-3

RIF1	Rap-Interacting Factor 1
RT-qPCR	Real Time quantitative Polymerase Chain Reaction
S phase	Synthesis phase
SAM	Sterile Alpha Motif
SLECs	Short Lived Effector Cells
snMCL1	small nuclear Myeloid-Cell Leukemia-1
TAD	Transactivation Domain
TAp73	Transcriptionally Active isoform of p73
TD	Tetramerization Domain
UV	Ultraviolet
VDAC	Voltage-Dependent Anion Channel
VLCAD	Very Long Chain Acyl CoA Dehydrogenase
WB	Western Blot
WCL	Whole Cell Lysate
WDR5	WD Repeat-containing protein-5
WRAD	WDR5, RBBP5, ASH2L, and a dimer of DPY30

INTRODUCTION

The Bcl-2 Family in Intrinsic Apoptosis

Cell death is a vital quality control function of all living life forms. It is an essential part of embryonic development, tissue regeneration, nutrient recycling, and the removal of damaged cells to prevent tumorigenesis[1,2]. Importantly, resisting cell death is one of the six seminal Hallmarks of Cancer, in addition to sustaining proliferative signaling, evading growth suppressors, and enabling replicative immortality among others[3,4]. These hallmarks are essential in reprogramming intracellular signaling networks to support cancer cell survival and growth. Here, we will discuss the intricacies of two essential signaling circuits that support cancer cell proliferation and viability[3].

In general, programmed cell death in response to intrinsic stimuli such as irreparable DNA damage or oxidative stress is called intrinsic apoptosis. Intrinsic apoptosis relies on the integrity of the outer mitochondrial membrane, which is controlled by more than 30 gate keeper proteins that are members of the Bcl-2 family[2]. The Bcl-2 family is comprised of three subgroups: (1) the anti-apoptotic proteins (MCL1, BCL2, BCLxL, BCLw, and BFL1/A1), (2) the pro-apoptotic BH3-only proteins (*e.g.* NOXA, PUMA, BIM), and (3) the pore forming effector proteins (BAK, BAX, and BOK)[5]. In general, these three subgroups interact with each other to modulate the oligomeric state and activity of the pore forming effectors. Upon intrinsic apoptotic stimulation, the anti-apoptotic proteins are downregulated to favor a pro-apoptotic reponse[6,7]. Furthermore, the pro-apoptotic BH3-only proteins can either bind and inhibit the anti-apoptotic proteins (*i.e.* sensitizers) or directly activate the oligomerization of BAK and BAX (*i.e.* activators)[5]. Thus, once

activated, effector proteins form oligomeric cytotoxic pores that insert into the outer mitochondrial membrane which initiates mitochondrial outer membrane permeabilization or MOMP[8]. Pore insertion is the rate-limiting step for apoptotic induction as they release intramitochondrial cytochrome c into the cytosol which binds and activates APAF-1 to an extended, active state[9]. The activated APAF-1/cytochrome c complex is collectively called the apoptosome, which initiates a caspase cascade, cleavage of intracellular proteins, and ultimately cell death[9-11] (Figure 1).

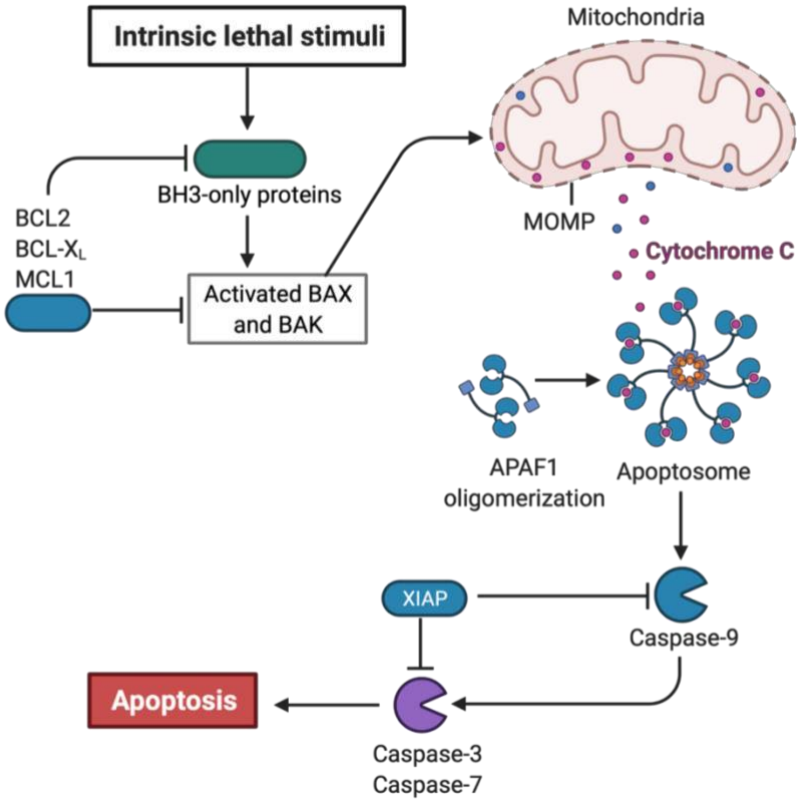

Figure 1. Pathway overview of the signaling cascade to initiate intrinsic apoptosis. This figure was created with BioRender.com.

Bcl-2 family members are classified by having a single conserved homologous Bcl2-homology or BH-motif[12]. While the BH3-only proteins only contain one BH-motif, the effectors and the anti-apoptotic proteins contain BH1-4[5]. Furthermore, the multi-motif

members form a globular protein structure with a hydrophobic binding cleft that mediates diverse protein interactions with BH3-containing proteins[12]. Therefore, the anti-apoptotic Bcl-2 family proteins, such as BCL2 or MCL1, inhibit apoptosis through binding and sequestering the pro-apoptotic BH3-containing proteins including both the effectors and BH3-onlys[5,12].

Under homeostatic, non-stressed cellular conditions, the proportion of pro- to antiapoptotic Bcl-2 family proteins is relatively equal, a concept that has become broadly understood as the 'rheostat model' or the 'anti-apoptotic neutralization model'[13]. Although the ratios are commonly considered equivalent, cells in a basal, unstressed state generally slightly favor the pro-survival proteins like MCL1 and BCL2 to endure a small amount of cellular stress without immediately initiating cell death[13,14]. Conversely, once an intrinsic lethal stimulus has been encountered, the pro-apoptotic Bcl-2 family members are significantly upregulated to overwhelm the pro-survival proteins to initiate apoptosis[13]. Upon the transformation of a normal cell to a malignant one, the anti-apoptotic proteins have been observed to be grossly upregulated to drive cancer cell survival in a hostile intracellular environment[15-17].

The Rise of BH3-Mimetics

Intrinsic apoptosis is one of the main mechanisms of cancer suppression in response to mutation, oxidative stress, mitotic defects, and other oncogenic cellular abberations[1]. Therefore, the selective induction of cancer cell death remains on the forefront of biomedical cancer research as tumor cells resist cell death by modulating the ratios of prosurvival and pro-death Bcl-2 family proteins. For example, overexpression of MCL1 has been identified across cancer cell types and can resist apoptosis under significant

intrinsic cell stress[17,18]. Furthermore, MCL1 upregulation promotes therapeutic resistance to conventional cancer treatments including chemotherapy and radiation[19-21]. Therefore, MCL1 has been a target for oncology drug discovery efforts for more than 10 years[21].

Selectively targeting one of the anti-apoptotic Bcl-2 family members has been a difficult drug discovery challenge due to the structural homology of the BH3-binding cleft. Early Bcl-2 family inhibitors such as gossypol and Sabutoclax were identified as pan-active inhibitors of all anti-apoptotic Bcl-2 family proteins, but they had a high level of doselimiting toxicities due to the lack of specificity for a specific target. At this time in the early 2000's, it had been shown that BH3-peptides have a selective affinity to specific antiapoptotic proteins, generating hypotheses of "BH3-mimietic" development to mimic these selective interactions[22-24]. Over the next several years, BH3-mimetics were identified through pre-clinical development and eventually tested in human patients.

In 2005, the first significant small molecule BH3-mimetic was ABT-737, a selective inhibitor of BCL2, BCLxL, and BCLw[25]. While ABT-737 showed significant promise in pre-clinical animal studies through intravenous administration, it was reformulated for oral-availability for human clinical trials and renamed Navitoclax (*i.e.* ABT-263)[26]. Once in clinic, Navitoclax displayed excellent pharmacokinetic

bioavailability and early signs of efficacy[27-29], but trials were halted due to the emergence of acute thrombocytopenia, which was attributed to the requirement of BCLxL for platelet survival[30]. In 2013, Venetoclax (*i.e.* ABT-199) was identified through structure-based fragment screening as a potent and selective small molecule inhibitor of BCL2 exclusively[31]. Venetoclax was a groundbreaking discovery as it showed remarkable antitumor activity while sparing platelets, eventually receiving FDA Breakthrough Therapy designation for the first time in 2015[31,32]. As of 2021, Venetoclax remains the only

FDAapproved BH3-mimetic, although there are numerous clinical trials underway with other inhibitors of the anti-apoptotic Bcl-2 family members, including MCL1, across hematologic maligangnies[21,33].

Venetoclax has proven success in multiple hematologic clinical trials and is currently FDA approved for combination therapy in Chronic Lymphocytic Leukemia (CLL) and Acute Myeloid Leukemia (AML)[34,35]. While the results have been impressive in leukemia, resistance mechanisms have been identified through extended use. Due to the redundant nature of the Bcl-2 family, upregulation of MCL1 creates an acquired resistance to Venetoclax treatment[36]. Furthermore, Venetoclax has not been shown to have potent efficacy in solid tumors, as MCL1 is typically the pro-survival Bcl-2 family member with the highest expression. Therefore, MCL1 selective small molecule inhibitors have been developed but remain in early Phase I/II clinical trials as a monotherapy and in combination studies with Venetoclax to combat resistance[21,37,38].

The Drug Discovery and Development Pipeline

All FDA-approved chemical therapeutics undergo a similar Drug Discovery and Development process to obtain approval by the Food and Drug Administration (FDA). On average, the Drug Discovery and Development process takes approximately 12 to 15 years to complete and can cost upwards of $800 million dollars prior to commercialization[39,40]. Outlined on fda.gov, there are five main phases of the Drug Discovery and Development Pipeline: Research and Development (R&D), Preclinical Research, Clinical Research, FDA Review and Approval, and FDA Post-Market Safety Monitoring. During the R&D and preclinical phases, biomedical research scientists are typically testing thousands of potential candidates for a select target. Target validation studies and a robust screening

assay are essential for on-target compound specificity and selectivity[40]. Once promising compounds have been identified, there is substantial chemical development to optimize the pharmacokinetic profile[39]. Upon completion of the chemical optimalization, studies using *in vitro* and *in vivo* model systems are implemented to characterize potential off-target effects, toxicities, and dosing strategies in preparation for First-In-Human studies[41,42].

While animal studies, particularly mice, are critical to characterize the potency and efficacy of novel therapeutics, they do not always recapitulate human disease and metabolism[43,44]. Therefore, once pre-clinical animal studies are complete, novel therapeutics are submitted under an Investigational New Drug (IND) application that is required for first-in-human clinical studies[45]. An IND is filed with all of the preclinical data, as well as manufacturing information and future clinical protocols for human studies[45]. Once accepted (or if 30 days passes past the IND submission), Phase I clinical trials may proceed. An IND must undergo three phases of clinical trials before submitting a New Drug Application (NDA) for FDA approval and ultimately commercialization. Each phase has its own objective from small-scale toxicity studies to large trials characterizing the on-target efficacy of a novel therapeutic.

Phase I clinical trials generally recruit less than 100 volunteers to monitor safety and determine the dosage for future Phase II/III studies. In many trials, Phase I studies are conducted with healthy participants, but cancer therapeutics are an exception as most drugs have a high risk of adverse events or toxic side effects. Therefore, Phase I clinical trials of novel anti-cancer agents will typically be tested in patients with the target cancer type. Of all the INDs that enter Phase I clinical trials, approximately 70% will move to Phase II. All descriptions and statistics of Clinical Trials are up-to-date information from fda.gov as of April 2021.

Phase II clinical trials scale up the number of patients and the length of the study. Typically, several hundred patients with the disease are selected to receive treatment for several months to two years. In these studies, toxicity, PK, and pharmacodynamic profiles of the drug are typical primary endpoints. While Phase II studies can be long enough to achieve a biological response, the primary goal of these trials is to evaluate the safety for long-term use. Of the drugs that enter Phase II studies, only one third progress to large scale Phase III clinical trials (fda.gov – April 2021).

In Phase III, hundreds to thousands of patients are recruited with the disease of interest. While safety and toxicities remain to be monitored, efficacy is the primary purpose of Phase III studies. These ongoing trials typically last from one to four years and require long term follow-up to monitor overall survival (OS) and other primary endpoints that are designed specifically for each trial. Of the Phase III studies that are completed, 25-30% will submit a New Drug Application (NDA) for FDA review (fda.gov – April 2021). FDA approval suggests that the drug has been rigorously tested and it is both safe and effective for an intended use[46]. Before the commercialization of a drug can begin after FDAapproval, new therapeutics must go through the 'labeling' process to outline all pertinent prescribing information (PI)[47,48]. Once the PI is complete, the drug can move forward with commercialization, large-scale manufacturing, and distribution.

After a drug is approved for use, it does not leave the FDA clinical trial program. Phase IV clinical trials are post-marketing surveillance studies to ensure the long-term safety and efficacy remains consistent with the pre-approval data. Additionally, the FDA regulates all prescription drug advertising efforts and promotional labeling. Lastly, Phase IV studies are critical for the accelerated approval for new indications, dosages, or formations, but a new IND filing is still required (fda.gov – April 2021).

According to the Food and Drug Administration (fda.gov), there are four possible distinctions used to accelerate the FDA clinical approval process. 'Fast Track' and 'Accelerated Approval' are designed for serious conditions or unmet medical needs. The Fast Track Designation facilitates the development and review of novel therapeutics and the Accelerated Approval Designation allows for the approval based on a surrogate endpoint. A surrogate endpoint is a measure that can predict clinical benefit but is not a measure of disease response itself. 'Breakthrough Therapy' is a designation that accelerates the development and review process because it demonstrates the potential to be an improvement over current standard of care. Lastly, 'Priority Review' sets the FDA-goal to six months for the application review, whereas the standard review window is ten months.

The BCL2-specific inhibitor Venetoclax received the Breakthrough Therapy Designation in April 2015 for hard-to-treat CLL patients. The accelerated approval followed a pivotal Phase II study showing that nearly 80% of CLL patients responded to Venetoclax[49]. Shortly after, the first NDA was approved for Venetoclax in January 2016 and another Breakthrough Therapy Designation was awarded for a second CLL population of patients harboring a 17p chromosomal deletion[50]. According to a press release from the manufacturer Abbvie, it was granted a third accelerated Breakthrough Therapy Designation in November 2018 for the treatment of AML in patients 75 years or older and not eligible for standard induction chemotherapy. The AML indication for Venetoclax ultimately received FDA approval in October 2020, and the BCL2 inhibitor remains under clinical investigation for other areas of malignant hematology in various combination therapies[50].

Goals and Hypotheses

The goal of this dissertation is to provide detailed insights into complex intracellular signaling pathways that are currently investigational therapeutic targets for cancer therapy. Like many druggable targets, MCL1 and other anti-apoptotic Bcl-2 members are involved in complex signaling networks that are often overlooked or undervalued in drug discovery efforts. In Chapter 1, we discuss the diverse role of MCL1 in multiple homeostatic cell signaling pathways in a literature review. In this chapter, we highlight MCL1's canonical regulation of apoptosis in specific cell types and describe numerous cell fate pathways that MCL1 participates in outside of intrinsic apoptosis. In addition to emphasizing other non-apoptotic pathways such as cell cycle regulation, DNA damage response, and autophagy which may contribute to MCL1 inhibitors efficacy in cancer therapy, we hypothesize MCL1 inhibitors as potential immunomodulatory drugs or novel applications for diseases such as Alzheimer's or allergic airway disease.

In Chapter 2, we characterize a specific protein-protein interaction briefly highlighted in Chapter 1. The overall goal of the Placzek lab is to characterize novel interactions mediated through a protein-motif capable of competitively binding into the BH3-pocket (*i.e.* rBH3), which is the druggable binding interface for BH3-mimetics. Here, we hypothesize that MCL1 and p73 interact through a direct protein-protein interaction and thereby modulate either the apoptotic or the transcriptional functions of these proteins.

Furthermore, we hypothesize that MCL1 and p73 could be predictive biomarkers for combination studies with MCL1-specific BH3 mimetics and platinum-based chemotherapeutics.

Through the first two chapters of this dissertation, the goal is to highlight the crosstalk amongst signaling pathways and how this can influence the response to anticancer therapies. Ultimately, this work will provide a guide for rational combination treatment strategies in oncology. Building upon this foundation, Chapter 3 highlights the translational impact of targeting a dynamic protein complex through a Drug Discovery project. The target of this project involves the epigenetic regulation of multiple pathways, similarly to the diverse crosstalk of MCL1 across all facets of cell regulation. This study is an ongoing collaborative effort through the Alabama Drug Discovery Alliance (ADDA) investigating a novel small molecule targeted therapeutic in MLL-rearranged leukemia. Through these studies, we hypothesize that a novel compound, herein called SRI-41155, targets the epigenetic SET/MLL histone methyltransferase complex. Furthermore, by inhibiting this complex, we hypothesize that we can epigenetically downregulate oncogenic gene expression and modulate aberrant H3K4 histone methylation in MLLrearranged leukemia.

Upon the completion of this dissertation, the overall goal is to provide a framework for investigating two complex signaling pathways involved in cancer cell survival: the Bcl2 family and epigenetic regulation by H3K4 histone methylation. By exploring these two pathways in detail, we have uncovered a novel drug discovery target in DPY30 and explored existing drug combination strategies for the future of multi-drug treatment regimens in cancer therapy, highlighting a new place for MCL1 inhibitors in the clinic.

THE MULTIPLE MECHANISMS OF MCL1 IN THE REGULATION OF CELL FATE

by

HAYLEY WIDDEN AND WILLIAM J. PLACZEK

In peer-review for *Communications Biology (Springer Nature)*

Format adapted for dissertation

Preface

MCL1 is a widely recognized pro-survival member of the Bcl-2 family and a promising target for cancer therapy. While the role MCL1 plays in apoptosis is well defined, its participation in emerging non-apoptotic signaling pathways is only beginning to be appreciated. Here, we synthesize studies characterizing MCL1s influence on cell proliferation, DNA damage response, autophagy, calcium handling, and mitochondrial quality control to highlight the broader scope that MCL1 plays in cellular homeostasis regulation. Throughout this review, we discuss which pathways are likely to be impacted by emerging MCL1 inhibitors, as well as highlight non-cancerous disease states that could deploy BH3-mimetics in the future.

Introduction

MCL1 (myeloid cell leukemia- 1) is a diverse cell regulatory protein, most notably recognized for its anti-apoptotic role in the Bcl-2 family. It was first identified in 1993 by Kozopas and colleagues in the laboratory of Ruth Craig while identifying genes that were associated with the transition from proliferation to differentiation in hematopoietic leukemia cells (ML-1)[1]. The novel gene was isolated during a phorbol-ester-induced differentiation experiment, which differentiates proliferating myeloblastic cells into nonproliferative monocytes or macrophages. The expression of *MCL1* was observed to increase just as the differentiation pathway was induced but before the appearance of canonical markers of differentiating cells or genes associated with the mature phenotype[1]. Soon after its identification, sequence homology of the *MCL1* gene with BCL2 (B-cell lymphoma protein 2) and subsequent confirmation that MCL1 shared anti-apoptotic functionality solidified its position as a regulatory protein in intrinsic apoptosis[1-3].

MCL1 and BCL2 are anti-apoptotic members of a large class of proteins that modulate cell viability at the outer mitochondrial membrane (OMM). The Bcl-2 family consists of three subgroups: the anti-apoptotic members (MCL1, BCL2, BCLxL, BCLW, and BFL1/A1), the pore-forming effectors (BAK, BAX, and BOK), and the pro-apoptotic BH3-only proteins (*e.g.* NOXA, BIM, and PUMA)[4]. All Bcl-2 family proteins directly interact through protein-protein interactions to regulate intrinsic apoptosis by maintaining the integrity of the OMM. Upon irreparable cellular stress, the cell commits to an apoptotic signaling cascade through the upregulation of one of the pro-apoptotic pore-forming effectors. Effector proteins, most notably BAK and BAX, homo-oligomerize to form cytotoxic pores in the OMM, releasing molecules such as cytochrome c into the cytosol which initiates the rapid induction of intrinsic apoptosis[5-7]. The other two classes of the

Bcl-2 family, the anti-apoptotic members, which include MCL1, and the pro-apoptotic BH3-only proteins, interact with both the pore-forming effectors and one another to modulate oligomerization and therefore, cell survival[4].

The functional interplay between the Bcl-2 family subgroups surrounds one pivotal polypeptide motif that is shared by all members – the Bcl-2 homology-3 (BH3) motif[8]. All members of the Bcl-2 family contain a BH3 motif, while some members contain additional BH-motifs, BH1, BH2, and/or BH4. The multi-motif members, which include all antiapoptotic proteins (i.e. MCL1) and the pore-forming effectors, adopt a conserved globular fold with a hydrophobic binding pocket that mediates interactions with the amphipathic BH3 helix of the pro-apoptotic BH3-only proteins[5,9,10]. Therefore, the BH3-motif is the central mediator of intrinsic apoptotic regulation as it both promotes oligomerization of the pro-death proteins BAK and BAX and is utilized by the BH3-only proteins to bind and sequester their anti-apoptotic counterparts[4].

Significantly during tumorigenesis, the anti-apoptotic Bcl-2 family members are often upregulated through copy number alterations (e.g. MCL1) or dysregulated as a result of chromosomal translocation (e.g. BCL2)[11,12]. This allows cancer cells to endure increased genotoxic stress that occurs during tumor development. To combat the dependance of cancer cell survival on anti-apoptotic protein expression, small molecule inhibitors mimicking the regulatory BH3-motif were designed (BH3 mimetics)[13-17]. Prior to the development of BH3-mimetics, the primary focus of anti-apoptotic Bcl-2 family research efforts primarily revolved around how the anti-apoptotic proteins interact with canonical BH3 sequences. Yet, increasing recent evidence shows that MCL1 and the other Bcl-2 family members can bind to a diverse set of cell regulatory proteins through interactions using both its BH3 binding cleft and through distal sites in its protein structure. While

recent reviews have discussed the non-apoptotic roles of BCL2 and BCLxL in detail[18], there has been a more limited discussion on the increasingly interesting body of research that directly connects MCL1 to the regulation of other cell signaling pathways beyond apoptosis. The literature summarized in this review synthesizes both studies that focus on the canonical BH3-binding cleft that may be impacted through BH3-mimetic targeting of MCL1, as well as other non-canonical protein interactions. Together, these studies demonstrate that MCL1 has many functions that alter cell fate, both as an anti-apoptotic Bcl-2 family protein and outside of that role through the regulation of cellular differentiation, cell cycle regulation, double stand DNA break repair, mitochondrial dynamics, and bioenergetic metabolism.

MCL1 is Required for Lineage-Specific Cell Survival, Differentiation, and Maintenance

Healthy tissues must maintain homeostasis between cellular differentiation, proliferation, and death. At the nexus of these three pathways lies embryonic development, where differentiation, proliferation, and death are critically timed and regulated to ensure the proper development of the organism. MCL1 was initially recognized as an early marker for differentiation, yet the identification of sequence and structural homology between MCL1 and BCL2 led to the hallmark observation of their shared role in regulating intrinsic apoptosis[1]. Subsequent interrogation of MCL1 specific functions found that unique from other Bcl-2 family members, MCL1 knockout mice exhibit peri-implantation lethality around E3.5[19]. During this developmental stage in mice, fertilized eggs are in the early blastocyst phase, which is comprised of two differentiated cell types: the inner cell mass and an outer layer of trophoblast cells. Of these two cell types, trophoblasts mature into the trophectoderm layer, which is required for implantation[20]. Recovered $MCL1^{-/-}$ blastocysts showed no signs of apoptosis and failed to hatch *in vitro*, suggesting a defect in

trophectoderm development[19]. These findings suggest that MCL1 is required for implantation and further establishes a role for MCL1 in cell biology that extends beyond apoptotic regulation.

Over the past two decades, MCL1 has proven to be essential for the survival and differentiation of many diverse cell types[21-24], most notably through hematopoiesis and neurogenesis[25-29]. Hematopoiesis is the process through which all blood cells are formed from self-renewing pluripotent stem cells that can differentiate into either myeloid or lymphoid cell types[30] (Figure 1). The inducible deletion of *Mcl1* promotes hematopoietic failure through loss of hematopoietic stem cells (HSCs), granulocyte monocyte progenitor cells (GMPs), and common myeloid progenitor cells (CMPs)[2,26,27,31]. In addition to the survival and differentiation of myeloid progenitor cells[2], MCL1 is also required for myeloid-derived cell types such as neutrophils[32], mast cells[33], basophils[33], and dendritic cells[34]. In contrast, MCL1 is not solely responsible for the survival of monocytes[32], macrophages[32], megakaryocytes[35,36], or platelets[35,37]. Furthermore, cellular dependence on MCL1 expression can be influenced by precise timing and developmental stage. For example, MCL1 is required for early-stage erythropoiesis, but is non-essential for maintenance of mature erythrocytes[38]. Moreover, while not specifically responsible for macrophage cell survival *in vivo*, MCL1 modulates the macrophage effector response during bacterial phagocytosis, where the knockdown of MCL1 enhances sensitivity to macrophage cell death[32,39]. This selective requirement of MCL1 expression creates a unique vulnerability for specific immune cell targeting through MCL1 inhibition. Phagocytes generally coordinate acute inflammation but also can cause inflammatory tissue damage through neutrophil recruitment or reduced eosinophil apoptosis[40]. Recently, the overexpression of MCL1 has been reported to exacerbate allergic airway inflammation

and resist eosinophilic apoptosis[40]. To this end, targeting MCL1 in inflammatory lung conditions that induce acute respiratory distress or allergic airway disease, such as eosinophilic asthma, has been evaluated using the cyclin-dependent kinase inhibitor (CDKi) AT7519[40-42]. These studies found that transcriptional silencing of MCL1 through CDKi's promotes neutrophil apoptosis, while sparing macrophages and the phagocytosis of neutrophils[42]. In a separate study, AT7519 was shown to sensitize resistant eosinophils to apoptosis in mice transgenically overexpressing MCL1[40]. Significantly, these studies suggest a therapeutic opportunity for targeting MCL1 in inflammatory conditions as it promotes the resolution of neutrophils and eosinophils while sparing other lineages of the host immune system.

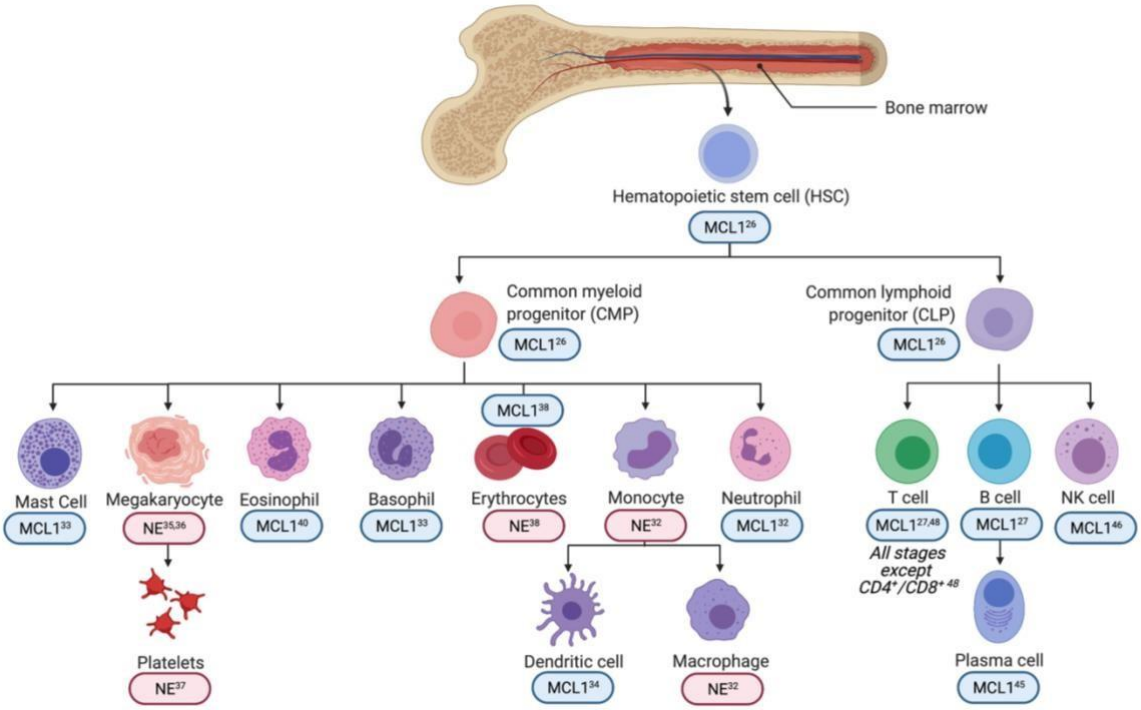

Figure 1. MCL1 differentially regulates hematopoietic cell survival and differentiation. Stem cell differentiation from bone marrow. Blue boxes (MCL1) highlight cell types using *in vivo* modeling that solely require MCL1 expression for differentiation and/or survival. These cell types undergo a significant amount of apoptosis *in vivo* when MCL1 is selectively knocked out using genetic manipulation. Red boxes (NE) highlight cell types that exhibit a no effect or a nonsignificant change in cell number compared to control mice when only MCL1 is knocked down.

Just as MCL1 is required for HSCs and myeloid progenitor populations, it is also essential for common lymphoid progenitor (CLPs) cell survival and differentiation[26,27,31] (Figure 1). In B-lymphocytes, MCL1 is required for the survival of germinal center Bcells[43,44] , memory B-cells[44] , and plasma cells[45]. Furthermore, MCL1 is required for natural killer (NK) cell survival[46] and throughout T-cell development[27]. MCL1 is essential for all stages of T-cell maturation with the exception of early $CD4^+/CD8^+$ (double positive or DP)

thymocytes[47,48]. While not essential for DP thymocyte survival, a conditional double knockout with BCLxL significantly decreases the survival of this T-cell population[48]. Furthermore, MCL1 enhances the survival of memory $CD8^+$ T-cells after viral infection and promotes the formation of long-term lymphocyte memory[49]. *In vivo* modeling using an *MCL1* transgene demonstrated that T-cells activated in response to viral infection shifted the population from short-lived effector cells (SLECs) to antigen specific memory precursor cells (MPECs). MPECs differentiate into the long-lived memory cell population, suggesting MCL1 promotes long-term T-cell memory formation[49]. Consistent with this study, MCL1 knockout mice with lymphocytic choriomeningitis viral infection exhibited decrease development of virus-specific T-cells[50]. Unlike other examples where MCL1 and BCLxL are redundant, the overexpression of BCLxL did not rescue the effect of MCL1 knockdown[50]. Taken together, these studies highlight the broad role that MCL1 plays in hematopoietic processes ranging from cellular differentiation, effector function, and cell maintenance/death (Figure 1).

Paralleled with its broad role in hematopoietic cell survival and maturation, MCL1 is also critical in the tissue-specific differentiation and cellular survival in the central nervous system (CNS)[28]. As shown through conditional knockout studies, MCL1 is required for neuronal development, where expression is high in neuronal precursor cells, promoting cellular survival throughout the process of neurogenesis[28]. Conditional Nestinmediated *Mcl1* knockout mice, which target both the neural stem cell (NSCs) and the intermediate NPC populations, are embryonic lethal at E16 with extensive cell death throughout the developing brain[28,51]. Moreover, MCL1 was recently identified as a critical survival factor in the midbrain dopaminergic neurons, whereas BCL2 and BCLxL promoted survival in non-dopaminergic cell lines[52]. Outside of the role in apoptotic

regulation, MCL1 is required for neural progenitor cells to differentiate into post-mitotic neurons through the regulation of cell cycle exit and terminal mitosis. Following upregulation of MCL1, there is an increase in immature neurons that undergo terminal mitosis and premature differentiation, which are dependent on the modulation of cell cycle inhibitor p27[53]. As characterized by the studies described here, MCL1 plays a unique role in differentiation, both in hemopoietic linages as well as in neurogenesis. BCL2 and BCLxL have independent and non-redundant roles compared with MCL1, many of which are reviewed elsewhere[18,29]. These studies together show that rather than serving as redundant regulators of cellular apoptosis, timing and expression of the Bcl-2 family is essential for proper cell differentiation, cell proliferation, and cell death across multiple cell types. Complete understanding of these mechanisms and cell-specific functions are still being characterized with transgenic mouse studies and the utilization of emerging novel BH3-mimetics that allow for specific inhibition of anti-apoptotic Bcl-2 family members.

MCL1 Modulates Cell Division Through Interactions with Cell Cycle Regulators

In addition to characterizing how MCL1 expression impacts specific cell lineages, it is also being interrogated for its impact on specific cell signaling pathways. MCL1 protein levels oscillate as cells progress through the cell cycle, with protein expression lowest in early G1 phase, increasing through S phase, and peaking in late S or early G2 phase[54]. Changes in MCL1 expression are a result of multiple levels of regulation from transcriptional activation, mRNA stability, non-coding RNA control, and post-translational modifications[55-58]. Specifically, during the cell cycle, MCL1 protein levels are regulated through two distinct phosphorylation sites on the MCL1 N-terminus, Ser64 and Thr92[55]. If there is a significant delay in mitotic progression (i.e. an unresolved problem in spindle

assembly), Thr92 is phosphorylated by the mitosis-promoting cyclin dependent kinase CDK1-cyclin B1, which initiates the destruction of MCL1 through a proteasomedependent mechanism[55]. This regulation of MCL1, in addition to the degradation by other E3 ligases such as FBW7 during mitosis, has led to its view as a mitotic clock that ensures timely exit from the cell cycle[59-61]. In cancer therapy, MCL1 degradation is an important event for apoptosis in cancer cells that are undergoing mitotic arrest by microtubule stabilizing agents[55,59,61]. As the half-life and protein stability of MCL1 is regulated through interactions with its unique amino terminus[62], it is unsurprising that BCL2 and BCLxL do not exhibit similar changes in protein expression through the cell cycle[55]. This specific protein level regulation makes the functionality of MCL1 in the cell cycle irreplaceable by other anti-apoptotic Bcl-2 family members[54].

Just as the precise regulation of MCL1 protein levels through the cell cycle ensures the successful completion of cell division through mitosis, there are also several MCL1 protein binding partners that impact cell cycle progression at different phases (Figure 2). Utilizing its canonical BH3-binding cleft, MCL1 negatively regulates the INK4 cell cycle inhibitor, p18, to promote the G1/S transition and cell cycle entry in an Rb-dependent manner (Figure 2A). Mechanistically, MCL1 inhibits the stability of the p18 protein by targeting it for proteolytic degradation[63]. Another direct MCL1 binding partner in the cell cycle includes proliferating cell nuclear antigen (PCNA), a DNA sliding clamp that acts as a co-factor to DNA polymerase G in S-phase (Figure 2B). In this specific study, overexpression of MCL1 inhibited cell cycle progression through S-phase[64]. Mutational analysis of the PCNA binding site (H224A, Glu225A, Thr226A, and Phe228A) demonstrated that mutant MCL1 still retains its anti-apoptotic function while promoting

DNA synthesis. While the interaction with p18 involves a BH3-like interaction with MCL1s canonical BH3-binding cleft, the interaction with PCNA only involves eight amino acid residues within the hydrophobic p3 pocket of the MCL1s binding interface[10,63,64]. It remains undetermined if these two interactions are mutually exclusive or if they solely depend on the phase of the cell cycle. Furthermore, it is still not fully elucidated if these interactions will be impacted by MCL1-specific BH3 mimetics, although a recent study suggests that the cell cycle functions of MCL1 are spared[65].

MCL1's function in the cell cycle is not limited to its traditional full-length isoform. A proteolytically cleaved variant termed small nuclear MCL1 (snMCL1) was identified through western blot analysis and was exclusively localized in the nuclear cell fraction[66]. The 36 kD snMCL1 isoform exhibits direct binding to CDK1 and thereby inhibits the CDK1 interaction with its binding partner cyclin B (Figure 2C). This complex is responsible for promoting MCL1 degradation in response to mitotic delay as discussed above[55]. Upon overexpression of snMCL1, the population of proliferating cells decreases consistent with a corresponding inhibition of the CDK1-cyclin B complex that promotes mitotic completion[66]. Through each of these interactions throughout the cell cycle, MCL1 overexpression has been demonstrated to promote cell proliferation or enable prolonged pausing in specific phases of the cell cycle, depending on the cell type, genetic background, and timing[53,63,64,66]. Further research is required to fully disentangle the mechanism by which MCL1 regulates cell proliferation and navigates cell cycle checkpoints. This is required for both cancerous and normal cell types to determine how these interactions facilitate lineage-specific cell proliferation and the checkpoint response to intrinsic stress.

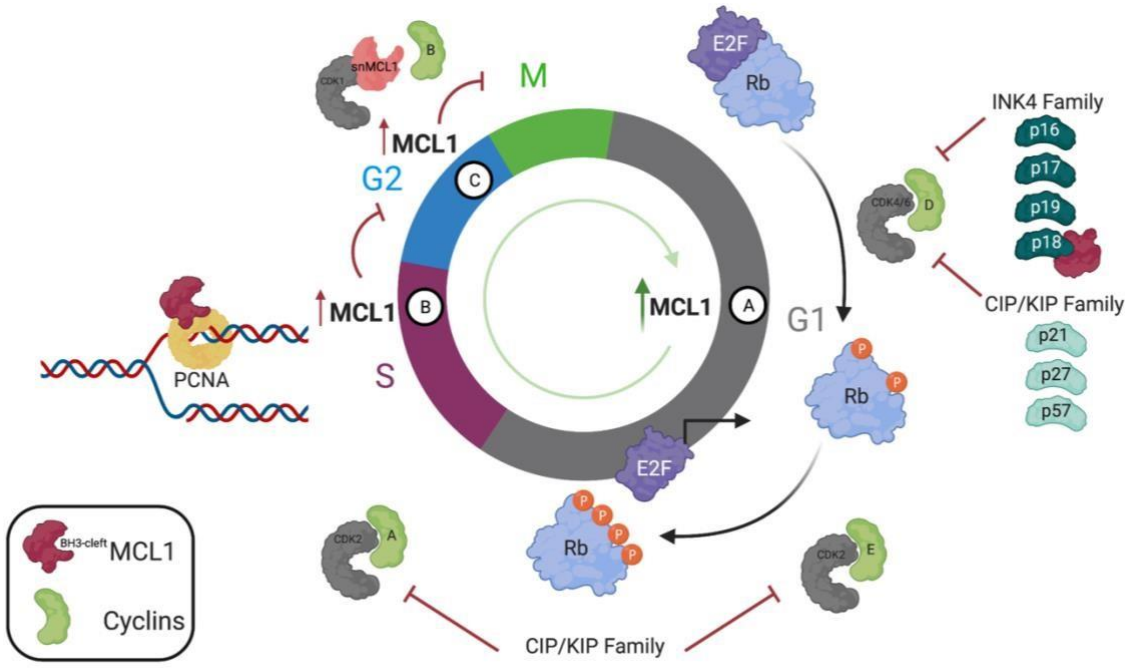

Figure 2. MCL1 modulates cell cycle entry and progression. A. In G1-phase, MCL1 binds and inhibits the stability of p18, an inhibitor of the G1/S transition. Decreased expression of p18 promotes cell cycle entry and proliferation in Rb-positive cells. **B.** In Sphase, MCL1 binds and inhibits PCNA, inhibiting DNA synthesis and cell cycle progression through G2. **C.** In G2-phase, a nuclear isoform of MCL1 (i.e. snMCL1) binds to CDK1, which preventing the interaction with canonical binding partner, cyclin B. Ultimately, this function of snMCL1 inhibits mitotic completion.

MCL1 Acts as a Molecular Switch for Double Strand Break DNA Repair

An important pathway intertwined with cell cycle regulation is DNA repair, which requires checkpoint activation to halt cell proliferation. Two hallmarks of cancer that go hand-in-hand are genomic instability and enabling replicative immortality (i.e. cell proliferation)[67]. DNA damage response (DDR) is one of the most exploited mechanisms by which cancer cells simultaneously maintain viability and permit genomic mutation. To this end, it presents a promising focus for therapeutic intervention[68]. As a regulator of apoptosis, MCL1's function in responding to DNA damage has now been assessed in detail. The impact of MCL1 in DDR continues to evolve as it has been found to act not

simply as an apoptotic switch, but also as a key determinant of DDR activation and double strand break (DSB) repair. MCL1 was first observed to be upregulated in response to DNA damage induced by ionizing radiation (IR), ultraviolet (UV) radiation, and alkylating agents in 1997[69]. This was the reciprocal effect observed for BCL2, whose expression decreases in response to DNA damage-induced therapy[69]. Likewise, expression of the proapoptotic effector protein, BAX, also increases following these treatments. Subsequent analysis found that while BAX and other members of the Bcl-2 family are regulated by the tumor suppressor p53[70], MCL1 is unique as it is upregulated through a p53-independent mechanism[69].

In response to DNA damage, MCL1 is upregulated, where it binds and promotes the phosphorylation and subsequent activation of CHK1, a protein kinase responsible for halting the cell cycle for DNA repair[71]. Knockdown of MCL1 delays CHK1 phosphorylation, making this account significant as it was the first to identify that MCL1 plays a functional role in DDR[66,72]. Furthermore, MCL1 binds to the early-response gene product-1, IEX-1, a protein that accumulates at sites of DNA damage. Through this interaction, MCL1 and IEX-1 cooperate to maintain CHK1 activation as the knockdown of either MCL1 or IEX-1 promotes genomic instability and results in increased sensitivity to replicative stress[73]. Ultimately, this could provide a novel area for combination therapy with MCL1 inhibition and DNA damaging agents as a novel therapeutic strategy in cancer. In addition to MCL1 facilitating the activation of DDR through CHK1, it also promotes specific mechanisms of DNA repair. The most lethal of all DNA lesions are double strand breaks (DSBs) which are resolved through one of two mechanisms – homologous recombination (HR) or non-homologous end joining (NHEJ)[68]. HR is the more accurate mechanism, though it requires more time for repair and is cell-cycle dependent as it

requires a sister chromatid to serve as a repair template[74]. Alternatively, NHEJ is non-cell cycle dependent, but it is more error-prone as it ligates two ends of DNA back together, irrespective of templating[74]. Through several protein interactions between MCL1 and DDR machinery, increased steady-state MCL1 levels promote cells to repair DSBs using the more accurate HR mechanism over NHEJ (Figure 3). Specifically, at the sites of DNA damage, MCL1 binds to the phosphorylated minor histone, JH2AX[72], and co-localizes with 53BP1, post-irradiation[75] (Figure 3A). Both JH2AX and 53BP1 are early signaling modifications at the sites of DNA damage, suggesting MCL1 plays a direct role at the site of DSBs[72,75]. MCL1 knockdown delays JH2AX foci formation and promotes higher expression of residual 53BP1 and RIF1 foci, resulting in the accumulation of chromosomal abnormalities[71,72,75] (Figure 3B). This accumulation of 53BP1-RIF1 foci promotes DNA end ligation required for NHEJ and attenuates DNA end-resection, a process required for repair through HR[74]. Moreover, MCL1 knockout cells exhibited reduced HR repair through a DSB reporter assay and decreased HR signaling protein foci (*i.e.* BRCA1, Rad51, and single-stranded RPA)[75], further suggesting repair through HR has been compromised (Figure 3B). These studies of DSB foci formation demonstrate that MCL1 overexpression leads to a net increase in HR, while knockdown of MCL1 leads to an increase in repair through NHEJ (Figure 3). This suggests that MCL1 serves as a functional switch between HR and NHEJ in DSB repair[54,75].

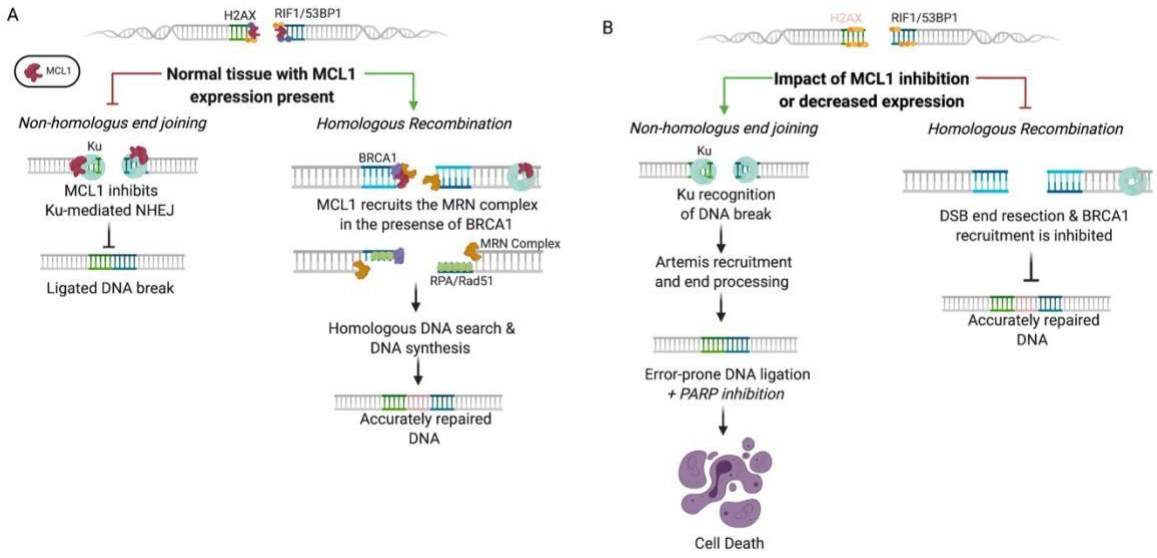

Figure 3. MCL1 facilitates double stand break (DSB) DNA repair by stimulating homologous recombination (HR) and inhibiting error-prone non-homologous end joining (NHEJ). A. MCL1 expression in normal tissue. At the sites of DSBs, MCL1 colocalizes and facilitates JH2AX signaling foci, which promotes repair through HR. Furthermore, HR is activated by MCL1 through the recruitment of the MRN complex, which promotes HR machinery such as BRCA1, ssRPA, and Rad51. MCL1 further inhibits NHEJ through the direct inhibition of the Ku protein complex. **B.** MCL1 inhibition as a therapeutic opportunity for combination therapy in cancer. Upon MCL1 inhibition, HR repair is compromised as highlighted by reduced JH2AX foci at the sites of DBSs and decreased recruitment of BRCA1, ssRPA, and Rad51. 53BP1-RIF1 foci are increased, which promotes error-prone repair through NHEJ. NHEJ is further activated by decreasing the negative MCL1 regulation on Ku. While MCL1 inhibition promotes genomic instability, compromised HR opens a therapeutic window for synthetic lethality approaches that have previously been successful in cancer therapy.

The effect of MCL1 on DSBs goes beyond its effects on DDR protein foci accumulation. MCL1 binds and inhibits Ku, an essential NHEJ protein that stabilizes the DNA ends to promote ligation[54] (Figure 3A). When MCL1 inhibits Ku and subsequently NHEJ in response to DSBs, it simultaneously promotes the HR machinery for more accurate DNA repair. DSBs repaired through HR require the assembly of three proteins, MRE11, RAD50, and NBS1, which are referred to as the MRN complex[74]. At the sites of DSBs, MCL1 facilitates the recruitment of MRE11[54] and binds to NBS1 in

coimmunoprecipitation experiments[72]. The inhibitory action of MCL1 on Ku and the recruitment of the MRN complex further establishes MCL1 as a central regulator for the decision between DDR repair mechanisms.

Characterizing these pathways in translational models provides insight into the benefit that cancer derives from the upregulation of MCL1, while also exposing possible combination therapies with emerging MCL1 inhibitors for cancer therapy. For instance, PARP inhibitors (e.g. olaparib) promote DSBs through inhibition of the base excision repair (BER) pathway[76]. Typically, these lesions are repaired through HR and if the cells are HR deficient (e.g. BRCA mutation), cells undergo apoptosis[76]. As knockdown of MCL1 drives cells from HR to the rapid, error-prone NHEJ, the combination of MCL1 and PARP inhibition was highlighted as a novel pathway to expose cancer cells to a targeted vulnerability[77]. To investigate if MCL1 inhibition mimics the BRCA synthetic lethality approach, a recent study interrogated the combination of MCL1 knockdown with PARP inhibitors in a panel of xenograft models for colon, lung, and brain malignancies[77]. As MCL1 protein is rapidly turned over[62], MCL1 inhibition was achieved through mTORC inhibition which halts new protein synthesis[78]. By depleting MCL1 protein expression, cells are inherently primed to repair DSBs through NHEJ. Combination therapy using either of the mTORC inhibitors (everolimus or AXD2014) with PARP inhibition significantly inhibited cancer cell growth both *in vitro* and *in vivo*[77]. This is the first study to exploit MCL1-mediated vulnerabilities through a DNA repair mechanism versus the BH3-mimetic approaches that aim to sensitize cancer cells to intrinsic apoptosis. Significantly, targeting MCL1 through this mechanism did not induce apoptosis, but rather resulted in activation of a necroptotic cell death pathway[77]. These findings pave the way

for alternative approaches to therapeutic targeting of MCL1 while simultaneously exploiting its regulation of DSB DNA repair.

Outside of tumorigenesis and cancer maintenance, cells still require DDR mechanisms to repair endogenous lesions to DNA. One family of proteins that is required for proper execution of DNA repair is the p53 family of transcriptional tumor suppressors[79]. The p53 family is comprised of three homologous members (p53, p63, and p73) which are activated in response in DNA damage. Upon activation, the p53 family promotes the upregulation of target genes involved in DNA damage response, halting the cell cycle, and precisely regulating apoptotic protein expression[79]. Interestingly, p63 and p73 contain a unique BH3-like sequence that specifically binds to the canonical BH3binding cleft of MCL1[80,81]. The MCL1-p73 interaction inhibits the p73 DNA binding capacity and transcriptional activation of DDR target genes[80]. Under normal circumstances, this mechanism could slow the induction of apoptotic target genes, such as BH3-only proteins NOXA and PUMA, to act as a time management sensor for repair before committing to the cell to apoptosis. Furthermore, under malignant conditions in which MCL1 is upregulated, the inhibition of MCL1 on p73 adds an additional layer of resistance on p73 activation. Specific inhibition of MCL1 using BH3-mimetic A-1210477 induces p73 target gene activation to promote cell cycle arrest, apoptosis, and DNA damage response target gene expression, suggesting MCL1 inhibition may reactivate p73 for more effective therapeutic response to platinum-based therapeutics[80]. This study provides yet another targeted protein interaction in the DDR pathway that could be exploited for combination therapy in cancer treatment regimens to activate DDR at the transcriptional

level.

MCL1 Regulates Autophagy and Mitophagy Through BH3-like Protein Interactions

Thus far, MCL1 has been described in cellular differentiation, cell cycle progression, and DNA damage response, all of which are mechanisms of cell viability and repair. Outside of its canonical apoptotic role, MCL1 has also been characterized in other processes of cell death. Autophagy is a catabolic mechanism in which cellular constituents are degraded and recycled by the lysosome[82]. Activation of autophagy occurs in response to nutrient deprivation where double-membrane vesicles called autophagosomes fuse with the lysosome for bulk degradation. Autophagosome nucleation is regulated by a protein complex that includes Beclin-1[82]. MCL1 and its anti-apoptotic homologs are able to directly bind and inhibit Beclin-1 through a consensus BH3-motif[83]. Inhibition of Beclin1 by MCL1 subsequently mediates the balance between autophagic and apoptotic cell death[84,85]. *In vitro* binding studies have shown that both canonical BH3-only proteins and BH3 mimetics are able to disrupt the binding interaction between anti-apoptotic Bcl-2 family members and Beclin-1[86-88]. Importantly, MCL1 protein degradation is induced in response to nutrient deprivation allowing activation of the autophagic pathway[84]. This suggests that the inhibition of MCL1 can either induce apoptosis or autophagy, which depends on the parallel expression levels of Beclin-1 and other anti-apoptotic Bcl-2 family members that are also capable of binding and inhibiting Beclin-1-mediated autophagy[85].

In a more specialized narrative, MCL1 regulates mitophagy, which is the selective degradation of mitochondria via autophagy. Mitophagy is a critical process in mitochondrial maintenance and is regulated by both Beclin-1-independent and Beclin-1dependent pathways[89]. Independent of Beclin-1, mitophagy is regulated through the Parkin/PINK1 pathway. Parkin is an E3 ligase that ubiquitinates depolarized mitochondria in a PINK1-dependent manner. Once tagged for degradation, damaged mitochondria have

enhanced mitochondrial fission and decreased fusion to promote elimination by the autophagosome[89]. Here MCL1 and other anti-apoptotic Bcl-2 family members, with the exception of BCL2 itself, inhibit mitophagy through the inhibition of Parkin translocation to depolarized mitochondria[90]. Furthermore, the selective elimination of damaged mitochondria was enhanced by BH3-mimetics ABT-737, which targets BCL2, BCLxL, and BCLW and UMI-77, which is an MCL1-specific inhibitor[90-92]. More recently, mitochondrial dysfunction and mitophagy pathways have a been evaluated as therapeutic targets in Alzheimer's Disease, highlighting a novel therapeutic area of BH3-mimetics in neurodegenerative diseases[91,92].

MCL1 also negatively regulates mitophagy through a Beclin-1-dependent pathway requiring pro-autophagic protein and mitophagy receptor, AMBRA1 and binding partner HUWE1. Like Beclin-1, both AMBRA1[93] and HUWE1 (i.e. MCL1 ubiquitin ligase E3 or MULE)[94] contain consensus BH3-motifs. When MCL1 is overexpressed, the recruitment of HUWE1 to the mitochondria is delayed, with a corresponding inhibition of mitochondrial ubiquitylation[95]. This finding was unique amongst the anti-apoptotic Bcl-2 family members, although an earlier publication by the same group identified an interaction between BCL2 and AMBRA1 as a crossroad between apoptosis and autophagic cell death

pathways[93,95]. These studies suggest that MCL1 plays a role in mitophagy regulation through modulation of the AMBRA1 and PARKIN-mediated mitophagy pathways. Interestingly, a study published in 2014 suggested that the anti-apoptotic Bcl-2 family proteins such as MCL1 only indirectly modulate autophagic pathways through the canonical sequestration of BAK and BAX[96]. This claim is supported through knockdown experiments in which MCL1 has no impact on induction of autophagy in the absence of

these effector proteins[96]. While there might be pathway and tissue-specific truth to these claims, the knockdown of Beclin-1, BAK, and BAX were all dispensable for Parkin/PINK1-dependent mitophagy[90]. The functional interplay between each of these pathways needs further investigation to fully elucidate the complete autophagic role of MCL1, which appears to be dependent on the expression of the other pro- and antiapoptotic Bcl-2 family members.

MCL1 Modifies Calcium Homeostasis at the ER and Mitochondrial Membranes

All anti-apoptotic members of the Bcl-2 family, aside from BFL1/A1, contain a conserved C-terminal transmembrane domain that enables anchorage into the outer mitochondrial membrane (OMM)[9] (Figure 3A). As the transmembrane domain is not specific for the mitochondria, MCL1 also localizes to the endoplasmic reticulum (ER) and the mitochondria-associated ER membranes (MAMs) where it functions to regulate basal calcium (Ca^{2+}) flux[97]. Calcium release from the ER is an acute stimulus for both apoptotic and non-apoptotic cellular responses. In apoptosis, calcium is discharged from the ER lumen into the cytosol in response to cytochrome c release from depolarized mitochondria[98]. Furthermore, calcium ions are important biological signaling molecules in physiological responses like muscle contraction and neurotransmitter release[99]. Specifically in cancer cells, Ca^{2+} signaling is required for cell proliferation, migration, and metastasis[100,101]. The Bcl-2 family proteins, BCL2 and BCLxL, have been studied and reviewed in detail describing their role in Ca^{2+} regulation at the ER[97]. While some ER functions of BCL2 and BCLxL appear to be redundant with MCL1, others are not, providing an interesting area of unique Bcl-2 family functionality[97].

At the ER membrane, MCL1 binds to the carboxy-terminus of inositol triphosphate receptor (IP3R), which is directly responsible for Ca^{2+} release from the ER lumen into the

cytosol[102] (Figure 4B). The IP3R channels regulate steady-state Ca^{2+} concentrations through active uptake and passive release. Upon binding to IP3R, MCL1 increases the rate of pro-survival spontaneous Ca^{2+} oscillations by impinging the gating activity of IP3R, promoting a lower concentration of ER-localized Ca^{2+} stores[102]. Furthermore, MCL1 has also been shown to bind and positively regulate all three isoforms of the mitochondrial Ca^{2+} voltage-dependent anion channel (VDAC) at the mitochondria[103,104] (Figure 4C). MCL1's interaction with VDAC promotes mitochondrial Ca^{2+} uptake and stimulates ROS production, which promotes cell migration in non-small cell lung carcinoma cells[103]. Conversely, knockdown of MCL1 was shown to inhibit cell migration without significantly impacting cell proliferation[103] (Figure 4C). Collectively, MCL1 elicits pro-survival functions outside of its canonical regulation as a Bcl-2 family member, as it increases calcium oscillations from the ER and induces mitochondrial calcium uptake, which ultimately promotes cancer cell migration[97,102,103]. While other members of the Bcl-2 family bind to VDAC channels, MCL1 was favored over BCLxL in competitive pulldown experiments[103]. Furthermore, while the effect of older generation BH3-mimetics that target BCL2 and BCLxL have been explored[105-107], the impact that emerging MCL1 inhibitors have on Ca^{2+} homeostasis remains unreported and should be an area of future investigation.

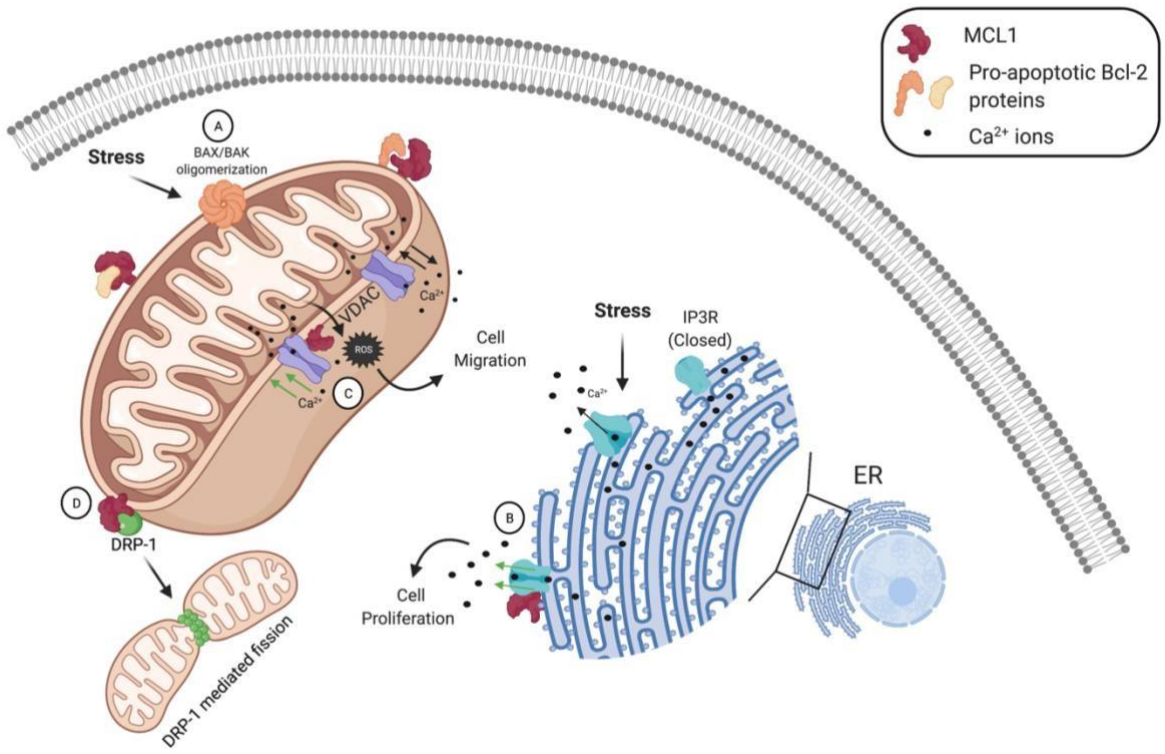

Figure 4. Membrane bound MCL1 dysregulates calcium homeostasis and mitochondrial dynamics. A. MCL1 at the outer mitochondrial membrane (OMM) binds to pro-apoptotic effector and BH3-only proteins (orange) to resist apoptosis. Upon irreparable cellular stress, MCL1 is down-regulated, promoting BAX and/or BAK oligomerization as the rate-limiting step to the apoptotic cascade. **B.** MCL1 localized to the ER-membrane binds and impinges the activity of IP3R channels (blue), promoting basal Ca^{2+} flux from the ER lumen into the cytosol, decreasing ER-stores that are required for an array of cellular functions. The dysregulation on IP3R by MCL1 promotes unstimulated Ca^{2+} release, activating cell proliferation. **C.** MCL1 binds to VDAC channels (purple) at the OMM, promoting mitochondrial Ca^{2+} uptake, ROS production, and cell migration. **B,C.** Black arrows indicate the normal flux of calcium ions, whereas green arrows indicate the change in calcium release and uptake in response to MCL1 binding. **D.** MCL1 binds to DRP-1 (green) at the OMM, modulating mitochondrial fission and fusion.

At the ER membrane, MCL1 binds to the carboxy-terminus of inositol triphosphate receptor (IP3R), which is directly responsible for Ca^{2+} release from the ER lumen into the cytosol[102] (Figure 4B). The IP3R channels regulate steady-state Ca^{2+} concentrations through active uptake and passive release. Upon binding to IP3R, MCL1 increases the rate of pro-survival spontaneous Ca^{2+} oscillations by impinging the gating activity of IP3R,

promoting a lower concentration of ER-localized Ca^{2+} stores[102]. Furthermore, MCL1 has also been shown to bind and positively regulate all three isoforms of the mitochondrial Ca^{2+} voltage-dependent anion channel (VDAC) at the mitochondria[103,104] (Figure 4C). MCL1's interaction with VDAC promotes mitochondrial Ca^{2+} uptake and stimulates ROS production, which promotes cell migration in non-small cell lung carcinoma cells[103]. Conversely, knockdown of MCL1 was shown to inhibit cell migration without significantly impacting cell proliferation[103] (Figure 3C). Collectively, MCL1 elicits pro-survival functions outside of its canonical regulation as a Bcl-2 family member, as it increases calcium oscillations from the ER and induces mitochondrial calcium uptake, which ultimately promotes cancer cell migration[97,102,103]. While other members of the Bcl-2 family bind to VDAC channels, MCL1 was favored over BCLxL in competitive pulldown experiments[103]. Furthermore, while the effect of older generation BH3-mimetics that target BCL2 and BCLxL have been explored[105-107], the impact that emerging MCL1 inhibitors have on Ca^{2+} homeostasis remains unreported and should be an area of future investigation.

MCL1 Facilitates Mitochondrial Bioenergetics and Dynamics

Thus far, we have demonstrated that MCL1 has critical homeostatic interactions with both BH3 and non-BH3 containing proteins in the nucleus, OMM, ER, and cytoplasm. MCL1 can also localize to the mitochondrial inner matrix (MIM) through a 33 amino acid mitochondrial matrix targeting sequence in its N-terminus[108,109]. This sequence is proteolytically cleaved following translocation to the MIM resulting in a unique 'N-MCL1 isoform[108]. Moreover, the MULE/Lasu1 binding site, which is the E3 ligase responsible for MCL1's rapid turnover, is removed, which reduces the steady-state ubiquitylation compared to the full-length isoform[110]. Initial identification of 'N-MCL1 demonstrated

conflicting evidence on the localization of the processed isoform, but MCL1 targeting to the MIM has now been confirmed by multiple studies[108-110].

While full-length MCL1 regulates intrinsic apoptosis and calcium flux at the OMM, 'N-MCL1 regulates mitochondrial dynamics and bioenergetic metabolism in the MIM[109,111]. 'N-MCL1, which is fully localized to the mitochondrial matrix, facilitates ATP production[111] and the maintenance of oligomeric ATP synthase[109]. MCL1 deletion in murine embryonic fibroblasts (MEFs) decreases the ability of complex I, complex II, and complex IV to transfer electrons through the electron transport chain[109]. Under these conditions, ATP production is reduced, which can be rescued with expression of MCL1[109,111]. Furthermore, MCL1 deletion induced mitochondrial morphological changes, including loss of the wild-type tubular mitochondrial networks and the appearance of mitochondrial puncta, neither of which were present in the control cells[109]. In these MCL1 knockout cells, there was a delay in mitochondrial fusion that could also be rescued through expression of wild type MCL1 or 'N-MCL1. An MCL1 transgene that only localizes to the OMM did not rescue the structural mitochondrial defects, demonstrating that 'NMCL1 is required for mitochondrial structure and bioenergetic metabolism[109].

Interestingly, 'N-MCL1 does not bind and sequester pro-apoptotic BH3-only proteins[109].
In a more recent report published, the MCL1 BH3-helix was shown to positively regulate VLCAD (very long-chain acyl-CoA dehydrogenase) to promote fatty acid Eoxidation in the MIM[112]. Here, knockdown of MCL1 or 'N-MCL1 dysregulated longchain fatty acid E-oxidation (FAO). Significantly, treatment with MCL1 small molecule inhibitor, S63845, had no impact on the rate of FAO of ^{3}H-palmitic acid[112]. Importantly, this finding is consistent with the earlier studies demonstrating that 'N-MCL1 does not bind to BH3-only

proteins[109]. This result is supported by multiple other observations: (1) the interaction between MCL1 and VLCAD implies MCL1 is in an altered conformational state as the BH3-helix of MCL1 mediates binding and is therefore, accessible[112], (2) lossof-function mutations of the MCL1 hydrophobic groove do not alter 'N-MCL1 mitochondrial functions[109], and (3) *in vivo* studies with S63845 showed minimal toxicity, suggesting that MIM-localized 'N-MCL1 is spared from inhibition[17,109]. Upon analysis of patient data, MCL1 amplification was significantly correlated with a FAO gene signature in two independent acute myeloblastic leukemia (AML) datasets, suggesting a link between MCL1 upregulation and FAO metabolism in cancer[112]. To this end, a recent report found that upregulation FAO pathways conferred resistance to FDA approved BCL2specific BH3-mimetic Venetoclax with Azacytidine treatment. In resistant leukemic stem cells, MCL1 inhibition did facilitate a decrease in FAO and confer sensitivity to the combination treatment with Azacytidine, prompting the need for further investigation into the crosstalk between the Bcl-2 family and fatty acid metabolism pathways[113].

Paralleled with the functional consequence of MCL1 in mitochondrial bioenergetics such as cellular respiration, the generation of ATP, and metabolism, MCL1 also facilitates normal mitochondrial fission and fusion and regulates the ultrastructure of mitochondrial cristae[109]. MCL1 interacts with two guanosine triphosphatases (GTPases) that are responsible for remodeling the mitochondrial network – DRP1[114] and OPA-1[115]. In mitochondrial dynamics, activated DRP1 forms oligomeric rings around the mitochondria at the OMM, dividing the organelle through mitochondrial fission[89]. Mitochondrial fission is a process that can mediate pro-survival or detrimental outcomes for the cell, especially in cardiac tissue where mitochondrial networks are extensive for energetic demands[116,117]. Conversely, OPA-1 mediates mitochondrial fusion at the MIM,

the process by which two mitochondria physically merge into one[89]. MCL1 binds and promotes the stability of DRP-1, promoting mitochondrial fragmentation at the OMM[115]. On the contrary, 'N-MCL1 inhibits OPA-1 protein stability at the mitochondrial matrix. While the stability of OPA-1 is decreased and fusion is repressed, MCL1 does not abolish its activity as mitochondria can still undergo fusion when MCL1 is inhibited[115]. Subsequent studies have since shown that MCL1-specific BH3-mimetics display fragmented mitochondrial networks, highlighting the shift in mitochondrial dynamics toward enhanced organelle fragmentation through fission[109,118,119]. MCL1 small molecule inhibitor, S63845, disrupted the mitochondrial network and MCL1's interaction with both DRP1 and OPA1, suggesting that the binding interface for these interactions is MCL1's hydrophobic BH3 cleft[115]. This is significant as it suggests that the use of MCL1 inhibitors will ultimately likely have an impact on the dynamic mitochondrial networks necessary for normal cellular homeostasis, contrary to earlier studies suggesting this pathway would be spared.

Concluding remarks: where are we now & where to go next?

As shown through the diverse functionality discussed here, MCL1 plays a critical role in cellular homeostasis, both through its canonical apoptotic and emerging nonapoptotic roles. MCL1 is a highly studied protein; it has >2,000 publications over the past five years with approximately 500 publications in 2020 alone. While a large portion of these studies, especially those since 2017, are characterizing MCL1-specific BH3mimetics in various cancer cell types, it is clear that MCL1 plays are larger, understudied role in many aspects of cellular maintenance and stress response. While ongoing studies characterizing the impact of BH3-mimetics is important to move these compounds from bench-to-bedside in

disease therapy, characterizing the underlying biological role of MCL1 is essential to designing the best combination strategies with existing therapy. Furthermore, the fundamental biology will be critical to predict and understand the etiology of adverse events in clinical trials as these inhibitors are deployed in Phase I and II human clinical trials.

One anecdotal observation that can be gleaned from synthesizing this review is that MCL1 is a very diverse protein, and many pathways must be monitored in deploying MCL1 inhibitors systemically. One tissue that relies heavily on mitochondrial metabolism and strict control over mitochondrial dynamics is the heart[120]. Cardiomyocytes must provide the energy required for circulation and oxygenation of organs throughout the body and mitochondria account for ~35% of cardiac tissue[120,121]. Comparatively to skeletal muscle, mitochondria only comprise 3-8% skeletal muscle volume, which is highly dependent on physical activity[120]. Conditional knockout of MCL1 in cardiomyocytes in mice induces rapid cardiomyopathy and death[122,123]. Interestingly, these cells do not undergo apoptosis but have impaired autophagy and endure necrotic cell death[122]. Tissue analysis reveals that the $MCL1^{-/-}$ cardiomyocytes have swollen mitochondria, leading to the swelling and rupture of the OMM[122]. Mitochondria isolated from these cells also have reduced respiration, consistent with reports of MCL1s role in the electron transport chain and ATP synthesis[109,122]. While MCL1-specific BH3 mimetics did not show significant toxicities in *in vivo* animal studies[17], there have been delays in ongoing Phase I/II clinical trials[124].

Outside characterizing emerging BH3-mimetics, there remains several areas of MCL1 biology that are underdeveloped as they have contradictory findings that suggest they are cell-type and tissue-specific. For example, MCL1s role in the cell cycle has been

demonstrated to be pro-proliferative, but also delays populations in the S and G2 phase[63,64,66]. Furthermore, specifically in autophagic cell death, MCL1 deletion activates an autophagy response in murine cortical neurons[84], whereas MCL1 deletion in cardiomyocytes displayed autophagic dysfunction[122]. In many areas, BCL2 and BCLxL have been more extensively characterized, demonstrating both similar and unique roles between the two Bcl-2 family homologs[18,125]. Thus, the role of MCL1 in these interactions requires further characterization to understand MCL1s functionality in greater detail.

Another new avenue of research in MCL1 biology encompasses a novel class of MCL1-binding proteins that contain a reverse BH3 (rBH3) motif, which specifically bind to MCL1 over the other anti-apoptotic Bcl-2 family members[81]. Recently, two rBH3mediated interactions have been identified and characterized between cell cycle regulator p18[63] and tumor suppressor p73[80]. Notably, while these proteins interact with MCL1 through the consensus BH3 pocket, they do not appear to impact MCL1s regulation of apoptosis at the OMM[63,80]. Instead, these novel protein interactions appear to impact their endogenous function in cell cycle regulation and transcriptional activation, respectively. The identification of the rBH3 has proven to be significant as these novel protein interactions are opening new avenues for non-canonical MCL1 protein regulation.

In conclusion, MCL1 is a dynamic, unique protein that is involved in a variety of cellular functions. These include but are not limited to cellular differentiation, cell cycle progression, DNA damage response, autophagy, mitochondrial dynamics, calcium handling, and metabolism. MCL1, like BCL2, is also proving to be a valuable anti-cancer therapeutic target[15-17]. Thus, understanding the role of MCL1 across diverse cancer cell types and endogenous tissues is critical as MCL1 inhibitors progress through clinical trials.

As we are currently in an era of personalized medicine, comprehending the immense role MCL1 executes in cellular physiology is critical. While the study of the Bcl-2 family over the past 30 years has focused on how signaling pathways transmit pro- and anti-apoptotic signals to regulate apoptosis, the emerging non-canonical functions of MCL1, BCL2, and BCLxL provide an improved model where these proteins can bind and promote prosurvival and pro-proliferative signaling pathways. These pathways support multiple central homeostatic regulatory systems including transcription factor activation, cell cycle control, mitochondrial biogenesis, and metabolism. Therefore, while MCL1 has thus far been viewed simply as an apoptotic regulator, the multiple functions that these studies begin to explore suggest it may be more significantly positioned as a rheostat that can report on cell stress on multiple levels that modulate ultimate cell fate decisions.

Acknowledgements

All figures were created using templates from BioRender.com

Chapter 1 References

1 Kozopas, K. M., Yang, T., Buchan, H. L., Zhou, P. & Craig, R. W. MCL1, a gene expressed in programmed myeloid cell differentiation, has sequence similarity to BCL2. *Proc Natl Acad Sci U S A* **90**, 3516-3520, doi:10.1073/pnas.90.8.3516 (1993).

2 Zhou, P., Qian, L., Kozopas, K. M. & Craig, R. W. Mcl-1, a Bcl-2 family member, delays the death of hematopoietic cells under a variety of apoptosis-inducing conditions. *Blood* **89**, 630-643 (1997).

3 Reynolds, J. E. *et al.* Mcl-1, a member of the Bcl-2 family, delays apoptosis induced by cMyc overexpression in Chinese hamster ovary cells. *Cancer Res* **54**, 6348-6352 (1994).

4 Kale, J., Osterlund, E. J. & Andrews, D. W. BCL-2 family proteins: changing partners in the dance towards death. *Cell Death Differ* **25**, 65-80, doi:10.1038/cdd.2017.186 (2018).

5 Uren, R. T., Iyer, S. & Kluck, R. M. Pore formation by dimeric Bak and Bax: an unusual pore? *Philos Trans R Soc Lond B Biol Sci* **372**, doi:10.1098/rstb.2016.0218 (2017).

6 Wei, M. C. *et al.* Proapoptotic BAX and BAK: a requisite gateway to mitochondrial dysfunction and death. *Science* **292**, 727-730, doi:10.1126/science.1059108 (2001).

7 Goldstein, J. C., Waterhouse, N. J., Juin, P., Evan, G. I. & Green, D. R. The coordinate release of cytochrome c during apoptosis is rapid, complete and kinetically invariant. *Nat Cell Biol* **2**, 156-162, doi:10.1038/35004029 (2000).

8 Aouacheria, A., Combet, C., Tompa, P. & Hardwick, J. M. Redefining the BH3 Death Domain as a 'Short Linear Motif'. *Trends Biochem Sci* **40**, 736-748, doi:10.1016/j.tibs.2015.09.007 (2015).

9 Youle, R. J. & Strasser, A. The BCL-2 protein family: opposing activities that mediate cell death. *Nat Rev Mol Cell Biol* **9**, 47-59, doi:10.1038/nrm2308 (2008).

10 Denis, C., Sopková-de Oliveira Santos, J., Bureau, R. & Voisin-Chiret, A. S. Hot-Spots of Mcl-1 Protein. *J Med Chem* **63**, 928-943, doi:10.1021/acs.jmedchem.9b00983 (2020).

11 Tsujimoto, Y., Cossman, J., Jaffe, E. & Croce, C. M. Involvement of the bcl-2 gene in human follicular lymphoma. *Science* **228**, 1440-1443, doi:10.1126/science.3874430 (1985).

12 Beroukhim, R. *et al.* The landscape of somatic copy-number alteration across human cancers. *Nature* **463**, 899-905, doi:10.1038/nature08822 (2010).

13 Zhang, L., Ming, L. & Yu, J. BH3 mimetics to improve cancer therapy; mechanisms and examples. *Drug Resist Updat* **10**, 207-217, doi:10.1016/j.drup.2007.08.002 (2007).

14 Szlavik, Z. *et al.* Discovery of S64315, a Potent and Selective Mcl-1 Inhibitor. *J Med Chem* **63**, 13762-13795, doi:10.1021/acs.jmedchem.0c01234 (2020).

15 Caenepeel, S. *et al.* AMG 176, a Selective MCL1 Inhibitor, Is Effective in Hematologic Cancer Models Alone and in Combination with Established Therapies. *Cancer Discov* **8**, 1582-1597, doi:10.1158/2159-8290.CD-18-0387 (2018).

16 Tron, A. E. *et al.* Discovery of Mcl-1-specific inhibitor AZD5991 and preclinical activity in multiple myeloma and acute myeloid leukemia. *Nat Commun* **9**, 5341, doi:10.1038/s41467-018-07551-w (2018).

17 Kotschy, A. *et al.* The MCL1 inhibitor S63845 is tolerable and effective in diverse cancer models. *Nature* **538**, 477-482, doi:10.1038/nature19830 (2016).

18 Chong, S. J. F. *et al.* Noncanonical Cell Fate Regulation by Bcl-2 Proteins. *Trends Cell Biol* **30**, 537-555, doi:10.1016/j.tcb.2020.03.004 (2020).

19 Rinkenberger, J. L., Horning, S., Klocke, B., Roth, K. & Korsmeyer, S. J. Mcl-1 deficiency results in peri-implantation embryonic lethality. *Genes Dev* **14**, 23-27 (2000).

20 Marikawa, Y. & Alarcón, V. B. Establishment of trophectoderm and inner cell mass lineages in the mouse embryo. *Mol Reprod Dev* **76**, 1019-1032, doi:10.1002/mrd.21057 (2009).

21 Watson, E. C., Whitehead, L., Adams, R. H., Dewson, G. & Coultas, L. Endothelial cell survival during angiogenesis requires the pro-survival protein MCL1. *Cell Death Differ* **23**, 1371-1379, doi:10.1038/cdd.2016.20 (2016).

22 Vick, B. *et al.* Knockout of myeloid cell leukemia-1 induces liver damage and increases apoptosis susceptibility of murine hepatocytes. *Hepatology* **49**, 627-636, doi:10.1002/hep.22664 (2009).

23 Sitailo, L. A., Jerome-Morais, A. & Denning, M. F. Mcl-1 functions as major epidermal survival protein required for proper keratinocyte differentiation. *J Invest Dermatol* **129**, 1351-1360, doi:10.1038/jid.2008.363 (2009).

24 Healy, M. E. *et al.* MCL1 Is Required for Maintenance of Intestinal Homeostasis and Prevention of Carcinogenesis in Mice. *Gastroenterology* **159**, 183-199, doi:10.1053/j.gastro.2020.03.017 (2020).

25 Perciavalle, R. M. & Opferman, J. T. Delving deeper: MCL-1's contributions to normal and cancer biology. *Trends Cell Biol* **23**, 22-29, doi:10.1016/j.tcb.2012.08.011 (2013).

26 Opferman, J. T. *et al.* Obligate role of anti-apoptotic MCL-1 in the survival of hematopoietic stem cells. *Science* **307**, 1101-1104, doi:10.1126/science.1106114 (2005).

27 Opferman, J. T. *et al.* Development and maintenance of B and T lymphocytes requires antiapoptotic MCL-1. *Nature* **426**, 671-676, doi:10.1038/nature02067 (2003).

28 Arbour, N. *et al.* Mcl-1 is a key regulator of apoptosis during CNS development and after DNA damage. *J Neurosci* **28**, 6068-6078, doi:10.1523/JNEUROSCI.4940-07.2008 (2008).

29 Opferman, J. T. & Kothari, A. Anti-apoptotic BCL-2 family members in development. *Cell Death Differ* **25**, 37-45, doi:10.1038/cdd.2017.170 (2018).

30 Jagannathan-Bogdan, M. & Zon, L. I. Hematopoiesis. *Development* **140**, 2463-2467, doi:10.1242/dev.083147 (2013).

31 Opferman, J. T. Life and death during hematopoietic differentiation. *Curr Opin Immunol* **19**, 497-502, doi:10.1016/j.coi.2007.06.002 (2007).

32 Dzhagalov, I., St John, A. & He, Y. W. The antiapoptotic protein Mcl-1 is essential for the survival of neutrophils but not macrophages. *Blood* **109**, 1620-1626, doi:10.1182/blood2006-03-013771 (2007).

33 Lilla, J. N. *et al.* Reduced mast cell and basophil numbers and function in Cpa3-Cre; Mcl1fl/fl mice. *Blood* **118**, 6930-6938, doi:10.1182/blood-2011-03-343962 (2011).

34 Carrington, E. M. *et al.* Prosurvival Bcl-2 family members reveal a distinct apoptotic identity between conventional and plasmacytoid dendritic cells. *Proc Natl Acad Sci U S A* **112**, 4044-4049, doi:10.1073/pnas.1417620112 (2015).

35 Kodama, T. *et al.* Mcl-1 and Bcl-xL regulate Bak/Bax-dependent apoptosis of the megakaryocytic lineage at multistages. *Cell Death Differ* **19**, 1856-1869, doi:10.1038/cdd.2012.88 (2012).

36 Debrincat, M. A. *et al.* Mcl-1 and Bcl-x(L) coordinately regulate megakaryocyte survival. *Blood* **119**, 5850-5858, doi:10.1182/blood-2011-12-398834 (2012).

37 Kodama, T. *et al.* BH3-only activator proteins Bid and Bim are dispensable for Bak/Baxdependent thrombocyte apoptosis induced by Bcl-xL deficiency: molecular requisites for the mitochondrial pathway to apoptosis in platelets. *J Biol Chem* **286**, 13905-13913, doi:10.1074/jbc.M110.195370 (2011).

38 Turnis, M. E. *et al.* Requirement for Anti-Apoptotic MCL-1 during Early Erythropoiesis. *Blood*, doi:10.1182/blood.2020006916 (2021).

39 Steimer, D. A. *et al.* Selective roles for antiapoptotic MCL-1 during granulocyte development and macrophage effector function. *Blood* **113**, 2805-2815, doi:10.1182/blood-2008-05-159145 (2009).

40 Felton, J. M. *et al.* Mcl-1 protects eosinophils from apoptosis and exacerbates allergic airway inflammation. *Thorax* **75**, 600-605, doi:10.1136/thoraxjnl-2019-213204 (2020).

41 Tibes, R. & Bogenberger, J. M. Transcriptional Silencing of MCL-1 Through CyclinDependent Kinase Inhibition in Acute Myeloid Leukemia. *Front Oncol* **9**, 1205, doi:10.3389/fonc.2019.01205 (2019).

42 Lucas, C. D. *et al.* Downregulation of Mcl-1 has anti-inflammatory pro-resolution effects and enhances bacterial clearance from the lung. *Mucosal Immunol* **7**, 857-868, doi:10.1038/mi.2013.102 (2014).

43 Krajewski, S. *et al.* Immunohistochemical analysis of Mcl-1 and Bcl-2 proteins in normal and neoplastic lymph nodes. *Am J Pathol* **145**, 515-525 (1994).

44 Vikstrom, I. *et al.* Mcl-1 is essential for germinal center formation and B cell memory. *Science* **330**, 1095-1099, doi:10.1126/science.1191793 (2010).

45 Peperzak, V. *et al.* Mcl-1 is essential for the survival of plasma cells. *Nat Immunol* **14**, 290297, doi:10.1038/ni.2527 (2013).

46 Sathe, P. *et al.* Innate immunodeficiency following genetic ablation of Mcl1 in natural killer cells. *Nat Commun* **5**, 4539, doi:10.1038/ncomms5539 (2014).

47 Campbell, K. J., Gray, D. H., Anstee, N., Strasser, A. & Cory, S. Elevated Mcl-1 inhibits thymocyte apoptosis and alters thymic selection. *Cell Death Differ* **19**, 1962-1971, doi:10.1038/cdd.2012.84 (2012).

48 Dzhagalov, I., Dunkle, A. & He, Y. W. The anti-apoptotic Bcl-2 family member Mcl-1 promotes T lymphocyte survival at multiple stages. *J Immunol* **181**, 521-528, doi:10.4049/jimmunol.181.1.521 (2008).

49 Gui, J. *et al.* MCL1 enhances the survival of CD8+ memory T Cells after viral infection. *J Virol* **89**, 2405-2414, doi:10.1128/JVI.02480-14 (2015).

50 Tripathi, P., Koss, B., Opferman, J. T. & Hildeman, D. A. Mcl-1 antagonizes Bax/Bak to promote effector CD4(+) and CD8(+) T-cell responses. *Cell Death Differ* **20**, 998-1007, doi:10.1038/cdd.2013.25 (2013).

51 Liang, H., Hippenmeyer, S. & Ghashghaei, H. T. A Nestin-cre transgenic mouse is insufficient for recombination in early embryonic neural progenitors. *Biol Open* **1**, 12001203, doi:10.1242/bio.20122287 (2012).

52 Robinson, E. J. *et al.* Survival of midbrain dopamine neurons depends on the Bcl2 factor Mcl1. *Cell Death Discov* **4**, 107, doi:10.1038/s41420-018-0125-7 (2018).

53 Hasan, S. M. *et al.* Mcl1 regulates the terminal mitosis of neural precursor cells in the mammalian brain through p27Kip1. *Development* **140**, 3118-3127, doi:10.1242/dev.090910 (2013).

54 Chen, G. *et al.* Targeting Mcl-1 enhances DNA replication stress sensitivity to cancer therapy. *J Clin Invest* **128**, 500-516, doi:10.1172/JCI92742 (2018).

55 Harley, M. E., Allan, L. A., Sanderson, H. S. & Clarke, P. R. Phosphorylation of Mcl-1 by CDK1-cyclin B1 initiates its Cdc20-dependent destruction during mitotic arrest. *EMBO J* **29**, 2407-2420, doi:10.1038/emboj.2010.112 (2010).

56 Cui, J. & Placzek, W. J. Post-Transcriptional Regulation of Anti-Apoptotic BCL2 Family Members. *Int J Mol Sci* **19**, doi:10.3390/ijms19010308 (2018).

57 Senichkin, V. V., Streletskaia, A. Y., Gorbunova, A. S., Zhivotovsky, B. & Kopeina, G. S. Saga of Mcl-1: regulation from transcription to degradation. *Cell Death Differ* **27**, 405419, doi:10.1038/s41418-019-0486-3 (2020).

58 Wu, X., Luo, Q. & Liu, Z. Ubiquitination and deubiquitination of MCL1 in cancer: deciphering chemoresistance mechanisms and providing potential therapeutic options. *Cell Death Dis* **11**, 556, doi:10.1038/s41419-020-02760-y (2020).

59 Whitaker, R. H. & Placzek, W. J. Regulating the BCL2 Family to Improve Sensitivity to Microtubule Targeting Agents. *Cells* **8**, doi:10.3390/cells8040346 (2019).

60 Haschka, M. D. *et al.* The NOXA-MCL1-BIM axis defines lifespan on extended mitotic arrest. *Nat Commun* **6**, 6891, doi:10.1038/ncomms7891 (2015).

61 Wertz, I. E. *et al.* Sensitivity to antitubulin chemotherapeutics is regulated by MCL1 and FBW7. *Nature* **471**, 110-114, doi:10.1038/nature09779 (2011).

62 Germain, M. & Duronio, V. The N terminus of the anti-apoptotic BCL-2 homologue MCL1 regulates its localization and function. *J Biol Chem* **282**, 32233-32242, doi:10.1074/jbc.M706408200 (2007).

63 Whitaker, R. H. & Placzek, W. J. MCL1 binding to the reverse BH3 motif of P18INK4C couples cell survival to cell proliferation. *Cell Death Dis* **11**, 156, doi:10.1038/s41419-0202351-1 (2020).

64 Fujise, K., Zhang, D., Liu, J. & Yeh, E. T. Regulation of apoptosis and cell cycle progression by MCL1. Differential role of proliferating cell nuclear antigen. *J Biol Chem* **275**, 39458-39465, doi:10.1074/jbc.M006626200 (2000).

65 Streletskaia, A. Y. *et al.* Upregulation of Mcl-1S Causes Cell-Cycle Perturbations and DNA Damage Accumulation. *Front Cell Dev Biol* **8**, 543066, doi:10.3389/fcell.2020.543066 (2020).

66 Jamil, S. *et al.* A proteolytic fragment of Mcl-1 exhibits nuclear localization and regulates cell growth by interaction with Cdk1. *Biochem J* **387**, 659-667, doi:10.1042/BJ20041596 (2005).

67 Hanahan, D. & Weinberg, R. A. Hallmarks of cancer: the next generation. *Cell* **144**, 646674, doi:10.1016/j.cell.2011.02.013 (2011).

68 de Almeida, L. C., Calil, F. A., Machado-Neto, J. A. & Costa-Lotufo, L. V. DNA damaging agents and DNA repair: From carcinogenesis to cancer therapy. *Cancer Genet* **252-253**, 624, doi:10.1016/j.cancergen.2020.12.002 (2021).

69 Zhan, Q., Bieszczad, C. K., Bae, I., Fornace, A. J. & Craig, R. W. Induction of BCL2 family member MCL1 as an early response to DNA damage. *Oncogene* **14**, 1031-1039, doi:10.1038/sj.onc.1200927 (1997).

70 Miyashita, T. *et al.* Tumor suppressor p53 is a regulator of bcl-2 and bax gene expression in vitro and in vivo. *Oncogene* **9**, 1799-1805 (1994).

71 Jamil, S., Mojtabavi, S., Hojabrpour, P., Cheah, S. & Duronio, V. An essential role for MCL-1 in ATR-mediated CHK1 phosphorylation. *Mol Biol Cell* **19**, 3212-3220, doi:10.1091/mbc.e07-11-1171 (2008).

72 Jamil, S., Stoica, C., Hackett, T. L. & Duronio, V. MCL-1 localizes to sites of DNA damage and regulates DNA damage response. *Cell Cycle* **9**, 2843-2855, doi:10.4161/cc.9.14.12354 (2010).

73 Pawlikowska, P. *et al.* ATM-dependent expression of IEX-1 controls nuclear accumulation of Mcl-1 and the DNA damage response. *Cell Death Differ* **17**, 1739-1750, doi:10.1038/cdd.2010.56 (2010).

74 Scully, R., Panday, A., Elango, R. & Willis, N. A. DNA double-strand break repairpathway choice in somatic mammalian cells. *Nat Rev Mol Cell Biol* **20**, 698-714, doi:10.1038/s41580-019-0152-0 (2019).

75 Mattoo, A. R. *et al.* MCL-1 Depletion Impairs DNA Double-Strand Break Repair and Reinitiation of Stalled DNA Replication Forks. *Mol Cell Biol* **37**, doi:10.1128/MCB.00535-16 (2017).

76 Rose, M., Burgess, J. T., O'Byrne, K., Richard, D. J. & Bolderson, E. PARP Inhibitors: Clinical Relevance, Mechanisms of Action and Tumor Resistance. *Front Cell Dev Biol* **8**, 564601, doi:10.3389/fcell.2020.564601 (2020).

77 Mattoo, A. R., Joun, A. & Jessup, J. M. Repurposing of mTOR Complex Inhibitors Attenuates MCL-1 and Sensitizes to PARP Inhibition. *Mol Cancer Res* **17**, 42-53, doi:10.1158/1541-7786.MCR-18-0650 (2019).

78 Li, H., Liu, L., Chang, H., Zou, Z. & Xing, D. Downregulation of MCL-1 and upregulation of PUMA using mTOR inhibitors enhance antitumor efficacy of BH3 mimetics in triplenegative breast cancer. *Cell Death Dis* **9**, 137, doi:10.1038/s41419-017-0169-2 (2018).

79 Nicolai, S. *et al.* DNA repair and aging: the impact of the p53 family. *Aging (Albany NY)* **7**, 1050-1065, doi:10.18632/aging.100858 (2015).

80 Widden, H., Kaczmarczyk, A., Subedi, A., Whitaker, R. H. & Placzek, W. J. MCL1 binds and negatively regulates the transcriptional function of tumor suppressor p73. *Cell Death Dis* **11**, 946, doi:10.1038/s41419-020-03068-7 (2020).

81 Placzek, W. J. *et al.* Identification of a novel Mcl-1 protein binding motif. *J Biol Chem* **286**, 39829-39835, doi:10.1074/jbc.M111.305326 (2011).

82 Li, X., He, S. & Ma, B. Autophagy and autophagy-related proteins in cancer. *Mol Cancer* **19**, 12, doi:10.1186/s12943-020-1138-4 (2020).

83 Erlich, S. *et al.* Differential interactions between Beclin 1 and Bcl-2 family members. *Autophagy* **3**, 561-568, doi:10.4161/auto.4713 (2007).

84 Germain, M. *et al.* MCL-1 is a stress sensor that regulates autophagy in a developmentally regulated manner. *EMBO J* **30**, 395-407, doi:10.1038/emboj.2010.327 (2011).

85 Germain, M. & Slack, R. S. MCL-1 regulates the balance between autophagy and apoptosis. *Autophagy* **7**, 549-551, doi:10.4161/auto.7.5.15098 (2011).

86 Maiuri, M. C. *et al.* BH3-only proteins and BH3 mimetics induce autophagy by competitively disrupting the interaction between Beclin 1 and Bcl-2/Bcl-X(L). *Autophagy* **3**, 374-376, doi:10.4161/auto.4237 (2007).

87 Maiuri, M. C. *et al.* Functional and physical interaction between Bcl-X(L) and a BH3-like domain in Beclin-1. *EMBO J* **26**, 2527-2539, doi:10.1038/sj.emboj.7601689 (2007).

88 Malik, S. A. *et al.* BH3 mimetics reveal the network properties of autophagy-regulatory signaling cascades. *Autophagy* **7**, 914-916, doi:10.4161/auto.7.8.15785 (2011).

89 Ashrafi, G. & Schwarz, T. L. The pathways of mitophagy for quality control and clearance of mitochondria. *Cell Death Differ* **20**, 31-42, doi:10.1038/cdd.2012.81 (2013).

90 Hollville, E., Carroll, R. G., Cullen, S. P. & Martin, S. J. Bcl-2 family proteins participate in mitochondrial quality control by regulating Parkin/PINK1-dependent mitophagy. *Mol Cell* **55**, 451-466, doi:10.1016/j.molcel.2014.06.001 (2014).

91 Cen, X. *et al.* Pharmacological targeting of MCL-1 promotes mitophagy and improves disease pathologies in an Alzheimer's disease mouse model. *Nat Commun* **11**, 5731, doi:10.1038/s41467-020-19547-6 (2020).

92 Cen, X., Xu, X. & Xia, H. Targeting MCL1 to induce mitophagy is a potential therapeutic strategy for Alzheimer disease. *Autophagy*, 1-2, doi:10.1080/15548627.2020.1860542 (2020).

93 Strappazzon, F. *et al.* Prosurvival AMBRA1 turns into a proapoptotic BH3-like protein during mitochondrial apoptosis. *Autophagy* **12**, 963-975, doi:10.1080/15548627.2016.1164359 (2016).

94 Zhong, Q., Gao, W., Du, F. & Wang, X. Mule/ARF-BP1, a BH3-only E3 ubiquitin ligase, catalyzes the polyubiquitination of Mcl-1 and regulates apoptosis. *Cell* **121**, 1085-1095, doi:10.1016/j.cell.2005.06.009 (2005).

95 Strappazzon, F. *et al.* HUWE1 controls MCL1 stability to unleash AMBRA1-induced mitophagy. *Cell Death Differ* **27**, 1155-1168, doi:10.1038/s41418-019-0404-8 (2020).

96 Lindqvist, L. M., Heinlein, M., Huang, D. C. & Vaux, D. L. Prosurvival Bcl-2 family members affect autophagy only indirectly, by inhibiting Bax and Bak. *Proc Natl Acad Sci U S A* **111**, 8512-8517, doi:10.1073/pnas.1406425111 (2014).

97 Vervliet, T. *et al.* Modulation of Ca. *Front Oncol* **7**, 75, doi:10.3389/fonc.2017.00075 (2017).

98 Giacomello, M., Drago, I., Pizzo, P. & Pozzan, T. Mitochondrial Ca2+ as a key regulator of cell life and death. *Cell Death Differ* **14**, 1267-1274, doi:10.1038/sj.cdd.4402147 (2007).

99 Kuo, I. Y. & Ehrlich, B. E. Signaling in muscle contraction. *Cold Spring Harb Perspect Biol* **7**, a006023, doi:10.1101/cshperspect.a006023 (2015).

100 Prevarskaya, N., Skryma, R. & Shuba, Y. Calcium in tumour metastasis: new roles for known actors. *Nat Rev Cancer* **11**, 609-618, doi:10.1038/nrc3105 (2011).

101 Roderick, H. L. & Cook, S. J. Ca2+ signalling checkpoints in cancer: remodelling Ca2+ for cancer cell proliferation and survival. *Nat Rev Cancer* **8**, 361-375, doi:10.1038/nrc2374 (2008).

102 Eckenrode, E. F., Yang, J., Velmurugan, G. V., Foskett, J. K. & White, C. Apoptosis protection by Mcl-1 and Bcl-2 modulation of inositol 1,4,5-trisphosphate receptordependent Ca2+ signaling. *J Biol Chem* **285**, 13678-13684, doi:10.1074/jbc.M109.096040 (2010).

103 Huang, H., Shah, K., Bradbury, N. A., Li, C. & White, C. Mcl-1 promotes lung cancer cell migration by directly interacting with VDAC to increase mitochondrial Ca2+ uptake and

reactive oxygen species generation. *Cell Death Dis* **5**, e1482, doi:10.1038/cddis.2014.419 (2014).

104 Weng, C., Li, Y., Xu, D., Shi, Y. & Tang, H. Specific cleavage of Mcl-1 by caspase-3 in tumor necrosis factor-related apoptosis-inducing ligand (TRAIL)-induced apoptosis in Jurkat leukemia T cells. *J Biol Chem* **280**, 10491-10500, doi:10.1074/jbc.M412819200 (2005).

105 Vervloessem, T., Ivanova, H., Luyten, T., Parys, J. B. & Bultynck, G. The selective Bcl-2 inhibitor venetoclax, a BH3 mimetic, does not dysregulate intracellular Ca. *Biochim Biophys Acta Mol Cell Res* **1864**, 968-976, doi:10.1016/j.bbamcr.2016.11.024 (2017).

106 Gerasimenko, J., Ferdek, P., Fischer, L., Gukovskaya, A. S. & Pandol, S. J. Inhibitors of Bcl-2 protein family deplete ER Ca2+ stores in pancreatic acinar cells. *Pflugers Arch* **460**, 891-900, doi:10.1007/s00424-010-0859-4 (2010).

107 Akl, H. *et al.* HA14-1, but not the BH3 mimetic ABT-737, causes Ca2+ dysregulation in platelets and human cell lines. *Haematologica* **98**, e49-51, doi:10.3324/haematol.2012.080598 (2013).

108 Huang, C. R. & Yang-Yen, H. F. The fast-mobility isoform of mouse Mcl-1 is a mitochondrial matrix-localized protein with attenuated anti-apoptotic activity. *FEBS Lett* **584**, 3323-3330, doi:10.1016/j.febslet.2010.07.013 (2010).

109 Perciavalle, R. M. *et al.* Anti-apoptotic MCL-1 localizes to the mitochondrial matrix and couples mitochondrial fusion to respiration. *Nat Cell Biol* **14**, 575-583, doi:10.1038/ncb2488 (2012).

110 Warr, M. R. *et al.* Mitochondrion-dependent N-terminal processing of outer membrane Mcl-1 protein removes an essential Mule/Lasu1 protein-binding site. *J Biol Chem* **286**, 25098-25107, doi:10.1074/jbc.M111.218321 (2011).

111 Anilkumar, U. *et al.* MCL-1 Matrix maintains neuronal survival by enhancing mitochondrial integrity and

bioenergetic capacity under stress conditions. *Cell Death Dis* **11**, 321, doi:10.1038/s41419-0202498-9 (2020).

112 Escudero, S. *et al.* Dynamic Regulation of Long-Chain Fatty Acid Oxidation by a Noncanonical Interaction between the MCL-1 BH3 Helix and VLCAD. *Mol Cell* **69**, 729743.e727, doi:10.1016/j.molcel.2018.02.005 (2018).

113 Stevens, B. M., Jones, C. L., Pollyea, D. A. & *al., e.* Vol. 1 1176–1187 (Nature Publishing Group, Nature Cancer, 2020).

114 Moyzis, A. G. *et al.* Mcl-1-mediated mitochondrial fission protects against stress but impairs cardiac adaptation to exercise. *J Mol Cell Cardiol* **146**, 109-120, doi:10.1016/j.yjmcc.2020.07.009 (2020).

115 Rasmussen, M. L. *et al.* A Non-apoptotic Function of MCL-1 in Promoting Pluripotency and Modulating Mitochondrial Dynamics in Stem Cells. *Stem Cell Reports* **10**, 684-692, doi:10.1016/j.stemcr.2018.01.005 (2018).

116 Youle, R. J. & van der Bliek, A. M. Mitochondrial fission, fusion, and stress. *Science* **337**, 1062-1065, doi:10.1126/science.1219855 (2012).

117 Coronado, M. *et al.* Physiological Mitochondrial Fragmentation Is a Normal Cardiac Adaptation to Increased Energy Demand. *Circ Res* **122**, 282-295, doi:10.1161/CIRCRESAHA.117.310725 (2018).

118 Milani, M. *et al.* DRP-1 functions independently of mitochondrial structural perturbations to facilitate BH3 mimetic-mediated apoptosis. *Cell Death Discov* **5**, 117, doi:10.1038/s41420-019-0199-x (2019).

119 Rasmussen, M. L. *et al.* MCL-1 Inhibition by Selective BH3 Mimetics Disrupts Mitochondrial Dynamics Causing Loss of Viability and Functionality of Human Cardiomyocytes. *iScience* **23**, 101015, doi:10.1016/j.isci.2020.101015 (2020).

120 Park, S. Y. *et al.* Cardiac, skeletal, and smooth muscle mitochondrial respiration: are all mitochondria created equal? *Am J Physiol Heart Circ Physiol* **307**, H346-352, doi:10.1152/ajpheart.00227.2014 (2014).

121 Lemieux, H. & Hoppel, C. L. Mitochondria in the human heart. *J Bioenerg Biomembr* **41**, 99-106, doi:10.1007/s10863-009-9211-0 (2009).

122 Thomas, R. L. *et al.* Loss of MCL-1 leads to impaired autophagy and rapid development of heart failure. *Genes Dev* **27**, 1365-1377, doi:10.1101/gad.215871.113 (2013).

123 Wang, X. *et al.* Deletion of MCL-1 causes lethal cardiac failure and mitochondrial dysfunction. *Genes Dev* **27**, 1351-1364, doi:10.1101/gad.215855.113 (2013).

124 Bolomsky, A. *et al.* MCL-1 inhibitors, fast-lane development of a new class of anti-cancer agents. *J Hematol Oncol* **13**, 173, doi:10.1186/s13045-020-01007-9 (2020).

125 Hardwick, J. M. & Soane, L. Multiple functions of BCL-2 family proteins. *Cold Spring Harb Perspect Biol* **5**, doi:10.1101/cshperspect.a008722 (2013).

MCL1 BINDS AND NEGATIVELY REGULATES THE TRANSCRIPTIONAL FUNCTION OF TUMOR SUPPRESSOR P73

by

HAYLEY WIDDEN, ANETA KACZMARCZYK, ASHOK SUBEDI, ROBERT H. WHITAKER, AND WILLIAM PLACZEK

Cell Death and Disease
Volume 11, Article 946 https://doi.org/10.1038/s41419-020-03068-7

Format adapted for dissertation

Abstract

MCL1, an anti-apoptotic protein that controls chemosensitivity and cell fate through its regulation of intrinsic apoptosis, has been identified as a high-impact target in anti-cancer therapeutic development. With MCL1-specific inhibitors currently in clinical trials, it is imperative that we understand the roles that MCL1 plays in cells, especially when targeting the Bcl-2 homology 3 (BH3) pocket, the central region of MCL1 that mediates apoptotic regulation. Here, we establish that MCL1 has a direct role in controlling p73 transcriptional activity, which modulates target genes associated with DNA damage response, apoptosis, and cell cycle progression. This interaction is mediated through the reverse BH3 (rBH3) motif in the p73 tetramerization domain, which restricts p73 assembly on DNA. Here, we provide a novel mechanism for proteinlevel regulation of p73 transcriptional activity by MCL1, while also framing a foundation for studying MCL1 inhibitors in combination with platinum-based chemotherapeutics. More broadly, this work expands the role of Bcl-2 family signaling beyond cell fate regulation.

Introduction

Complex decisions of cell fate occur in response to genomic stress, mutation, nutrient deprivation, and hypoxia. In response to extensive or irreparable stress, cells maintain the ability to commit suicide through a process of programmed cell death called intrinsic apoptosis. Deciding whether cellular aberrations represent a significant impedance to the integrity of the cell requires a delicate balance between cell survival and cell death. At the heart of the decision to initiate intrinsic apoptosis lies the B-cell lymphoma 2 (Bcl-2) family of pro- and anti-apoptotic proteins[1]. Bcl-2 family members take part in a complex

interaction network that regulates the integrity of the outer mitochondrial membrane. Ultimately, the Bcl-2 family is the gate-keeper for cell survival[1].

Members of the Bcl-2 family are sub-divided into three classes based on their role in apoptotic regulation: the anti-apoptotic proteins, the pore-forming effector proteins, and the proapoptotic Bcl-2 homology 3 (BH3) only proteins. Despite these three classes, all Bcl-2 family members share a core amphipathic alpha-helical BH3-motif that mediates binding between family members of opposing roles[2]. The anti-apoptotic members (BCL2, BCLxL, MCL1, BCLW, and BFL1/A1) have a conserved tertiary fold that forms a hydrophobic binding groove. This groove mediates interactions with the BH3 motif that is accessible in the pro-apoptotic members[3]. When the anti-apoptotic members bind and sequester the pro-apoptotic proteins through this canonical BH3mediated protein-protein interaction, the cell is void of apoptotic signaling. In response to intrinsic stress, the cell transiently upregulates expression or stabilization of the proapoptotic Bcl-2 proteins, while concomitantly downregulating the expression of antiapoptotic members[4]. When pro-apoptotic expression surpasses that of the anti-apoptotic proteins, this allows the pore-forming effectors, BAK and BAX, to be released and induces their oligomerization. Effector oligomerization creates pores in the outer mitochondrial membrane (*i.e*. MOMP), which leads to release of cytochrome c into the cytosol, caspase activation, and apoptotic body formation[1,2,4].

Over the past fifteen years, targeting the anti-apoptotic Bcl-2 family members with small molecule BH3 mimetics has emerged as an anti-cancer therapeutic strategy to sensitize cells to intrinsic stress[5-7]. However, small molecules which were initially designed to target BCLW, BCLxL, and/or BCL2 have shown an acquired resistance due to the

upregulation of MCL1[8,9]. In addition, more recent studies have directly highlighted MCL1 amplification as a common driver of tumorigenesis[10]. We therefore searched for novel binding sequences to strategically inhibit MCL1 using phage display. Through this screen, we identified two novel sequences that specifically bind MCL1 over the other anti-apoptotic Bcl-2 family members. These sequences are a reversal of the homologous organization of hydrophobic and acidic amino acid residues within the canonical BH3 sequence (Table 1)[11]. Therefore, we refer to these sequences as having a reverse-BH3 or rBH3 motif. Using BLAST sequence analysis of the human proteome, we identified a series of native proteins that contain rBH3-like sequences, thereby establishing a pool of potential novel MCL1 binding partners[11,12].

Table 1. Sequence comparison between canonical and non-canonical BH3 motif and the putative reverse BH3 (rBH3) motif.

	H1 H2 H3 H4
BH3 Motif	XΦXXXLXXΦGDXΦ
BAK_{BH3}	VVGRQLAIIGDDINR
$NOXA_{BH3}$	ECATQLRRFGDKLNF
rBH3-1	HLYAQMLEVTEN-$_{NH2}$
rBH3-2	YYYTLMTNVTEN-$_{NH2}$
$p73_{rBH3}$	QPVLEMLELSEKL-$_{NH2}$

One of the rBH3-containing proteins identified is p73, a transcription factor in the p53 family of tumor suppressors[11,13]. Like p53, p73 plays a role in DNA damage response, cell cycle progression, and apoptosis through transcriptional activation of target gene expression[14,15]. In p53-mutant cells, which is the case for >50% of human cancers, p73 has been suggested to play a critical role in executing these tumor suppressive functions[14,16,17]. Structurally, p73 has four core domains: a transactivation domain (TAD), a DNA binding domain (DBD), a tetramerization domain (TD), and a sterile alpha motif

(SAM)[15]. While there is sequence conservation between p53 and p73 among their TAD, DBD, and TD domains, p73 has a higher level of complexity due to its alternative promoter usage and C-terminal alternative splicing[17]. Importantly, p73 has two promoters that generate functionally distinct N-terminal isoforms from a single gene[18]. The fulllength isoform from the P1 promotor contains a complete transactivation domain (TAp73) and functions similarly to p53, while transcription initiating at the P2 promoter, located in intron 3, gives rise to a truncated protein with 13 unique amino acids on its Nterminus (ΔNp73)[19]. ΔNp73 acts as a dominant negative regulator over TAp73, thus the two N-terminal p73 isoforms perform opposing roles in the cell[20,21]. Furthermore, both the full length TAp73 and the truncated ΔNp73 isoforms can be alternatively spliced at their C-termini (ΔN/TAp73α, β, δ, ε, φ, γ, η), generating up to seven C-terminal isoforms per N-terminal variant. There are two additional alternatively spliced N-terminal isoforms, ΔEx2-p73 and ΔEx2/3-p73, generating up to 28 hypothetical p73 variants in total[19], many of which are currently of unknown significance[22]. All of these p73 isoforms retain their DNA binding domain and the tetramerization domain, suggesting that they all maintain the ability to bind DNA and associate with one another[19,22].

While MCL1 and p73 are both known regulators of cell fate, these two proteins have never been shown to bind through a direct protein-protein interaction. Here, we confirm the direct interaction between the rBH3-containing tetramerization domain of p73 and the hydrophobic BH3 binding pocket of MCL1. Further, we demonstrate that the interaction between MCL1 and p73 inhibits p73 binding to DNA, thereby acting as a novel p73 transcriptional suppressor. This work develops a unique mechanism for the cross-communication between the Bcl-2 family-mediated regulation of intrinsic apoptosis and the p73 tumor suppressive transcriptional program.

Results

p73 Contains a Putative rBH3-Motif in the Tetramerization Domain (TD)

Based on our previously published phage display screen that identified the putative reverse BH3 (rBH3) motif and its specific association with MCL1[11], we sought to determine if rBH3 sequences found in native proteins are able to mediate direct interactions with the Bcl-2 family. BLAST analysis of the human proteome for rBH3-1 homologous sequences identified a putative rBH3 motif in the tetramerization domain (TD) of p73[11] (Table 1). Consistent with the rBH3-1 and rBH3-2 sequences identified in the phage display, the p73 rBH3 sequence contains three of the four conserved hydrophobic amino acids found in the homologous BH3 motif (H2, H3, and H4 listed in **Table 1**). These hydrophobic residues in the canonical BH3 motif mediate binding to the p2, p3, and p4 hydrophobic pockets previously described in the MCL1 BH3 groove[5,23]. This includes the placement of a conserved methionine at the hydrophobic position H2 which was observed to be integral in maintaining MCL1 affinity. In addition, the rBH3 sequence in p73 employs a homologous substitution for the conserved aspartic acid residue between H3 and H4, which is a persistent substitution observed in the other rBH3 sequences (i.e. aspartic acid in the BH3 versus glutamic acid in the rBH3)[11] (Table 1).

All Native p73 Isoforms Can Interact with MCL1

Based on the observation that p73 contains an rBH3 sequence, we sought to determine if MCL1 and p73 interact in a cell culture model system. To assess this, we cotransfected HEK-293T cells with plasmids that express MCL1 and FLAG-tagged TAp73α (Figure 1a). Following co-transfection, MCL1 and p73 proteins were coimmunoprecipated (Co-IP) in the resulting HEK293T lysates through pulldown of either MCL1 or the FLAG-tag attached to the p73 protein. Protein immunoprecipitation (IP) was

analyzed through western blot analysis. We observed that IP of either MCL1 or the FLAG-TAp73α resulted in pull-down of the partnered protein. As a negative control, a transfection containing the FLAG tag alone did not Co-IP MCL1 protein.

We then assessed the ability of two additional native p73 isoforms to IP with MCL1 (ΔNp73α and TAp73β) (Figure 1b). As these isoforms lack either the transactivation domain (ΔNp73α) or the sterile alpha motif (TAp73β) (Figure 1b)[22], they aid in defining the p73 domain responsible for binding to MCL1. We observed that both ΔNp73α and TAp73β Co-IP with the pulldown of MCL1 protein (Figure 1c). These studies demonstrate that MCL1 interacts with p73 in cell lysates. In addition, they demonstrate the ability for all three native p73 isoforms to bind to MCL1 thereby reducing the binding of p73 to its DNA binding domain (DBD) and/or the rBH3containing tetramerization domain (TD) in HEK-293T cells. As the DBD and the TD are conserved amongst all p73 isoforms, this would suggest that MCL1 can bind to all native p73 protein variants[19].

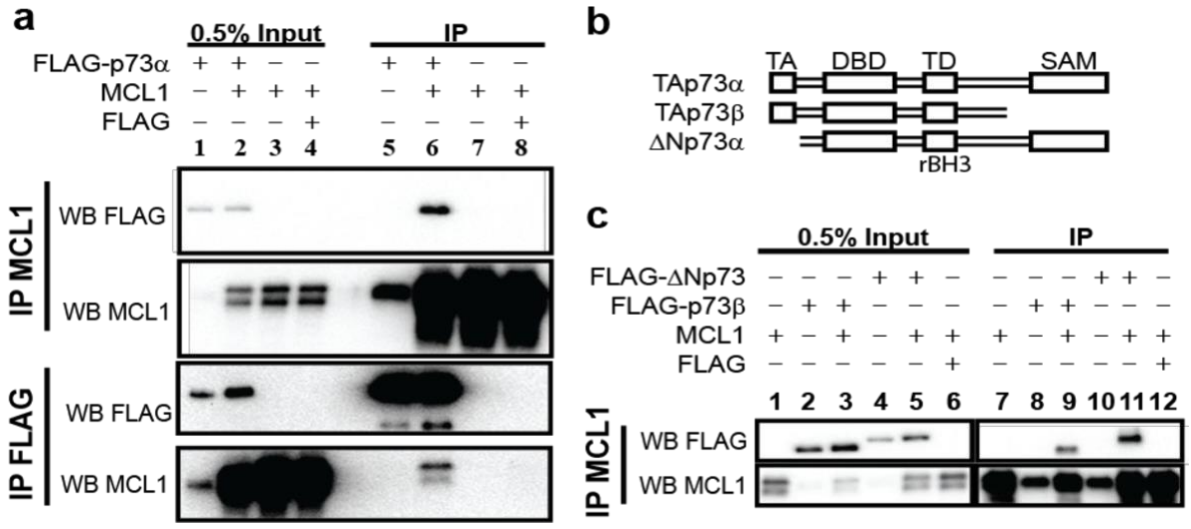

Figure 1. MCL1 interacts with native p73 isoforms. a MCL1 and either FLAGTAp73α or a FLAG control were transiently overexpressed in HEK293T cells. Reciprocal co-immunoprecipitations were performed with either anti-MCL1 captured by Protein G dynabeads or with pre-conjugated anti-FLAG magnetic beads. Western blot analysis was used to confirm protein overexpression and reciprocal pulldown of full length p73 or MCL1 protein. **b** Visual representation of the domain structure of the native p73 constructs. **c** MCL1 and either FLAG-ΔNp73, FLAG-p73β, or a FLAG control were transiently overexpressed in HEK293T cells. MCL1 was immunoprecipitated and western blots were analyzed for either the FLAG tag or MCL1. Only lanes expressing FLAG-p73β and FLAG-ΔNp73 co-immunoprecipitated with MCL1.

The rBH3-Containing TD of p73 Mediates Binding to MCL1

We next sought to determine which core domain, the DBD or the TD, of p73 mediates binding to MCL1. We were unable to express either of these protein domains independently in cell culture models due to protein stability and therefore moved to *in vitro* biochemical methods to characterize the protein-protein interaction. Prior studies have demonstrated that the DBD of p53 is able to directly interact with another antiapoptotic protein, BCL2[24]. Therefore, we expressed and purified recombinant $p73_{DBD}$ and tested its ability to associate with MCL1 using competitive fluorescence polarization assay (FPA) analysis and NMR chemical shift perturbation studies (Figure 2a, Supplemental Figure 1). FPA is a biochemical assay that can either determine the binding constant between a recombinant protein and a fluorescently labeled small molecule or peptide (i.e. direct FPA as a measure of K_D) or it can determine the concentration in which an unknown binding partner can compete with bound fluorescently labeled ligand (competitive FPA as a measure of IC_{50}). Neither NMR nor competitive FPA analysis exhibited significant changes that would indicate that the $p73_{DBD}$ associates with MCL1. Consequently, we focused our subsequent studies on the rBH3-containing $p73_{TD}$.

To study the $p73_{TD}$, we synthesized a corresponding 23 amino acid peptide ($p73_{23mer}$) that parallels the homologous BH3 peptides used for other Bcl-2 family binding studies[12,25,26] (Table 2). Through an N-terminally labeled FITC-$p73_{23mer}$ peptide, we determined that p73 binds MCL1 with a K_D that is $\leq$ 5nM (limit of detection for our probe) (Figure 2b). This is comparable to the K_D of the BH3 peptide derived from BAK that has previously been used as a standard model for anti-apoptotic Bcl-2 family binding studies[26] (Figure 2b). Although the exact binding constant could not be determined, a direct FPA K_D of $\leq$ 5nM indicates that these are both high affinity binding proteins.

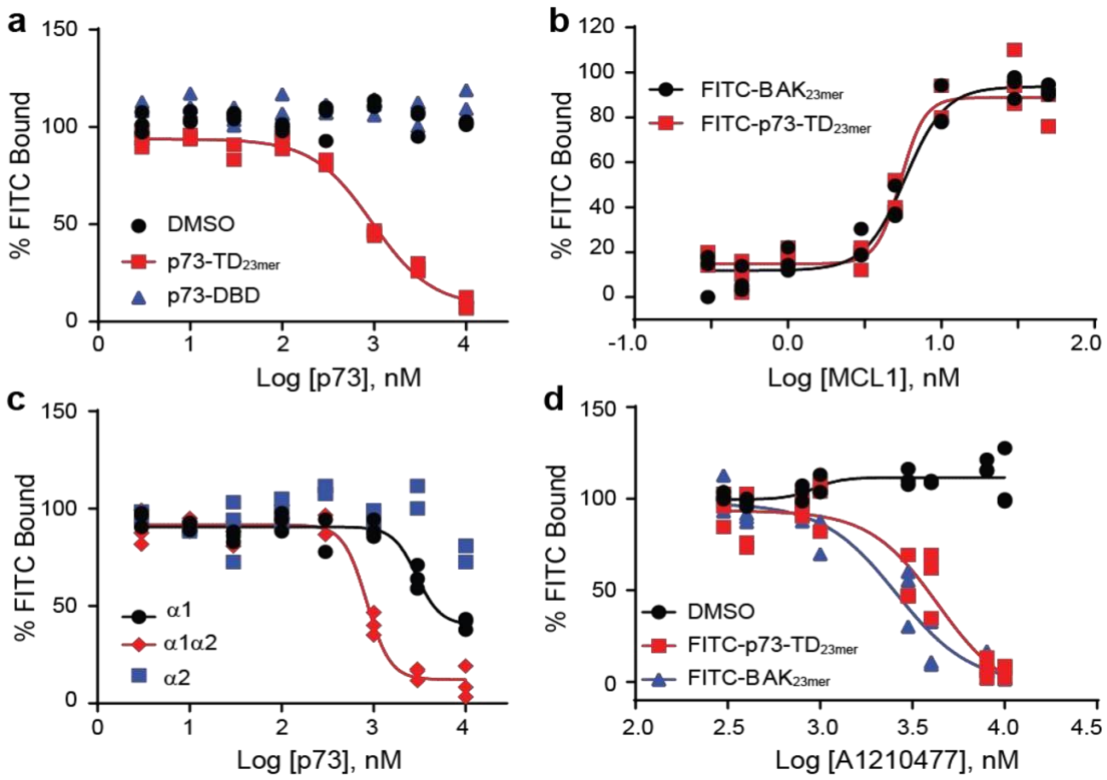

Figure 2. The p73TD α1 helix contains the rBH3 sequence that mediates binding to MCL1. a and **c** Competitive FPA consisting of 50 nM recombinant MCL1, 10 nM FBAK, and an unlabeled titration of the p73TD derived peptides. **a** The p7323mer (red) is representative of the TD versus the full length p73 DBD (blue). A constant concentration of DMSO is used as a negative control (black). **b** Direct FPA with two N-terminally labeled FITC peptides, the known MCL1 binding partner BAK (black) and p73TD derived peptide p7323mer (red). The KD value for both peptides is ≤ 5 nM, which is at or approaching the limit of detection. **c** Competitor peptides include examples of the secondary structural components α1 (black), α2 (blue), or a combinatory peptide, α1α2 (red). **d** Competitive FPA consisting of 50 nM recombinant MCL1, 10 nM F-p7323mer
(red) or 10 nM F-BAK (blue), and a titration of MCL1-specific inhibitor A1210477. A DMSO vehicle control is labeled in black. The plot shown is one representative assay in technical triplicate. The IC50s for F-p73 and F-BAK were 4.336 μM and 2.590 μM respectively. All FPAs were performed in biological and technical triplicate. Each plot shows the three data points from one representative assay. All statistical analysis with the standard deviation for each peptide is listed in Table 2.

Supplemental Figure 1. The p73 DNA binding domain does not bind to MCL1. a ^{15}N

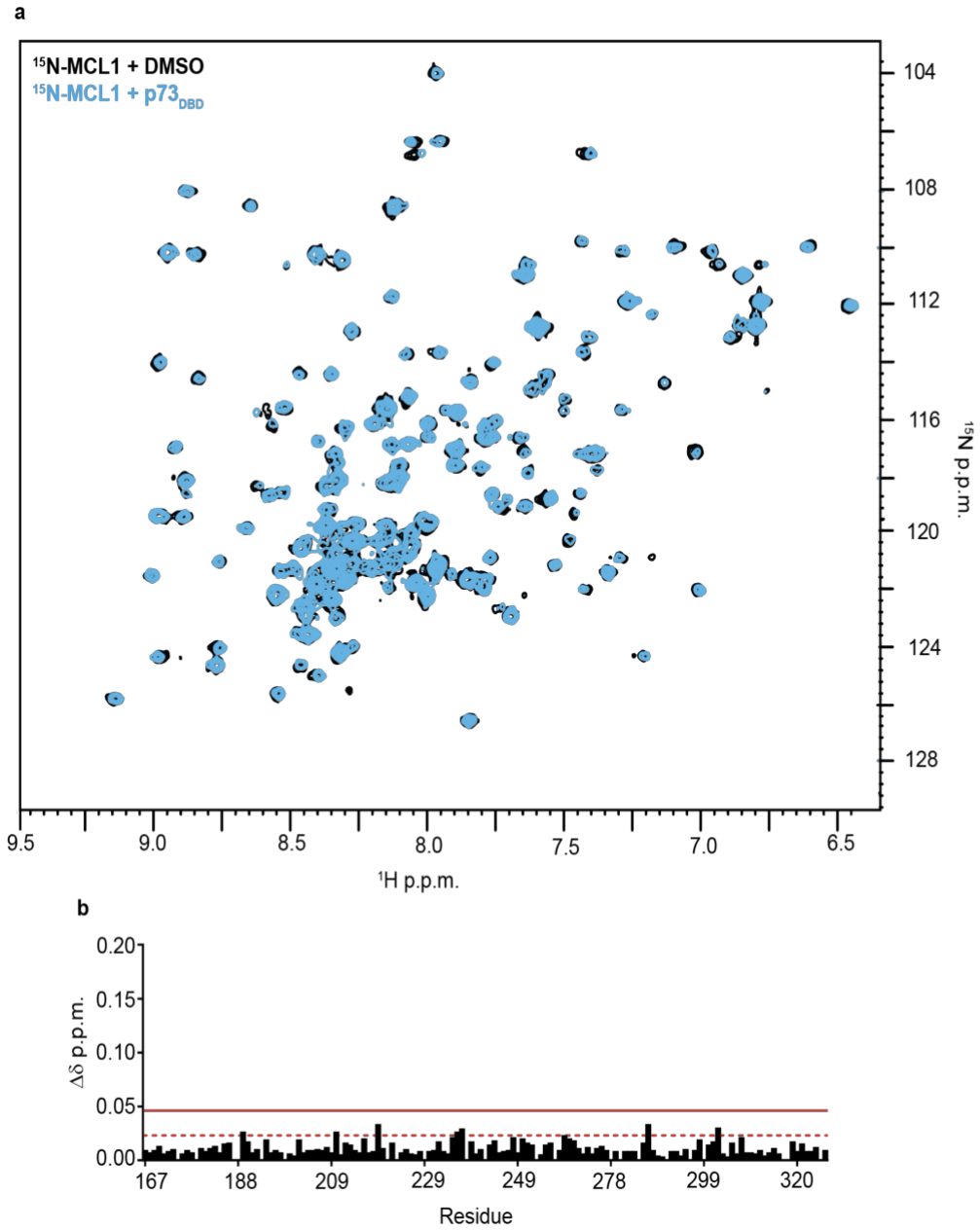

HSQC spectra with 50 µM ^{15}N MCL1 + 2% DMSO (black) superimposed with 50 µM ^{15}N MCL1 + 200 µM p73DBD (blue) **b** CSP quantified as a function of δΔ p.p.m. for each amino acid residue. The two cut offs represent the 1 and 2 SD cut offs determined through the 50 µM 15N hMCL1 + 200 µM p7323mer spectra in Figure 2. No amino acids in this spectra exhibited significant shifts designated by the 2 SD from the mean cut-off.

The full length $p73_{TD}$ is composed of three secondary structural units (β1, α1, α2)[27]. To determine the key components of the $p73_{TD}$ that mediates its interaction with MCL1, we prepared a series of $p73_{TD}$-derived peptides. These peptides encompass the structural components of the single $p73_{TD}$ monomer (β1, α1, α2) or combinations thereof (β1α1, α1α2)[27] (Table 2). Using a competitive fluorescence polarization assay (FPA), we tested each peptides' binding to MCL1 in competition with a 23 amino acid peptide derived from the known binding partner, BAK (FITC-AHX-BAK or F-BAK)[28]. The IC_{50} of the $p73_{23mer}$ binding to MCL1 in competition with F-BAK is 0.982 μM. Similarly, all of the α1, rBH3-containing peptides including α1, β1α1, and α1α2 exhibited comparable competition with F-BAK to the $p73_{23mer}$ (Table 2). As demonstrated in Figure 2c, the complete binding of the α1-peptide alone is not fully achieved in the absence of other structural components of the p73 tetramerization domain. The β1 and α2 subunits likely facilitate helicity of the α1 helix, which is consistent with the FPA results obtained with the monomer subunits versus the combinatory β1α1 or α1α2 peptides. More importantly, the peptides that did not contain the putative rBH3 sequence, β1 and α2, had no detectable binding to MCL1 (IC_{50} >10 μM). All of the IC_{50}s determined through the competitive FPA for the p73 structural subunits are summarized in Table 2, along with the corresponding peptide sequences.

Through the p73 peptide competitive FPA analysis, we concluded that the rBH3containing α1 helix mediates the protein-protein interaction between the $p73_{TD}$ and MCL1. To determine if this interaction could be inhibited with an MCL1 inhibitor, we performed a competitive FPA between MCL1 and FITC-$p73_{23mer}$ using the MCL1-specific inhibitor A1210477 (Figure 2d). Using this inhibitor, we were able to inhibit the MCL1-p73 interaction with an IC_{50} of 4.37 μM. These values are comparable to the competition between MCL1 and F-BAK, which has an IC50 of 2.59 μM in our system

(Figure 2d). Together, these studies demonstrate that the $p73_{TD}$ binds with a biologically relevant strength to MCL1 and is comparable to known binders like the BH3-only protein BIM and the pore-forming effector BAK[26]. Additionally, the interaction between MCL1 and p73 can be inhibited using MCL1 specific inhibitors, which are now in Phase 1 clinical trials.

Table 2. Fluorescence polarization assay results with $p73_{TD}$-derived peptides reduce MCL1 binding to the rBH3-containing α1 helix of p73 (highlighted in red).

	Peptide sequence	FPA IC_{50} (μM)
$p73_{TD}$	351 DEDTYYLQVR GRENFEILMK LKESLELMEL VPQPLVDSYR QQQQLLQR 398 ----β1---- ----------α1--------- ---------α2---------	
$p73_{23mer}$	351 GRENFEILMK LKESLELMEL VPQ 398	0.982 ± 0.195
β1	351 DEDTYYLQVR 360	ND (>10 μM)
β1α1	351 DEDTYYLQVR GRENFEILMK LKESLELMEL 380	1.091 ± 0.159
α1	361 GRENFEILMK LKESLELMEL 380	2.633 ± 0.659
α1α2	361 GRENFEILMK LKESLELMEL VPQPLVDSYR QQQQLLQR 398	0.882 ± 0.054
α2	381 VPQPLVDSYR QQQQLLQR 398	ND (>10 μM)

p73 Binds into the Canonical BH3 Binding Pocket of MCL1

Interactions between pro-apoptotic BH3-containing proteins and MCL1 occur through a hydrophobic BH3 binding groove formed by BH motifs 1-3 of MCL1[26,29]. As the rBH3 motif in the $p73_{TD}$ is the reverse of the canonical BH3 sequence, we hypothesized that p73 similarly binds to MCL1's BH3 binding pocket. To localize p73 binding to MCL1, we mapped the chemical shift perturbation of 2D [^{1}H, ^{15}N]-HSQC spectra of ^{15}N-labeled MCL1 following the addition of unlabeled $p73_{23mer}$ peptide. We observed that addition of the peptide induced significant chemical shift perturbation primarily localized to the BH3 binding groove of MCL1, corresponding to the three hydrophobic pockets that mediate

BH3 binding (homologous rBH3 residues H2, H3, and H4 in Table 1) – p2, p3, and p4. Amongst these, amino acids required for hydrophobic interactions, including the L267 of the p2 pocket, F228 of the p3 pocket, and the V265 of

the p4 pocket, were all significantly perturbed[30,31]. There were also several amino acids in which the corresponding peaks had line broadening beyond detection (red in Figure 3b and 3c). Amongst these, R263 is the most significant as it mediates a critical stabilizing salt bridge with the conserved acidic amino acid within the BH3 or rBH3 helices[31] (Table 1). Additionally, V243 of the p2 pocket and V216 and V220 of the p4 pocket could no longer be detected[31]. Of note, R263 and the hydrophobic pockets p2 and p3, are core interaction sites for the emerging MCL1-specific BH3 mimetics[30,32].

In addition to perturbations in the BH3 pocket, we also observed a cluster of residues that were impacted at the base of MCL1. This region corresponds with a loop that follows alpha helix 5 (α5) that lies in the core of the MCL1 fold and is oriented perpendicular to the BH3 binding groove. This helix has a series of residues that help form the back of the BH3 binding groove. We and others have observed that when peptides and small molecules bind to the BH3 pocket, residues on this helix are impacted and that often, the perturbation of this helix extends beyond the residues that make direct contact with the ligand[33]. Thus, binding to the BH3 groove also induces allosteric perturbation to the MCL1 structure through this central alpha helix.

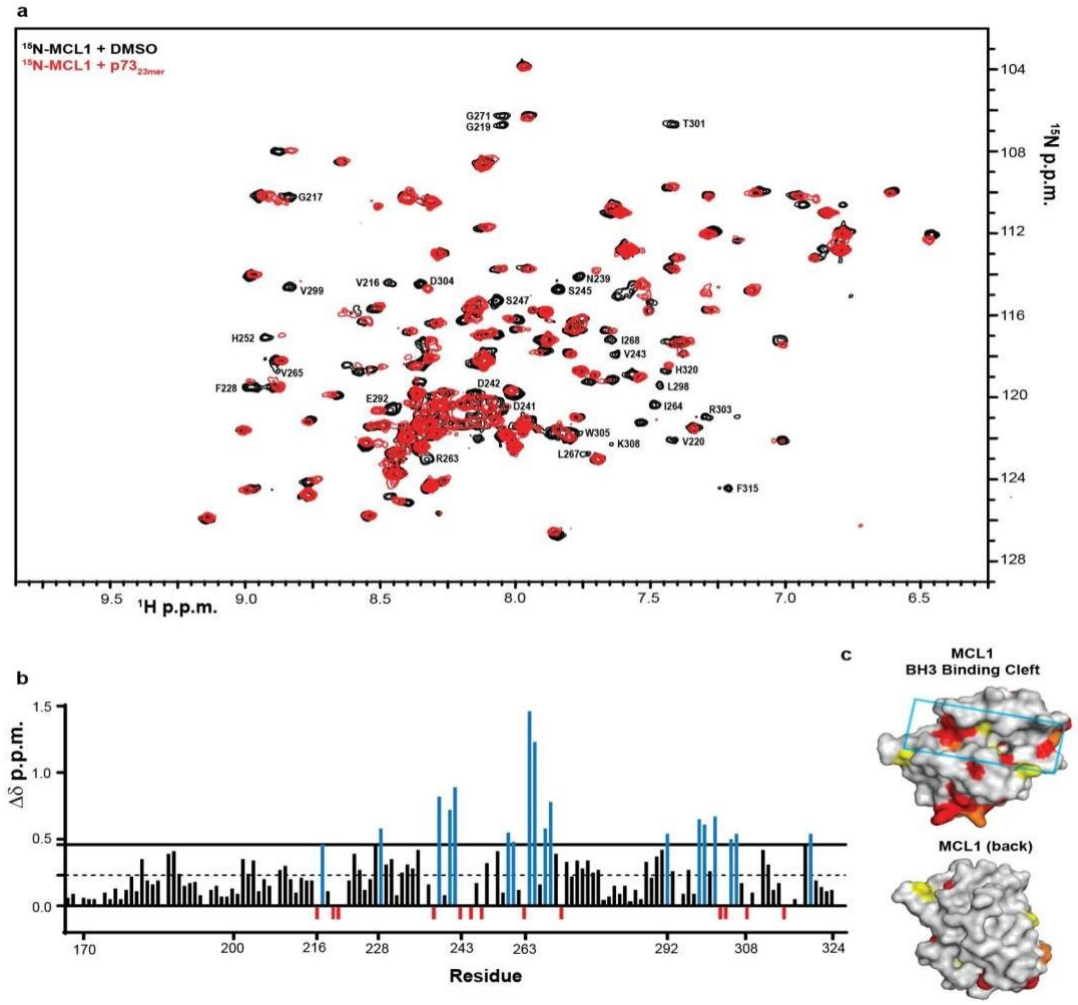

Figure 3. p73 binds to the BH3 binding groove of MCL1. a 2D [^{15}N, ^{1}H]-HSQC spectra of 50 µM 15N MCL1 + 2% DMSO (black contours) or 50 µM 15N MCL1 + 200 µM p73$_{23mer}$ TD-derived peptide (red contours). Amino acids with significant CSP (Δδ >0.046 p.p.m.: G217, F228, N239, D241, D242, H252, I264, V265, L267, I268, E292, L298, V299, T301, D304, and H320) or residues that were unable to be identified in the bound spectra (V216, G219, V220, V243, S435, S247, R263, G271, R303, K308, and F315) are labeled for reference. **b** CSP quantified as a function of Δδ ppm for each amino acid residue. The first dotted line indicates 1 SD from the mean (0.023) and the solid line indicates 2 SD from the mean (0.046). Amino acids with significant CSP were identified as >2 SD above the mean (blue). Amino acids that were unable to be identified in the bound spectra were set to -0.01 to differentiate them from peaks with no CSP (red). All colored amino acid peak positions are labeled in **a**. The numerical labels are used as a reference to identify significant peaks. Amino acids that were unable to be identified in the apo-MCL1 protein were not plotted as a function of Δδ ppm (residues 171, 254-261, 269, 289, 306). **c** Space filling diagram of MCL1 with the significant CSP colored as follows: Δδ ppm 0.046 – 0.060 (yellow), Δδ ppm 0.061 – 0.146 (orange), unable to be identified in the p73$_{23mer}$ spectra (red). A cluster of significant CSP is localized in or around the BH3 binding groove, which is highlighted with the cyan box (top). A 180° rotation of MCL1 shows limited CSP impact on the reverse of the protein (bottom).

Taken together, the biochemical data provided thus far demonstrate that MCL1 and p73 interact through a direct protein-protein interaction. This novel interaction is driven by the rBH3 motif located in the α1 helix of the $p73_{TD}$. The $p73_{TD}$ binds to the conserved BH3 binding groove of MCL1 which mediates interactions between MCL1 and the pro-apoptotic BH3-containing Bcl2 family members[1,26,29]. Additionally, small molecule inhibitors that target MCL1 mimic the BH3-mediated interactions and would therefore target rBH3-mediated interactions such as the identified interaction with p73 herein described[34,35].

MCL1 and Endogenous p73 Exclusively Co-Localize in the Nucleus

Once we confirmed the direct interaction between MCL1 and p73 in cells and through various biochemical assays, we sought to determine the biological implication of this novel interaction. Canonically, the two proteins are localized in different cellular compartments with MCL1's primary function as an anti-apoptotic member of the Bcl-2 family, positioning it outside the nucleus in the cytosol and often anchored into the outer mitochondrial membrane[1]. Yet, prior studies have observed nuclear MCL1 and proposed that it functions to regulate cell cycle progression and mediate DNA damage response through interactions with a number of nuclear proteins including IEX-1[36] and PCNA[37]. Unlike p73, these nuclear binding partners do not contain putative rBH3 motifs and the binding sites exist in regions outside the canonical BH3-binding pocket. Likewise, while p73's function as a transcription factor positions it predominantly in the nucleus, there have been a few studies identifying cytosolic functions of p73 and p73 fragments[38,39]. We therefore started by fractionating two cell lines into cytosolic and nuclear fractions to identify the cellular localization of our two proteins of interest in our model systems. For the remaining *in vitro* cell studies, we chose the $p53^{-/-}$ cell lines, PC-3 and H1299, to

separate p73 activity from the overlapping functions with its homolog, p53[40-42]. Through the fractionation studies, MCL1 was identified primarily in the cytosolic fraction, but nuclear MCL1 accounted for 26% and 13% of the total MCL1 protein population in PC-3 and H1299 cells, respectively (Figure 4). We observed no evidence of cytosolic fulllength p73 at endogenous levels or following low dose cisplatin treatment, which we utilize as a chemical agent to upregulate the p73 transcriptional activation in subsequent experiments (Figure 4, Supplemental Figure 2). Interestingly, we observed that treatment with cisplatin did increase MCL1 levels in both the cytoplasmic and nuclear compartments. These studies strongly suggest that the interaction between MCL1 and p73 occurs in the nucleus.

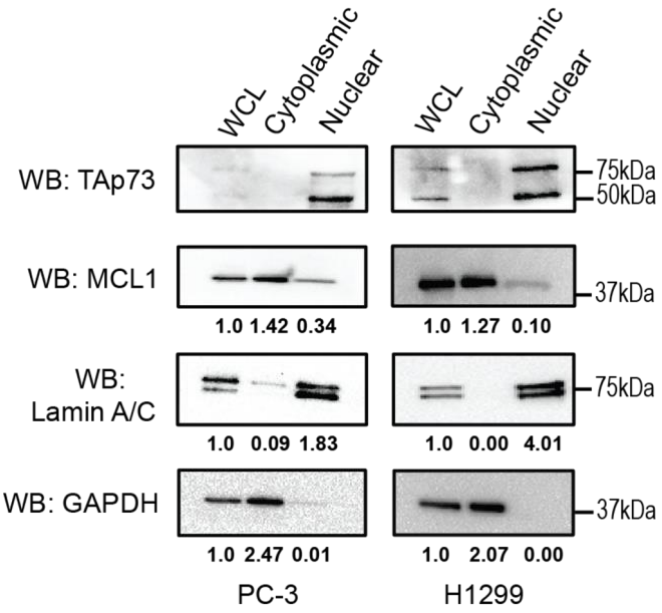

Figure 4. Endogenous MCL1 and full length p73 exclusively co-localize in the nucleus. Cellular fractionation of untreated PC-3 and H1299 cells into cytoplasmic and nuclear fractions. Western blot analysis was performed to determine the endogenous protein localization. GAPDH was used for a cytoplasmic control and Lamin A/C was used for a nuclear control for fractionation. The quantification provided is normalized to the whole cell lysate (WCL). Experiments were completed in biological triplicate with representative western blots shown.

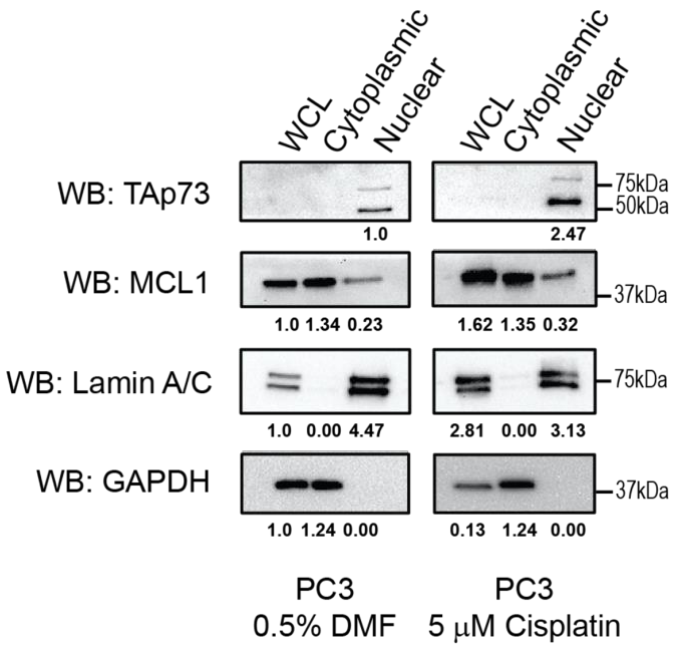

Supplemental Figure 2. p73 is exclusively localized to the nuclear compartment following low dose Cisplatin treatment. PC-3 cells were treated with 5 mM Cisplatin or the respective vehicle control, 0.5% DMF, for 24 hours. Cells were fractionated in cytosolic and nuclear compartments. Protein localization was analyzed through Western Blot analysis. Lamin A/C and GAPDH were used for fractionation controls. Band quantifications using the adjusted volume for each individual band are below for reference. All paired samples are normalized to the WCL treated with DMF alone.

MCL1 Negatively Impacts p73 DNA Binding

Prior studies have suggested that the $p73_{TD}$ increases the association of p73 with target DNA sequences[43]. To activate target genes, p73 forms a tetramer on specific DNA response elements[44]. The location of the rBH3 is at the center of the tetrameric assembly within the TD[27]. This suggests that MCL1 binding should inhibit p73 tetramer formation and sequester p73 in a monomeric or dimeric state. It should be noted that p73 dimerization can be induced through an interaction within the DNA binding domain and therefore, we do not anticipate that this interaction would inhibit all oligomeric states of p73[45]. Further, we observe that MCL1 and p73

exclusively co-localize in the nucleus (Figure 4), thus we hypothesized that MCL1 binding to p73 should decrease affinity to target DNA sequences. Prior studies have implied that tetramer formation of p73 should increase the affinity for DNA[43]. We validated this phenomenon using recombinant p73 proteins in FPA binding assays with two canonical FITC-labeled response elements, FITC-NOXA (F-NOXA) and FITC-GADD45 (F-GADD45)[46,47] (Figure 5a).

To characterize the impact that MCL1 has on p73 DNA binding due to its interaction with the $p73_{TD}$, we utilized an *in vitro* DNA Electrophoretic Mobility Shift Assay (EMSA). For these studies, we used a FITC-labeled consensus response element from GADD45 (F-GADD45)[46]. To visualize the p73 DNA binding, we purified two recombinant p73 protein constructs: one that contains the DBD alone ($p73_{DBD}$, amino acids 112-311) and another which contains both the DBD and TD that includes the rBH3 motif ($p73_{DBD-TD}$, amino acids 112-398). In Figure 5c, we observed that MCL1 does not impact the migration of either the free F-GADD45 DNA (lane 3) or binding of FGADD45 DNA by $p73_{DBD}$ (lanes 5-9). Conversely, the titration of recombinant MCL1 into a solution containing $p73_{DBD-TD}$ and F-GADD45 DNA reduces p73 DNA binding by 27% (Figure 5b and d). This data demonstrates that MCL1 binding to p73 can negatively impact p73 binding to canonical DNA response elements in a $p73_{TD}$-dependent manner. It also suggests that the binding of MCL1 to the $p73_{TD}$ inhibits the higher order oligomeric states that enhance high affinity DNA binding resulting in activation of target genes.

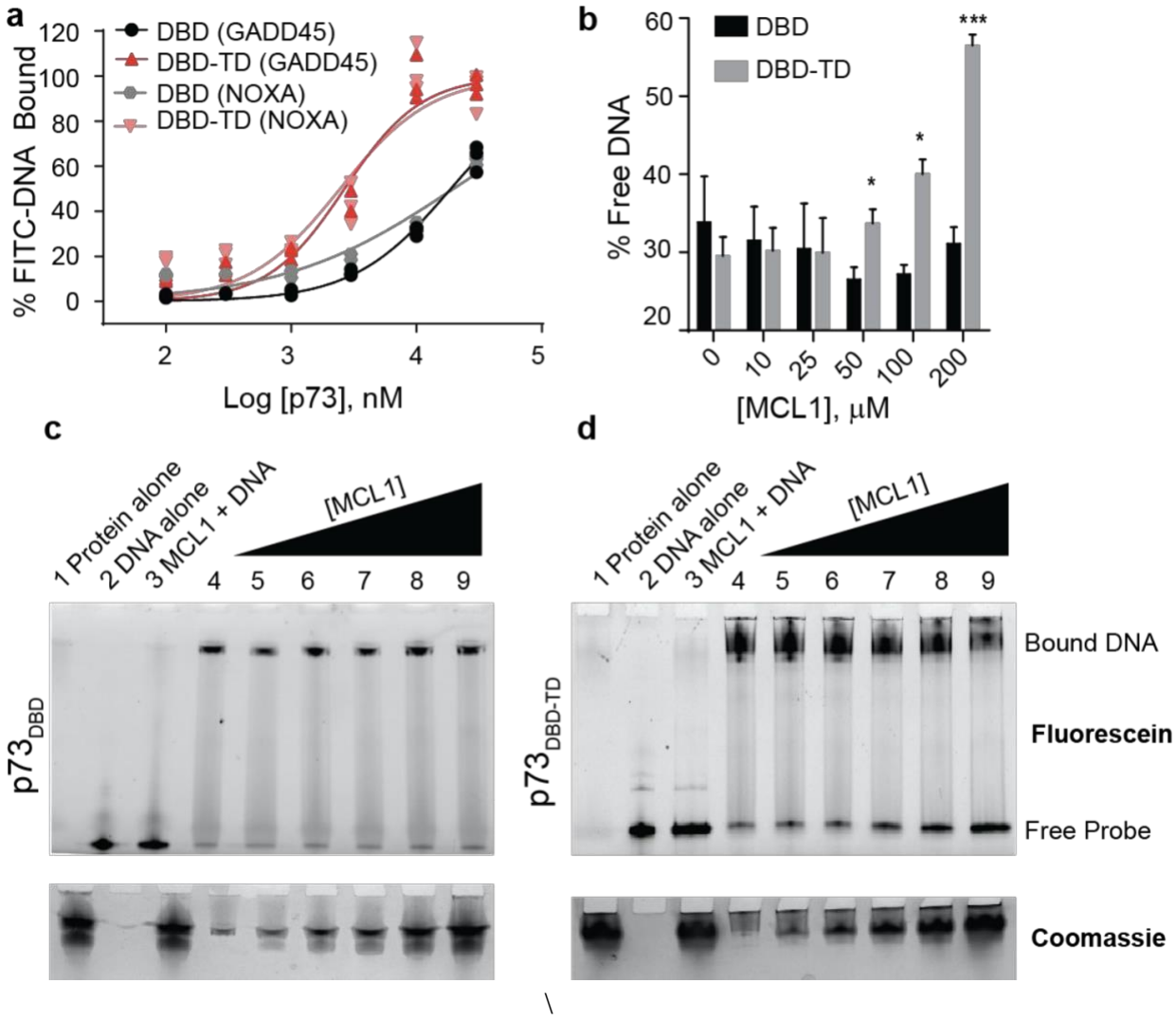

Figure 5. MCL1 negatively impacts p73 DNA binding in a p73TD-dependent manner. **a** Direct FPA between p73 (either $p73_{DBD}$ alone or $p73_{DBD\text{-}TD}$) and FITC-labeled DNA response elements (i.e. FITC-GADD45 or FITC-NOXA). All FPAs were performed in biological and technical triplicate. Each plot shows the three data points from one representative assay. **b** Quantification of the EMSA using $p73_{DBD}$ or $p73_{DBD\text{-}TD}$ with an increasing concentration of recombinant MCL1. The amount of unbound DNA was quantified through intensity values calculated by the free probe. An unpaired t-test was used for each concentration of MCL1 (DBD vs. DBD-TD), N = 3. Error is the SEM. p-value for 50 μM = 0.043, 100 μM = 0.0153, 200 μM = 0.0005. **c** and **d** Representative EMSAs on native TGX gels visualizing FITC-GADD45 DNA (F-DNA). **c** is the $p73_{DBD}$ alone whereas **d** is the $p73_{DBD\text{-}TD}$. Coomassie staining is used to visualize the protein with increasing amounts of MCL1 added into the reaction. Lanes for both gels are as follows: (1) 200 μM MCL1 alone (No F-DNA), (2) F-DNA alone (no protein), (3) 200 μM MCL1 + F-DNA, (4) 10 μM p73 protein with 1 μM F-DNA, (5–9) 10 μM p73 with F-DNA + increasing concentration of MCL1 (10–200 μM).

MCL1 is a Novel p73 Transcriptional Suppressor

To determine if the MCL1-p73 interaction has an impact on the transcriptional activation of p73 target genes, we used TaqMan RT-qPCR to look at the cellular response of four known p73 target genes – p21, NOXA, GADD45, and PUMA[48-50]. For these studies, we utilized the $p53^{-/-}$ cell lines PC-3 and H1299 to study gene expression following modulation of p73 and MCL1 protein expression. Prior studies have identified that p73 protein and/or target genes are upregulated in response to cisplatin treatment. We found that we could mimic this upregulation of p73 protein levels and/or resulting upregulation of p73 target gene activation using a sublethal dose of cisplatin in each cell line for 24 hours. We confirmed that this dose of cisplatin did not induce apoptosis during this time frame using Annexin V/PI flow cytometry where we observed no change in the Annexin V/PI +/- cell population that is associated with apoptotic cells (Supplemental Figure 3). Using this sub-lethal cisplatin treatment, we were able to generate a baseline for changes in the p73 target gene expression relative to an increase in activation of the native isoforms of p73 protein[51] (Figure 6). In both cell lines, we observed statistically significant increases in expression in at least three of the four p73 target genes (Figure 6a, Supplemental Figure 4). It should be noted that while both cell lines are $p53^{-/-}$, the ratio and dependence of TAp73α versus TAp73β varies between the two cell lines. For example, as H1299 cells are predominantly driven by TAp73α expression and the PUMA target gene is more potently activated through TAp73β, it is unsurprising that PUMA is not significantly upregulated following sub-lethal cisplatin treatment in H1299 cells[52] (Figure 6a).

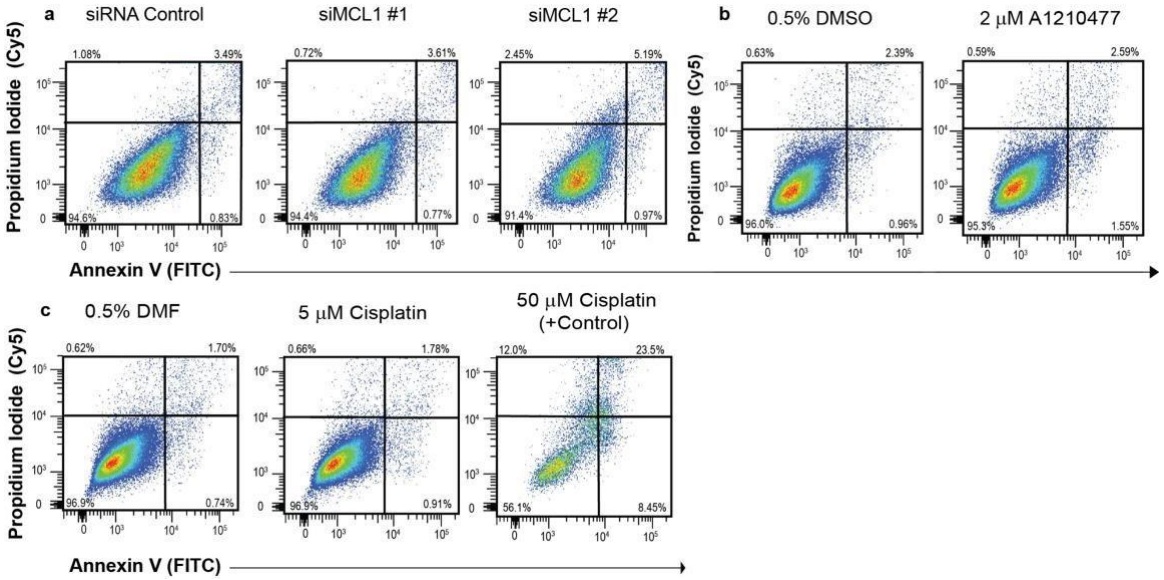

Supplemental Figure 3. Modulation of MCL1 or TAp73 does not induce apoptosis. a PC-3 cells are treated with two siRNAs targeting MCL1 or an siRNA control for 48 hours. Cells were stained with Annexin V and Propidium Iodide (PI) to determine the apoptotic cell population. There is no significant increase in apoptosis with the knockdown of MCL1 over the siRNA control. **b** PC-3 cells are treated with MCL1 specific BH3 mimetic 2 μM A1210477 or the respective chemical control, 0.5% DMSO, for 24 hours. There is no increase in apoptotic induction similarly to the RNAi knockdown approach. **c** PC-3 cells are treated with 5 μM Cisplatin or the respective chemical control, 0.5% DMF, to intrinsically induce the endogenous p73 protein expression for 24 hours. As a positive control for the Annexin V/PI staining, cells treated with 50 μM Cisplatin showed a significant increase in apoptosis. All plots shown here are representative plots of the data set, N=4.

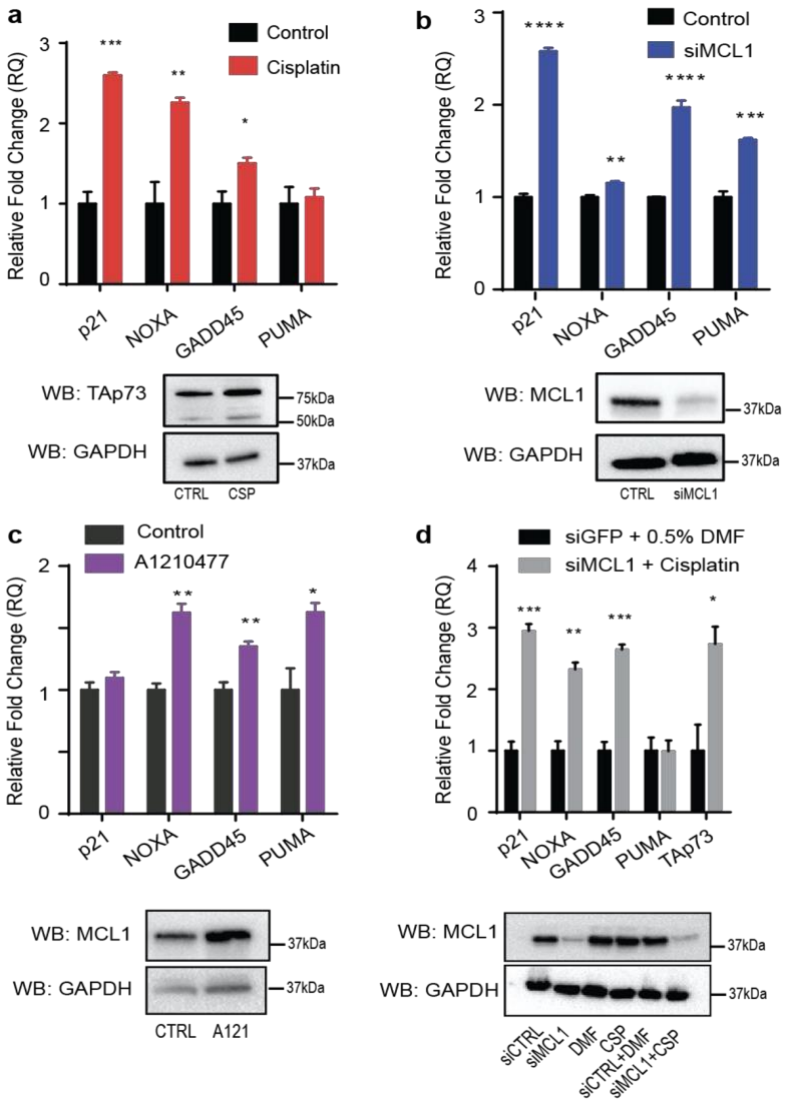

Figure 6. MCL1 inhibits the transcriptional function of TAp73. **a** H1299 cells were treated with 10 μM cisplatin for 24 hours to upregulate endogenous p73 protein expression to generate a baseline to p73 target gene activation. Four known p73 target genes were analyzed by TaqMan RT-qPCR. After a baseline was established, H1299 cells were treated with **b** an siRNA targeting MCL1 (48 h) or **c** 2 μM MCL1 inhibitor A1210477 (24 h). The four known p73 target genes show comparable increases in comparison with the sub-lethal cisplatin. **d** H1299 cells were treated with a combination of an siRNA-targeting MCL1 (48 h) and 10 μM cisplatin (24 h). All experiments were performed in biological and technical triplicate. Bar graphs shown with SEM of one representative assay. A Student's t-test was applied to each target gene for each treatment for statistical analysis, p-values: *$p < 0.05$, **$p < 0.01$, ***$p < 0.001$, ****$p < 0.0001$.

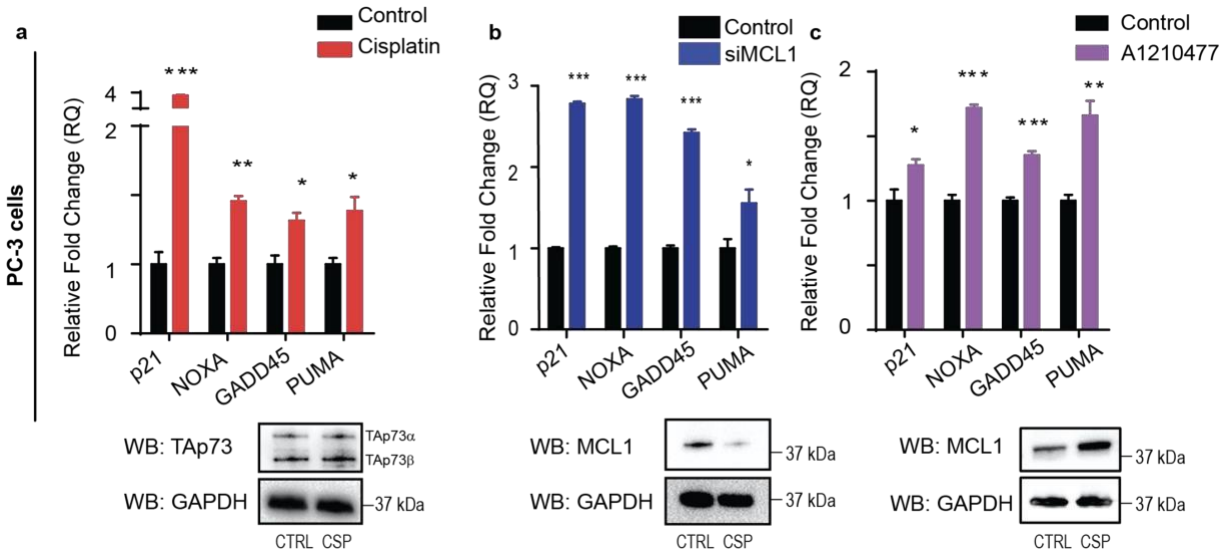

Supplemental Figure 4. MCL1 inhibits the transcriptional function of TAp73. a PC3 cells were treated with 5 μM cisplatin to upregulate endogenous target gene activation. Four known p73 target genes were analyzed by TaqMan RT-qPCR. After a baseline was established, cells were treated with **b** an siRNA targeting MCL1 or **c** 2 μM MCL1 inhibitor A1210477. The four known p73 target genes show comparable increases following siMCL1 or A1210477 compared to cisplatin. All experiments were performed in biological and technical triplicate. Bar graphs shown with SEM of one representative assay. A Student's t-test was applied to each target gene for each treatment for statistical analysis, p-values: * $p < 0.05$, ** $p < 0.01$, *** $p < 0.001$, **** $p < 0.0001$.

To examine if MCL1 acts as a novel p73 suppressor, we inhibited MCL1 expression using siRNA knockdown or direct protein inhibition using the MCL1-specific BH3 mimetic A1210477 (Figure 6b and 6c, Supplemental Figure 4)[53]. Although BH3mimetics inhibit the interacting binding site of MCL1, A1210477 and other MCL1 inhibitors increase the MCL1 protein expression as they inhibit protein binding partners that regulate MCL1 turnover[53]. Based on our hypothesis following the *in vitro* biochemical experiments, we anticipated an increase in p73 target gene expression would occur following inhibition of MCL1, as the knockdown would promote enhanced p73 tetramer formation and DNA binding. In each of the treatments above, we observed that when MCL1 is inhibited through a specific BH3-mimetic or knocked down, the treatment induced significant increases in

gene expression in at least three of the four p73 target genes in the cell lines H1299 and PC-3 (Figure 6b and Figure 6c, Supplemental Figure 4). The observed changes in expression were comparable to those observed following p73 activation through cellular treatment with sub-lethal cisplatin (Figure 6a).

To verify that these findings were not an artifact of subsequent apoptotic induction following treatment with cisplatin or knockdown of MCL1, we performed Annexin V/PI staining with FACS analysis. None of the cell treatments induced a significant amount of cellular apoptosis, suggesting that the MCL1-p73 interaction is primarily responsible for these findings (Supplemental Figure 3). This data supports our hypothesis that MCL1 can inhibit p73 transcriptional activation of target genes through a novel rBH3-mediated interaction.

Discussion

In this study, we have described and characterized a novel protein-protein interaction between anti-apoptotic MCL1 and the p53-homolog, p73. Biochemically, we have reduced this binding to the specific elements that mediate this interaction: the rBH3 motif in the tetramerization domain of p73 ($p73_{TD}$) and the canonical hydrophobic binding groove of MCL1. This data establishes a novel role for MCL1 where it acts as a transcriptional suppressor capable of inhibiting p73. Prior studies have highlighted how activation of p73 is essential for the transactivation of canonical response elements that regulate DNA damage response, apoptosis, and cell cycle progression[45]. Thus, MCL1's ability to regulate p73 transactivation expands on the canonical role of MCL1 as a prosurvival and pro-proliferative protein. These findings support and expand on the role that the rBH3 motif plays in extending MCL1 function in cells. Recently, we published a

study showing that MCL1 directly modulates protein stability of the cell cycle regulator P18 through a homologous rBH3-mediated interaction[12]. Our work here provides further evidence that the rBH3 motif is capable of mediating interactions with MCL1 and implies other rBH3-containing proteins should be explored.

The identified direct interaction between MCL1 and p73 poses an interesting intersection between cell survival and cell death. While this study is the first account of MCL1 modulating the activity of a transcription factor in cells, as shown in Figure 1, we also demonstrate that MCL1 is able to bind to all alternatively spliced C-terminal isoforms as well as the dominant-negative oncogenic ΔNp73 variants. The pull-down is weaker than we may have liked, but this is not unanticipated as MCL1 has many other binding partners in the cell and p73 protein functions as a tetramer with the site of MCL1 interaction buried in this tetrameric interface. MCL1 binding may therefore impact the tetramerization of p73, an area that would be of interest for future studies as this interplay between monomeric and tetrameric p73 lies at the heart of p73 affinity to DNA as well as the heterotetrameric regulation mediated by TA and ΔN p73 isoforms. Further, as the tetramerization domain is conserved amongst all p73 isoforms, we hypothesize that MCL1 modulates all p73 activity[19]. Thus, it is possible that in cases wherein ΔNp73 variants are predominantly expressed, MCL1 would act to negatively regulate their suppressive effects and thereby activate normal p73 function. In our cell models used for these studies, we were unable to detect endogenous ΔNp73 protein using commercially available antibodies, consistent with previous accounts using these cell lines, suggesting there is no detectable endogenous ΔNp73 present[54,55]. Therefore, our studies primarily focus on the impacts that MCL1 has on the pro-apoptotic transcriptional regulation by TAp73. This alternative mechanism generates additional avenues to be explored in regard to ΔNp73 regulation.

MCL1 as a nuclear protein is not a novel finding. In 2010, a study conducted by Pawlikowska and colleagues elucidated a role for nuclear MCL1 accumulation in response to DNA damage[36]. Following genotoxic stress, early-response gene product IEX-1 is upregulated by ataxia telangiectasia mutant (ATM) and acts as a carrier protein to promote MCL1 nuclear translocation. They identified that MCL1 was an integral component of the DNA damage response pathway as the knockdown of MCL1 increased the sensitivity to genotoxic stress[39]. While we show that p73 interacts with the canonical BH3 binding pocket of MCL1, the interaction site between MCL1 and IEX-1 is localized to the C-terminal MCL1 transmembrane domain and thus, these sites are not mutually exclusive[36]. Therefore, there could be a scenario in which MCL1 has dual binding to both proteins, bound to IEX-1 at the C-terminus and to p73 through its BH3 binding pocket.

Consistent with the findings from Pawlikowska and colleagues above, several other studies over the past decade have elucidated a role for MCL1 in DNA repair, consistently reaching the conclusion that knockdown of MCL1 inhibits double stand break (DSB) repair and improves sensitivity to genotoxic therapies[56,57]. Through these studies, it has been shown that MCL1 colocalizes with DSB-induced 53BP1 foci[56]. It has also been published that ΔNp73β binds 53BP1[58]. Based on the data shown here, it could be proposed that MCL1 localizes to sites of DSBs through a MCL1-ΔNp73β-53BP1 complex. Mattoo and colleagues proposed a model in which the knockdown of MCL1 increases 53BP1 at DSBs, which inhibits homologous recombination via impaired BRCA1 recruitment[56]. To support previous suggested hypotheses and the proposed above, we suggest that the knockdown of MCL1 may free the ΔNp73β-53BP1 complex to bind at these DSBs. This mechanism could be exploited to target vulnerable populations with genotoxic anti-cancer therapies in combination with emerging MCL1

inhibitors[32].

In addition to several DNA damage response studies, nuclear MCL1 has also been implicated in cell cycle regulation[12,37,59]. In 2000, Fujise and colleagues identified that MCL1 interacts with proliferating cell nuclear antigen (PCNA) in the nucleus to regulate cell cycle progression through S-phase. Like the MCL1 interaction defined here, the interaction between MCL1 and PCNA was shown to be exclusive to MCL1 supporting the idea that MCL1 has a unique role in the nucleus that is not redundant amongst other anti-apoptotic Bcl-2 family members[37]. Additionally, snMCL1 was shown to bind to CDK1 to regulate the G2/M transition[59].

Outside its role in general cellular homeostasis, p73 expression has been evaluated in several cancer cell types and patient tumor tissues. While not commonly mutated like p53, p73 isoform dysregulation has been described in various cancer lineages in both solid and hematopoietic malignancies[60]. In the absence of wild type p53,

there is a functional redundancy amongst the p53 family[13,17]. For cancers that rely on TAp73 for efficacy of chemotherapeutics such as platinum reagents, dose limiting toxicities and resistance remain a therapeutic hurdle[61-64]. Based on the novel interaction characterized here, there is a foundation to characterize MCL1 inhibition in combination with cisplatin and/or carboplatin. By targeting MCL1 with a specific BH3 mimetic such as AZD5991 (AstraZeneca)[34], AMG-176 (Amgen)[35], or S64315 (Servier/Novartis)[32], the interaction between MCL1 and p73 would be inhibited according to **Figure 2**. The BH3 mimetics identified specifically target the BH3 binding pocket and would therefore inhibit not only interactions with the pro-apoptotic Bcl-2 family members, but also all rBH3-mediated interactions[12]. All three inhibitors listed above have shown promising clinical efficacy and their or related MCL1 inhibitor impact in combination therapy is worth pursuing[32]. By

combining novel MCL1 inhibitors with low dose cisplatin, we could potentially combat cisplatin resistance and/or decrease the therapeutic dosing. This rationale is supported by recent accounts that knockdown of MCL1 sensitizes cancer cells to cisplatin-induced apoptosis[65,66].

Our work shown here defines a novel protein interaction between MCL1 and p73 and supports previous studies aimed at understanding the non-canonical role of nuclear MCL1 in DNA damage response. Here, we establish a unique function of MCL1 in transcriptional regulation that has never been previously described. As this is the second account of an rBH3-mediated interaction with MCL1, our work provides further validation that the rBH3 motif is a biologically relevant and available mechanism for mediating interactions between the Bcl-2 family and other protein signaling networks[11,12]. By characterizing these rBH3-mediated interactions, we gain a better understanding of the core homeostatic mechanisms regulating MCL1. Further, knowledge of these signaling networks will better guide combination treatment of emerging BH3-mimetic based therapies into clinic with chemotherapeutics and other genotoxic anti-cancer agents.

Materials and Methods

Cell Culture

H1299, PC-3, and HEK293T cells were maintained in humidified atmosphere with 5% CO_2 in RPMI-1640 medium supplemented with 10% fetal bovine serum, 2.05 mM L-glutamine, 100 units/ml each of penicillin and streptomycin, and 0.25 μg/ml of Fungizone antimycotic (Life Technologies, Grand Island, NY). Cell lines were obtained from the ATCC and are regularly validated through STR profiling at the Heflin Center Genomics Core Facility at

UAB. Before lysis, cells were rinsed with sterile Dulbecco's Phosphate Buffered Saline (1X

DPBS, Corning cellgro). Cell lysates for Western Blot and Immunoprecipitation were prepared in RIPA Lysis Buffer (Pierce, 89900) or in Immunoprecipitation Lysis Buffer (IP lysis buffer, Pierce, 87788). Lysis buffers are supplemented with 1X Halt Protease Inhibitor Cocktail with EDTA (ThermoScientific, 1861279). All experiments in this manuscript were completed in biological triplicate.

Transfections

All transient transfections for exogenous overexpression or RNA interference were performed using Lipofectamine 3000 or Lipfectamine RNAiMax, respectively (Invitrogen). All expression constructs for exogenous overexpression were made in pcDNA3.1 plasmid. Full length human MCL1 (clone ID 3138465) and p73α (clone ID 40125802) cDNA clones were obtained from Invitrogen. Coding sequences were amplified with Failsafe polymerase (Epicentre, Madison, WI) and tagged with N-terminal HA and FLAG tag respectively using primers: forward AGAATGGGATACCCATACGATGTTCCAGATTACGCTTTTGGCCTCAAAAGAA ACG and reverse CTATCTTATTAGATATGCCAAACCAGC for MCL1 and forward AGAATGGGAGATTACAAGGATGACGATGACAAGGCCCAGTCCACCGCCACC and reverse TCAGTGGATCTCGGCCTCC for FLAG-p73α. The fragments were inserted into the plasmid using TOPO cloning method (Invitrogen). ΔNp73 and TAp73β constructs were made by deletion using Phusion site directed mutagenesis kit (Thermo Scientific) using as a template pcDNA3.1 containing FLAG-p73α insert. TAp73β was amplified with the following primers: reverse TCAGGGCCCCCAGGTCCTGACGAGGCTGGGGTCGGCGTGGTAG, which

includes a fragment coding for the C-terminal amino acid sequence ArgThrTrpGlyPro that is distinct from the p73α isoform and forward primer complementary to vector sequence, TGAAGGGCAATTCTGCAGATATCC. To make ΔNp73α construct forward primer CTGTACGTCGGTGACCCCGCACGGCACCTCGCCACGGCCCAGTTCAATCTGCT GAGCAGCAC and reverse primer CTTGTCATCGTCAT CCTTGTAATCTCCCATTCTaag were used. The correct sequence was confirmed for all constructs by Sanger sequencing. All RNA interference experiments were performed by the manufacturer's protocol for Lipfectamine RNAiMAX. The final concentration of siRNA was 10 pmol/well for a 12 well dish. Silencer Select siRNA (Ambion) sequences for MCL1 are as follows: siMCL1 #1 (s8585) – GTAATTAGGAACCTGTTTCtt and siMCL1 #2 (s8583) – CCAGUAUACUUCUUAGAAAtt.

Immunoprecipitation

Four μg pcDNA3.1 plasmid DNA were premixed with 500 μl OptiMEM, 16 μl reagent P3000 and 10 μl Lipofectamine 3000 (Invitrogen). The mixture was incubated for 10 min at RT. Transfection mix was then added to cells in fresh RPMI-1640 medium supplemented with 10% fetal bovine serum, without antibiotics. 24 hours after transfection, the medium was removed and fresh medium containing 50 nM bortezomib diluted from DMSO stock was added. Cells were harvested after another 24-hour incubation and approximately 500 μg total protein was used for immunoprecipitation. The day before transfection, HEK-293T cells were seeded at $2.5x10^6$ on 6 cm cell culture dish. Mouse monoclonal IgG was used for MCL1 immunoprecipitation (RC-13, Santa Cruz Biotechnology) at 1 μg per sample. Following a one-hour incubation with respective antibodies at 4ºC, immune complexes were captured overnight on protein G magnetic beads

(Dynabeads, Invitrogen). For capturing FLAG-tagged p73 constructs, 25 µl antiFLAG magnetic beads with covalently attached mouse monoclonal G2a kappa antibody were used (Clontech). Immune complexes were washed 3 times with IP buffer, followed by one wash with water. Proteins were eluted from beads with Pierce pH 2.0 IP elution buffer for 15 min at RT shaker, subsequently neutralized with neutralization buffer pH 8.5 (Pierce Classic Magnetic IP/Co-IP Kit) and denatured for 5 min at 95 C with Laemmli sample buffer containing β-mercaptoethanol.

Western Blot Analysis

Cells were lysed with RIPA Lysis Buffer (Pierce, 89900) supplemented with 1X Halt Protease Inhibitor with EDTA (ThermoScientific, 1861279). Lysates were mixed with 4X Laemmli sample buffer containing β-mercaptoethanol and denatured at 95ºC for 10 minutes. Proteins were resolved using SDS polyacrylamide gel electrophoresis at 150V for 45 minutes and transferred to an activated PVDF membrane in a BioRad wet transfer system for 1 hour at 100V. Membranes were blocked in 5% w/v nonfat milk in PBS with 0.01 % Tween (PBST) for 1 hour. Membranes were then incubated with primary antibodies overnight at 4ºC. All antibodies were diluted into 1% milk-PBST solution. Secondary antibody was applied for 1 hour at RT. Western Blots were developed using ECL2 Reagent and Western Blotting Substrate (Pierce) and western blots were visualized on a BioRad ChemiDoc MP imaging system.

Primary Antibodies

MCL1: MCL1 protein in Figure 1 was detected with anti-MCL1 polyclonal rabbit antibody (D35A5, Santa Cruz), diluted 1:1000. MCL1 Western Blots in subsequent figures were detected by anti-MCL1 rabbit mAb (D2W9E, Cell Signaling), diluted to 1:1000. FLAG: Rat monoclonal IgG anti-Flag L5 antibodies (MA1-142, Pierce), diluted

1:10000. p73: anti-TAp73 mouse mAb (5B429, Novus) diluted 1:500. GAPDH: anti-GAPDH XP (R) mouse mAb (D16H11, Cell Signaling), diluted 1:1000. Lamin A/C: anti-Lamin A/C rabbit polyclonal IgG (H-110, sc20681, Santa Cruz), diluted 1:1000.

Secondary Antibodies

Rabbit: Goat anti-rabbit IgG-HRP, diluted 1:2000 (Cell Signaling), Rat: Goat anti-rat IgG conjugated with HRP, diluted 1:100000 (Pierce), Mouse: Horse anti-mouse IgG-HRP diluted 1:2000 (Cell Signaling).

Peptide Synthesis p73-derived peptides and the FITC-BAK peptide used in the fluorescence polarization assay and NMR Spectroscopy were synthesized using a standard, doubleaddition, FMOC, solid-phase peptide synthesis strategy on a Prelude peptide synthesis system (Gyros Protein Technologies, Sweden). 4-(2′,4′-dimethoxyphenylfmocaminmethyl)-phenoxyacetamidomethylbenzhydryl amine resin (rink amide MBHA resin, Anaspec) was swelled in *N*,*N*-Dimethylformamide (DMF, Fisher Scientific) followed by methylene chloride (DCM, Fisher Scientific) to increase surface area availability for bonding. Using a double-addition FMOC strategy, the N-terminal FMOC on the growing peptide chain was deprotected with 0.8 M piperidine (Fisher Scientific) in DMF for 2 minutes and 30 seconds. The following amino acid (200 mM) was added to the N-terminus and activated with 0.4 M O-(1H-6-Chlorobenzotriazole1-yl)-1,1,3,3tetramethyluronium hexafluorophosphate (HCTU, Anaspec) in DMF for nucleophilic attack of the N-terminal peptidyl-resin. Next, 800 mM 4-Methylmorpholine (NMM, Fisher Scientific) in DMF was added, and the peptidyl-resin, HCTU, NMM slurry was mixed for 30 minutes followed by four 30 second DMF washes. Peptidyl resin was cleaved using 88% TFA, 5% Water, 5% phenol, and 2% triisopropylsilane for 180 minutes. The cleaved peptide was filtered by hand using the Prelude reaction vessels away from the

resin. Filtered, cleaved peptide was cold-ether precipitated and centrifuged at 14,000 x g to pellet the resin-cleaved, crude peptide. Crude peptides were lyophilized and resuspended in 80% water/20% acetonitrile and purified over a Zorbax Eclipse XDBC18 column (Agilent) on a 1260 Infinity HPLC (Agilent) with a 5-60% acetonitrile gradient. Following purification, the peptides were lyophilized and resuspended to 10 mM in DMSO. The purity of the peptide was confirmed by MALDI.

Recombinant Protein Purification

MCL1 and the p73 constructs were transformed into BL21 (DE3) *E. coli* using the New England BioLabs protocol. Cells were grown in 1L cultures (250 mL/flask) under kanamycin selection at 37°C for 1 hour. When an optical density (OD_{600}) of 0.5 – 0.7 was obtained, the protein expression was induced with 1M Isopropyl β-d1thiogalactopyranoside (IPTG, Fisher BioReagents). The optical density is monitored over several hours until a plateau is reached using the cuvette reading on a Nanodrop 2000c Spectrophotometer. At maximal density, the cells are harvested through centrifugation at 4,700 x g. At this point, the pellet is either frozen at -80°C for future purification or resuspended in 20 mL protein lysis buffer. Once resuspended, the lysate is supplemented with 2 EDTA-free mini protease inhibitor tablets (Pierce, A32955) and Lysozyme (0.25 mg/mL). For lysis, cells are subjected to probe sonication for 6 – 8 minutes on ice. Once complete, the cell debris is pelleted at 14,000 x g and the supernatant is filtered through a 0.45 µm syringe filter (Millex). Following preparation, the protein is purified on an Biorad NGC FPLC system using nickel chromatography (1 mL HisTrap, GE Healthcare) followed by subsequent gel filtration (S100, GE Healthcare). Both column purifications were followed by a polyacrylamide gel run at 150 V for 45 minutes to confirm the presence of the protein of interest. Final protein identity was confirmed through MALDI. Both p73 constructs and MCL1 are in a final buffer of

1X PBS, pH 6.8.

Direct Fluorescence Polarization Assay

In a flat-bottom, untreated black 96 well microplate (ThermoScientific), 90 µL recombinant protein is incubated with 10 µL 10X FITC-peptide or annealed FITC-DNA. The FITC-BAK sequence used in the peptide FPAs is FITCAhxGQVGRQLAIIGDDINRRYD. The two FITC-labeled response elements were ordered from ThermoScientific and annealed in 5 mM Tris, 5 mM KCl, 0.01% Triton, 0.2 mM DTT (pH 8.6). The sequences are as follows: GADD45 (fwd): 5'-FITC-GAACATGTCTAGGCATGCTG-3' and NOXA (fwd): 5'-FITC-GAGCGTGTCCGGGCAGGTCG-3'. The plate is covered with an opaque lid to shake for 30 minutes. Once complete, the plate is read using the FP-Fluorescein setting (1.0s, CW lamp filter – F485, emission filter, F535) on a Perkin Elmer Victor X5 plate reader. The buffer used for all assays is 1X PBS, pH 7.4. All experiments were completed in technical and biological triplicate. Data plotted in Figure 2 is one representative assay in technical triplicate.

Competitive Fluorescence Polarization Assay

In a flat-bottom, untreated black 96 well microplate (ThermoScientific), 80 µL recombinant protein is incubated with 10 µL 10X unlabeled peptide or small molecule inhibitor shaking at 300 rpm for 20 minutes to allow for binding. Once complete, 10 µL of 10X FITC-peptide is added per well. The plate is covered with an opaque lid to shake for an additional 40 minutes. After 1 hour incubation is complete, the plate is read using the FP-Fluorescein setting (1.0s, CW lamp filter – F485, emission filter, F535) on a Perkin Elmer Victor X5 plate reader. The buffer used for all assays is 1X PBS, pH 7.4.
All experiments were completed in technical and biological triplicate. All data plotted in Figure 2 is one representative assay in technical triplicate.

Nuclear Magnetic Resonance (NMR)

The NMR HSQC spectra were acquired using a Bruker 600 MHz magnet at the Central Alabama High Field NMR Facility. Samples were prepared the day of collection in 1X PBS, pH 6.8 supplemented with sodium azide (Fisher BioReagents) and deuterium oxide (99%, Cambridge Isotope Laboratories, Inc). For any samples containing peptides, the control spectra were also supplemented with DMSO for comparison. The resulting spectra were analyzed using CARA (Computer Aided Resonance Assignment) and the peak lists were exported to Microsoft Excel for the chemical shift perturbation (CSP) quantification and calculation of the mean and standard deviation. Any peaks exhibiting significant CSP (>2 SD) were mapped to the space filling model of MCL1 on PyMOL, using PBD file 6QFI: Structure of human Mcl-1 in complex with BIM BH3 peptide. The BIM peptide was removed to display the BH3 binding pocket.

Cellular Localization

Cellular localization was performed using the NE-PER Nuclear and Cytoplasmic Extraction Reagent Kit (ThermoScientific, 78833) per the manufacturer's protocol. The western blot quantification analysis was completed in the Image Lab 6.0.1 software using the Adjusted Volume tool. All assays were completed in biological triplicate with one representative image for each treatment group and/or cell line.

Electrophoretic Mobility Shift Assay (EMSA)

Recombinant p73 protein (DBD or DBD-TD) was incubated with 1 µM annealed FITC-GADD45 on ice (sequence above). After 15 minutes, recombinant MCL1 is added into each reaction for a total reaction volume of 10 µL for each sample. All reactions are mixed at 300 rpm in an Eppendorf MixMate plate shaker for 1 minute, followed by a 15 minute incubation on ice. After the second incubation, 5 µL Native Sample Buffer (BioRad,

#161-0738) was added to each reaction. Samples were run under native conditions on Any Kd Mini-PROTEAN TGX gels (BioRad, #456-9036) in cold 1X Tris/Glycine Running Buffer (BioRad, #161-0771) for 20 minutes at 200V. Gels were imaged on a BioRad ChemiDoc Imaging System for Fluorescein to visualize FITClabeled DNA. Following imaging, gels were stained with Bio-Safe Coomassie G-250

Stain (BioRad, #1610787) per manufacturer's protocol. Gels were imaged on the BioRad ChemiDoc Imaging System for Coomassie Blue to protein visualization. EMSAs were completed in biological triplicate with multiple protein purification preparations. The gels presented in Figure 4 are one representative gel. The quantification and statistical analysis includes all biological triplicate values.

RNA Extraction and cDNA Synthesis

RNA was purified from human cancer cell lines for RTqPCR with the SurePrep TrueTotal RNA Purification Kit (Fisher BioReagents, BP2800-50) by the manufacturer's protocol. The final concentration of purified RNA was measured using a Nanodrop 2000c Spectrophotometer. Once RNA concentration was determined, a single step cDNA synthesis reaction was made in TempAssure PCR 8-Tube Strips (USA Scientific, 14022500) in technical duplicate as follows: 100 ng RNA, 16 µL Nuclease-Free Water (Ambion, 1512103), and 4 µL qScript cDNA SuperMix (Quanta BioSciences Inc., 84034). The cDNA synthesis reaction per the qScript cDNA SuperMix protocol is 25°C for 5 minutes, 42°C for 30 minutes, and 85°C for 5 minutes with a 4° hold. Concentration was determined after the cDNA synthesis on the Nanodrop 2000c Spectrophotometer. cDNA was diluted to 25 ng/µL into Molecular Biology Grade Water (Corning, 46-000-CM) and stored at -20°C for future use. Remaining RNA was stored at -80°C.

TaqMan RT-qPCR

All RT-qPCR reactions were performed in biological triplicate. A master mix for each target or housekeeping gene was made with 15 µL RNAse-Free water, 3 µL 20X RTqPCR Primer Mix (ThermoScientific), 12 µL 25 ng/µL cDNA, and 30 µL TaqMan Universal Master Mix II, with UNG (Applied Biosystems, 2020-02-29). The mix was aliquoted out 20 µL/well in technical triplicate with the final concentration of cDNA at 100 ng/reaction. PCR reactions were performed on an Applied Biosystems ViiA 7 RealTime PCR System for 40 cycles starting at 25°C. Each cycle is 50°C for 2 minutes, 95°C for 10 minutes and 15 seconds, and 60°C for 1 minute. Temperature shifts at 1.6°C/sec. All data is collected and analyzed using Applied Biosystems QuantStudio Real-Time PCR Software. All target genes analyzed were normalized to GAPDH. All primers had FAM-MGB probes. All TaqMan primers were ordered from ThermoFisher Scientific with the target gene and Assay ID included: CDKN2A/p21 (Hs00355782_m1), PMAIP1/NOXA (Hs00560402_m1), GADD45A (Hs00169255_m1), BBC3/PUMA (Hs00248075_m1), GAPDH (Hs02758991_g1). Graphs in Figure 6 are one representative assay in technical triplicate.

Annexin V/PI Staining with Fluorescence-activated cell sorting (FACS)

Cells were seeded in a 6 well plate and treated through various treatments to modulate MCL1 or p73 expression as they were in previous experiments. After the 24 or 48 hour treatment, cells were collected through trypsin dissociation and washed twice with sterile DPBS. Cell number was counted on a BioRad Automated Cell Counter. After final wash, cells were pelleted at 1000 x g for 10 minutes. The cell pellet was resuspended in 1X Annexin V Binding Buffer (BD Pharmingen, 556454) and $5x10^5$ cells were transferred to a FACS tube containing 5 µL Propidium Iodide (PI) Staining Solution (BD Pharmingen, 51-66211E) and 5 µL FITC-Annexin V (BD Pharmingen, 556419).

Cells were incubated for 15 minutes in the dark. FACS was collected on a BD LSRFortessa and analyzed using FlowJo v10. Compensation controls used for analysis include unstained cells and cells stained for each individual fluorophore (FITC-Annexin V and Cy5-PI). Gating strategy eliminated cell debris and doublets through forward and side scatter plots.

Reagents

The following reagents were used throughout the experiments above: MCL1specific inhibitor A1210477 (SelleckChem, S7790); cisplatin (SelleckChem, S1166). All other reagents were described in the applicable section above.

Statistical analyses

All experiments were repeated with at least three biologic replicates using two or three technical replicates, as reported, with data expressed as the mean ± S.D. No samples were excluded. Differences between two data sets were calculated using a two-tailed unpaired Student t-test with $P<0.05$ considered statistically significant. Statistical analysis was performed in Prism (Graphpad Inc.) or Microsoft Excel. *P<0.05, **P<0.01, ***P<0.001.

Acknowledgements

We would like to thank Nathan Ruppert for assistance in collecting preliminary FPA experiments. This work was supported, in part, by funding from the National Institutes of Health Grants R01GM117391 (to W.J.P.) and T32-NS048039 (to R.H.W.). This study used the UAB CCC NMR Shared Facility (P30CA013148 and S10RR022994).

Author Contributions

H.N.W., A.K., and W.J.P. conceived and designed the experiments. A.K. did the coimmunoprecipitations. A.S. and R.H.W. did the peptide synthesis. H.W. collected and analyzed the NMR and performed all FPA, cellular localization, EMSA, western blots, RT-qPCR, and cell viability analysis. H.N.W. and W.J.P. wrote the manuscript. All authors contributed to the data interpretation, troubleshooting, manuscript writing, and editing. All of the authors read and approved the final manuscript.

Conflicts of Interest

The authors declare no conflicts of interest.

Chapter 2 References

1 Chipuk, J. E., Moldoveanu, T., Llambi, F., Parsons, M. J. & Green, D. R. The BCL-2 family reunion. *Mol Cell* 2010 **37**, 299-310.

2 Kale, J., Osterlund, E. J. & Andrews, D. W. BCL-2 family proteins: changing partners in the dance towards death. *Cell Death Differ* 2018 **25**, 65-80.

3 Kvansakul, M. & Hinds, M. G. Structural biology of the Bcl-2 family and its mimicry by viral proteins. *Cell Death Dis* 2013 **4**, e909.

4 Singh, R., Letai, A. & Sarosiek, K. Regulation of apoptosis in health and disease: the balancing act of BCL-2 family proteins. *Nat Rev Mol Cell Biol* 2019 **20**, 175193.

5 Cory, S., Roberts, A. W., Colman, P. M. & Adams, J. M. Targeting BCL-2-like Proteins to Kill Cancer Cells. *Trends Cancer* 2016 **2**, 443-460.

6 Letai, A. BH3 domains as BCL-2 inhibitors: prototype cancer therapeutics. *Expert Opin Biol Ther* 2003 **3**, 293-304.

7 Leverson, J. D. *et al.* Found in Translation: How Preclinical Research Is Guiding the Clinical Development of the BCL2-Selective Inhibitor Venetoclax. *Cancer Discov* 2017 **7**, 1376-1393.

8 Choudhary, G. S. *et al.* MCL-1 and BCL-xL-dependent resistance to the BCL-2 inhibitor ABT-199 can be overcome by preventing PI3K/AKT/mTOR activation in lymphoid malignancies. *Cell Death Dis* 2015 **6**, e1593.

9 Zhu, H. & Almasan, A. Development of venetoclax for therapy of lymphoid malignancies. *Drug Des Devel Ther* 2017 **11**, 685-694.

10 Consortium, I. T. P.-C. A. o. W. G. Pan-cancer analysis of whole genomes. *Nature* 2020 **578**, 82-93.

11 Placzek, W. J. *et al.* Identification of a novel Mcl-1 protein binding motif. *J Biol Chem* 2011 **286**, 39829-39835.

12 Whitaker, R. H. & Placzek, W. J. MCL1 binding to the reverse BH3 motif of P18INK4C couples cell survival to cell proliferation. *Cell Death Dis* 2020 **11**, 156.

13 Dotsch, V., Bernassola, F., Coutandin, D., Candi, E. & Melino, G. p63 and p73, the ancestors of p53. *Cold Spring Harb Perspect Biol* 2010 **2**, a004887.

14 Jost, C. A., Marin, M. C. & Kaelin, W. G., Jr. p73 is a simian [correction of human] p53-related protein that can induce apoptosis. *Nature* 1997 **389**, 191-194.

15 Levrero, M. *et al.* Structure, function and regulation of p63 and p73. *Cell Death Differ* 1999 **6**, 1146-1153.

16 Rufini, A. *et al.* p73 in Cancer. *Genes Cancer* 2011 **2**, 491-502.

17 Yoon, M. K., Ha, J. H., Lee, M. S. & Chi, S. W. Structure and apoptotic function of p73. *BMB Rep* 2015 **48**, 81-90.

18 Seelan, R. S. *et al.* The human p73 promoter: characterization and identification of functional E2F binding sites. *Neoplasia* 2002 **4**, 195-203.

19 Murray-Zmijewski, F., Lane, D. P. & Bourdon, J. C. p53/p63/p73 isoforms: an orchestra of isoforms to harmonise cell differentiation and response to stress. *Cell Death Differ* 2006 **13**, 962972.

20 Stiewe, T., Theseling, C. C. & Putzer, B. M. Transactivation-deficient Delta TAp73 inhibits p53 by direct competition for DNA binding: implications for tumorigenesis. *J Biol Chem* 2002 **277**, 14177-14185.

21 Grob, T. J. *et al.* Human delta Np73 regulates a dominant negative feedback loop for TAp73 and p53. *Cell Death Differ* 2001 **8**, 1213-1223.

22 Vikhreva, P., Melino, G. & Amelio, I. p73 Alternative Splicing: Exploring a Biological Role for the C-Terminal Isoforms. *J Mol Biol* 2018 **430**, 1829-1838.

23 Whitaker, R. H. & Placzek, W. J. Regulating the BCL2 Family to Improve Sensitivity to

Microtubule Targeting Agents. *Cells* 2019 **8**.

24 Tomita, Y. *et al.* WT p53, but not tumor-derived mutants, bind to Bcl2 via the DNA binding domain and induce mitochondrial permeabilization. *J Biol Chem* 2006 **281**, 8600-8606.

25 Zhai, D., Jin, C., Huang, Z., Satterthwait, A. C. & Reed, J. C. Differential regulation of Bax and Bak by anti-apoptotic Bcl-2 family proteins Bcl-B and Mcl1. *J Biol Chem* 2008 **283**, 9580-9586.

26 Stewart, M. L., Fire, E., Keating, A. E. & Walensky, L. D. The MCL-1 BH3 helix is an exclusive MCL-1 inhibitor and apoptosis sensitizer. *Nat Chem Biol* 2010 **6**, 595-601.

27 Coutandin, D. *et al.* Conformational stability and activity of p73 require a second helix in the tetramerization domain. *Cell Death Differ* 2009 **16**, 1582-1589.

28 Zhai, D., Jin, C., Satterthwait, A. C. & Reed, J. C. Comparison of chemical inhibitors of antiapoptotic Bcl-2-family proteins. *Cell Death Differ* 2006 **13**, 1419-1421.

29 Czabotar, P. E. *et al.* Structural insights into the degradation of Mcl-1 induced by BH3 domains. *Proc Natl Acad Sci U S A* 2007 **104**, 6217-6222.

30 Kump, K. J. *et al.* Discovery and Characterization of 2,5-Substituted Benzoic Acid Dual Inhibitors of the Anti-apoptotic Mcl-1 and Bfl-1 Proteins. *J Med Chem* 2020.

31 Denis, C., Sopkova-de Oliveira Santos, J., Bureau, R. & Voisin-Chiret, A. S. HotSpots of Mcl-1 Protein. *J Med Chem* 2020 **63**, 928-943.

32 Hird, A. W. & Tron, A. E. Recent advances in the development of Mcl-1 inhibitors for cancer therapy. *Pharmacol Ther* 2019 **198**, 59-67.

33 Lee, D. H. *et al.* A conserved mechanism for binding of p53 DNA-binding domain and antiapoptotic Bcl-2 family proteins. *Mol Cells* 2014 **37**, 264-269.

34 Tron, A. E. *et al.* Discovery of Mcl-1-specific inhibitor AZD5991 and preclinical activity in multiple myeloma and acute myeloid leukemia. *Nat Commun* 2018 **9**, 5341.

35 Caenepeel, S. *et al.* AMG 176, a Selective MCL1 Inhibitor, Is Effective in Hematologic Cancer Models Alone and in Combination with Established Therapies. *Cancer Discov* 2018 **8**, 1582-1597.

36 Pawlikowska, P. *et al.* ATM-dependent expression of IEX-1 controls nuclear accumulation of Mcl-1 and the DNA damage response. *Cell Death Differ* 2010 **17**, 1739-1750.

37 Fujise, K., Zhang, D., Liu, J. & Yeh, E. T. Regulation of apoptosis and cell cycle progression by MCL1. Differential role of proliferating cell nuclear antigen. *J Biol Chem* 2000 **275**, 39458-39465.

38 Aqeilan, R. I. *et al.* Functional association between Wwox tumor suppressor protein and p73, a p53 homolog. *Proc Natl Acad Sci U S A* 2004 **101**, 4401-4406.

39 Liu, T., Roh, S. E., Woo, J. A., Ryu, H. & Kang, D. E. Cooperative role of RanBP9 and P73 in mitochondria-mediated apoptosis. *Cell Death Dis* 2013 **4**, e476.

40 Fontemaggi, G. *et al.* Identification of direct p73 target genes combining DNA microarray and chromatin immunoprecipitation analyses. *J Biol Chem* 2002 **277**, 43359-43368.

41 Kravchenko, J. E. *et al.* Small-molecule RETRA suppresses mutant p53-bearing cancer cells through a p73-dependent salvage pathway. *Proc Natl Acad Sci U S A* 2008 **105**, 6302-6307.

42 Dar, A. A., Belkhiri, A., Ecsedy, J., Zaika, A. & El-Rifai, W. Aurora kinase A inhibition leads to p73dependent apoptosis in p53-deficient cancer cells. *Cancer Res* 2008 **68**, 8998-9004.

43 Brandt, T., Petrovich, M., Joerger, A. C. & Veprintsev, D. B. Conservation of DNA-binding specificity and oligomerisation properties within the p53 family. *BMC Genomics* 2009 **10**, 628.

44 Ethayathulla, A. S., Nguyen, H. T. & Viadiu, H. Crystal structures of the DNAbinding domain tetramer of the p53 tumor suppressor family member p73 bound to different full-site response elements. *J Biol Chem* 2013 **288**, 4744-4754.

45 Ethayathulla, A. S. *et al.* Structure of p73 DNA-binding domain tetramer modulates p73 transactivation. *Proc Natl Acad Sci U S A* 2012 **109**, 6066-6071.

46 Kearns, S., Lurz, R., Orlova, E. V. & Okorokov, A. L. Two p53 tetramers bind one consensus DNA response element. *Nucleic Acids Res* 2016 **44**, 6185-6199.

47 Scoumanne, A., Harms, K. L. & Chen, X. Structural basis for gene activation by p53 family members. *Cancer Biol Ther* 2005 **4**, 1178-1185.

48 Harms, K., Nozell, S. & Chen, X. The common and distinct target genes of the p53 family transcription factors. *Cell Mol Life Sci* 2004 **61**, 822-842.

49 Martin, A. G., Trama, J., Crighton, D., Ryan, K. M. & Fearnhead, H. O. Activation of p73 and induction of Noxa by DNA damage requires NF-kappa B. *Aging (Albany NY)* 2009 **1**, 335-349.

50 Melino, G. *et al.* p73 Induces apoptosis via PUMA transactivation and Bax mitochondrial translocation. *J Biol Chem* 2004 **279**, 8076-8083.

51 Gong, J. G. *et al.* The tyrosine kinase c-Abl regulates p73 in apoptotic response to cisplatininduced DNA damage. *Nature* 1999 **399**, 806-809.

52 Nyman, U. *et al.* Full-length p73alpha represses drug-induced apoptosis in small cell lung carcinoma cells. *J Biol Chem* 2005 **280**, 34159-34169.

53 Leverson, J. D. *et al.* Potent and selective small-molecule MCL-1 inhibitors demonstrate on-target cancer cell killing activity as single agents and in combination with ABT-263 (navitoclax). *Cell Death Dis* 2015 **6**, e1590.

54 Marrazzo, E., Marchini, S., Previdi, S. & Broggini, M. Questioning the oncogenic role of

DeltaNp73alpha in different cell lines expressing p53 or not. *Cancer Biol Ther* 2006 **5**, 794-803.

55 Guan, M. & Chen, Y. Aberrant expression of DeltaNp73 in benign and malignant tumours of the prostate: correlation with Gleason score. *J Clin Pathol* 2005 **58**, 1175-1179.

56 Mattoo, A. R. *et al.* MCL-1 Depletion Impairs DNA Double-Strand Break Repair and Reinitiation of Stalled DNA Replication Forks. *Mol Cell Biol* 2017 **37**.

57 Chen, G. *et al.* Targeting Mcl-1 enhances DNA replication stress sensitivity to cancer therapy. *J Clin Invest* 2018 **128**, 500-516.

58 Wilhelm, M. T. *et al.* Isoform-specific p73 knockout mice reveal a novel role for delta Np73 in the DNA damage response pathway. *Genes Dev* 2010 **24**, 549-560.

59 Jamil, S. *et al.* A proteolytic fragment of Mcl-1 exhibits nuclear localization and regulates cell growth by interaction with Cdk1. *Biochem J* 2005 **387**, 659-667.

60 Rodriguez, N., Pelaez, A., Barderas, R. & Dominguez, G. Clinical implications of the deregulated TP73 isoforms expression in cancer. *Clin Transl Oncol* 2018 **20**, 827-836.

61 Nishioka, K. *et al.* [A complete response (CR) case of multiple lung metastases after radical lobectomy for non-small-cell-lung cancer obtained by cisplatin+vindesine]. *Gan To Kagaku Ryoho* 2008 **35**, 2210-2212.

62 Al-Bahlani, S. *et al.* P73 regulates cisplatin-induced apoptosis in ovarian cancer cells via a calcium/calpain-dependent mechanism. *Oncogene* 2011 **30**, 4219-4230.

63 Tanida, S. *et al.* Mechanisms of Cisplatin-Induced Apoptosis and of Cisplatin Sensitivity: Potential of BIN1 to Act as a Potent Predictor of Cisplatin Sensitivity in Gastric Cancer Treatment. *Int J Surg Oncol* 2012 **2012**, 862879.

64 Dasari, S. & Tchounwou, P. B. Cisplatin in cancer therapy: molecular mechanisms of action. *Eur J Pharmacol* 2014 **740**, 364-378.

65 Yu, X. *et al.* Targeting MCL-1 sensitizes human esophageal squamous cell carcinoma cells to cisplatin-induced apoptosis. *BMC Cancer* 2017 **17**, 449.

66 Wang, H. *et al.* MALAT1/miR-101-3p/MCL1 axis mediates cisplatin resistance in lung cancer.

SRI-41155 INHIBITS HISTONE 3, LYSINE 4 METHYLATION AND MLL-REARRANGED LEUKEMIC PROLIFERATION

by

HAYLEY WIDDEN, ALEXUS ACTON, REBECCA BOOHAKER, CORINNE AUGELLI-SZAFRAN, MARK SUTO, HAO JIANG, AND WILLIAM J. PLACZEK

Manuscript preparation pending New Patent Application
Intellectual Property Disclosures filed in collaboration with the Bill L. Harbert Institute for Innovation and Entrepreneurship at UAB and Southern Research

Format adapted for dissertation

Abstract

Aggressive acute leukemias in children, adolescents, and adults arise due to a chromosomal translocation and subsequent protein fusion that occurs at chromosome 11q23 at the mixed-linage leukemia-1 (*MLL1)* gene. MLL-rearranged leukemias comprise 10% of all human leukemias, and comparatively, have poor therapeutic outcomes compared to non-MLL hematologic malignancies. *MLL1* encodes the large, interchangeable catalytic subunit of the SET/MLL histone methyltransferase that specifically regulates the gene activating epigenetic pattern of Histone 3, Lysine 4 methylation (H3K4me). Dysregulation of SET/MLL complex, such as fusion partners with *MLL1*, causes epigenetic dysregulation promoting tumorigenic pathways, such as oncogenic MYC expression. MYC dysregulation is one of the most common features across solid and hematologic malignancies, and historically has been a therapeutic challenge for drug discovery efforts. Here, we propose that targeting the DPY30 subunit of the SET/MLL complex will inhibit aberrant H3K4 histone methylation patterns and downstream oncogenic MYC expression. Prior to this study, we designed a high throughput screen to identify small molecules that specifically inhibit the DPY30-ASH2L protein interaction. Through pre-clinical characterization studies, we have validated the ontarget efficacy of a first-in-class chemical scaffold herein called SRI-41155, which significantly downregulates H3K4me3 and MYC expression. Additionally, SRI-41155 inhibits MLL-rearranged leukemic cell proliferation *in vitro* and significantly decreased MLL tumor burden *in vivo.* Through these proof-of-concept studies, we have identified a novel therapeutic target in MLL-rearranged leukemias through inhibition of the DPY30ASH2L interaction of the histone SET/MLL complex capable of modulating MYC expression and the H3K4 epigenome.

Keywords: Mixed Lineage Leukemia (MLL), SET/MLL histone methyltransferase complex, histone 3, lysine 4 methylation (H3K4me), DPY30, high throughput screen

Introduction

Mixed Lineage Leukemia or MLL-rearranged leukemias account for 5-10% of acute leukemia cases in adults, but more significantly, comprise 70% of infant acute lymphoblastic leukemia (ALL) cases[1,2]. Unfortunately, patients with MLL-rearrangements have significantly lower 5-year survival rates and high rates of relapse of 50-60%[1]. The current standard of care in MLL-rearranged leukemia remains multiagent cytotoxic therapy, despite the high percentage of patients who relapse[1,3]. Therefore, there is an unmet need in acute lymphoid and myeloid leukemias that harbor this genomic aberration for novel targeted therapeutics to improve the quality of life and the duration of therapeutic response.

MLL-rearranged leukemia is characterized by a chromosomal rearrangement arising at the long arm of chromosome 11, band 23 (11q23)[4]. The gene at the 11q23 locus is *MLL1/KMT2A* which codes for one of six homologous catalytic subunits of the histone 3, lysine 4 methyltransferase complex (*i.e.* H3K4 HMT complex). The wild type MLL1 subunit is comprised of two protein fragments as a result of post-translational processing: MLL1-N/p320 (*i.e.* the N-terminal MLL-1 fragment with a MW of 320 kD) and MLL1C/p180[5]. The full length 500 kDa MLL1 protein is cleaved by taspase1, and the two fragments interact with each other to form a stable complex post-cleavage that is required for endogenous epigenetic activity[6]. Uniquely in MLL-rearranged leukemia, fusion

proteins with MLL1-N inhibit the wild-type interaction with the MLL1-C fragment. There are nine common pathologic fusion partners with MLL1-N, but more than 130 MLLrearrangements have been identified making the development of pan-active targeted therapeutics difficult[3,7].

Critically for the functionality of the MLL1-complex, the C-terminal fragment of MLL1 contains the SET domain responsible for the methyltransferase activity. Typically, these malignancies have a low mutational burden, but the MLL1-N fusion proteins cause epigenetic dysregulation that coordinates a specific transcriptional gene signature that promotes leukemogenesis[8-11]. Over the past decade, there has been success in targeting epigenetic modifiers such as bromodomains (*i.e.* BRD4, JQ1), histone deacetylases (HDACs), and the H3K27 histone methyltransferase EZH2 (FDA-approved tazematostat), but thus far, there are no FDA approved therapies targeting the SET/MLL complex that is ubiquitously disrupted in MLL-rearranged leukemogenesis[12-14].

The wild type SET/MLL HMT complex is comprised of six subunits: one catalytic domain and five core subunits important for methylation efficacy[1]. The catalytic domain (**MLL1,** MLL2, MLL3, MLL4, SET1A, or SET1B) is responsible for the methyltransferase activity and recruits other chromatin remodeling proteins to generate target gene specificity[1,10,15]. The MLL1-C or the C-terminus of another catalytic subunit binds and tethers the WRAD complex comprised of **W**DR5, **R**BBP5, **A**SH2L, and a dimer of **D**PY30. These subunits individually have unique functions, but together coordinate H3K4 methylation by the SET/MLL catalytic domain[1,16]. Two pivotal structural studies of the WRD5, RBBP5, and ASH2L subunits showed that WDR5 and RBBP5 act as a tether between the WRAD complex and the SET/MLL catalytic domain[16]. Furthermore, RBBP5 and ASH2L form a heterodimer that stabilizes the catalytic conformation of the SET/MLL subunit and is therefore essential for all SET/MLL-mediated H3K4 methylation

activity[16,17]. Lastly, DPY30, which is the primary focus of this study, binds as an asymmetric dimer to ASH2L through a single a-helix bridge and specifically coordinates H3K4me3, a pattern typically associated with poised and active transcriptional start sites[1820]. The mechanism of how and why DPY30 selectively promotes trimethylation over mono- or dimethylation remains to be determined as the mechanistic studies of the MLLcomplex have not included DPY30[16,17].

H3K4 methylation is an important epigenetic regulatory protein modification associated with transcriptional activation. There are three methylation states with unique signatures that alter transcription at different areas of the genome: one methyl group or H3K4me1 marks active enhancer regions, H3K4me2 marks transcriptional activation of the gene body, and H3K4me3 marks poised or activated start sites in promoter regions[20]. Due to the epigenetic dysregulation observed in MLL-rearranged leukemias, *MLL1* and the core subunits have been highlighted as novel therapeutic targets in this subset of cancers[2123]. Importantly for this study, aberrant H3K4 methylation activates oncogenes required for MLL-rearranged leukemogenesis, notably MYC, which has been notoriously difficult to target for drug discovery efforts[10,16,20,24]. However, recent success over the past decade using epigenetic complex inhibitors, such as JQ1, have been shown to successfully downregulate MYC expression by modulating the epigenome[25-27]. Thus far, inhibitors of MLL1 and its interaction with the core subunit WDR5 (*i.e.* MM-102[28], MM-589[29], or OICR-9429[30]) have been identified, but these inhibitors remain in pre-clinical characterization and development[31-33]. Nevertheless, a small molecule inhibitor of the DPY30-ASH2L interface has not been identified and may provide a new opportunity for targeting MLL-rearranged leukemia and ultimately, other MYC-dependent malignancies[24,34].

The goal of this study was to develop a novel small molecule inhibitor targeting the

DPY30-ASH2L binding interface, identifying a first-in-class targeted therapeutic for MLL-rearranged leukemias (Figure 1A). The premise for this project is based on our previously published proof-of-concept target validation study using a cell-penetrating ASH2L-peptide mimetic that selectively inhibits growth of MYC-driven acute lymphoblastic leukemia cells and multiple MLL-rearranged leukemic cell lines[34]. Furthermore, there was a significant downregulation of H3K4me3 using *in vitro* methylation assays and Western Blot analysis[34]. Using a high throughput MTS Cell Viability screen, we identified a small molecule compound with potent, low nanomolar activity herein called SRI-41155. SRI-41155 selectively targets the MLL-rearranged leukemia cell line MOLM13, harboring a MLL1-AF9 fusion protein. Importantly, it does not show efficacy in K562 cells that have WT-MLL1 expression[35,36]. Ultimately, we have discovered a compound that selectively targets MLL-rearranged leukemic cell growth both *in vitro* and *in vivo* with a broad therapeutic window that exhibits minimal toxicities. While this compound does not have the properties to be tested in human clinical trials, it can be utilized as a tool compound to characterize DPY30 regulation in Mixed Lineage Leukemia and will provide insight for future chemical design in pursuit of developing the first small molecule inhibitor of DPY30.

Results

SRI-41155 was Identified as a Potent Inhibitor of MLL-Rearranged Leukemia Cells

SRI-41155 was identified through a collaboration between Southern Research and UAB that sought to identify novel small molecule inhibitors of the DPY30/ASH2L protein interaction. Using a biochemical fluorescence polarization assay (FPA), molecules were selected based on their inhibition of a FITC-ASH2L peptide bound to recombinant DPY30 protein (method highlighted in Figure 1B)[37]. Compounds with a positive response, or hits, from the biochemical screen were characterized using two validated *in vitro* cell culture

leukemia model systems, MOLM13 and K562 suspension cell lines[34]. MOLM13 cells are highly sensitive to the knockdown of core subunits of the SET/MLL complex including DPY30 or alternatively, to decreased MYC expression[24,38]. Stable knockdown of DPY30 promotes cell cycle arrest and ultimately senescence, an important phenotype for our future studies[38-40]. Conversely, K562 cells are uninhibited by the knockdown of DPY30, making this cell model an ideal candidate for studying off-target cytotoxicity[34,38]. Thus, the goal of the *in vitro* cell line screening was to identify hits that selectively inhibited MOLM13 cells but had no effect in K562 cells, suggesting that they remain on-target through the inhibition of the DPY30/ASH2L interaction.

Using these two cell models, we tested the positive hits from our biochemical screen using an MTS assay, a high throughput, cost-effective metabolic viability assay. This assay relies on the oxidation of tetrazolium salt by the NADPH-dependent dehydrogenase to generate a colored dye detectable at the 490 nm wavelength (protocol description adopted from abcam.com). Uniquely from the other compounds screened, SRI41155 showed low nanomolar IC50s in the MTS Assay of 0.133 nM versus K562 cells that showed no change in viability or metabolic response up to 10 μM (Figure 1C). Due to the highly selective and potent nature of this compound, we proceeded to characterize SRI41155 using more selective readouts to identify the mechanism of action of our lead candidate from the high throughput screen.

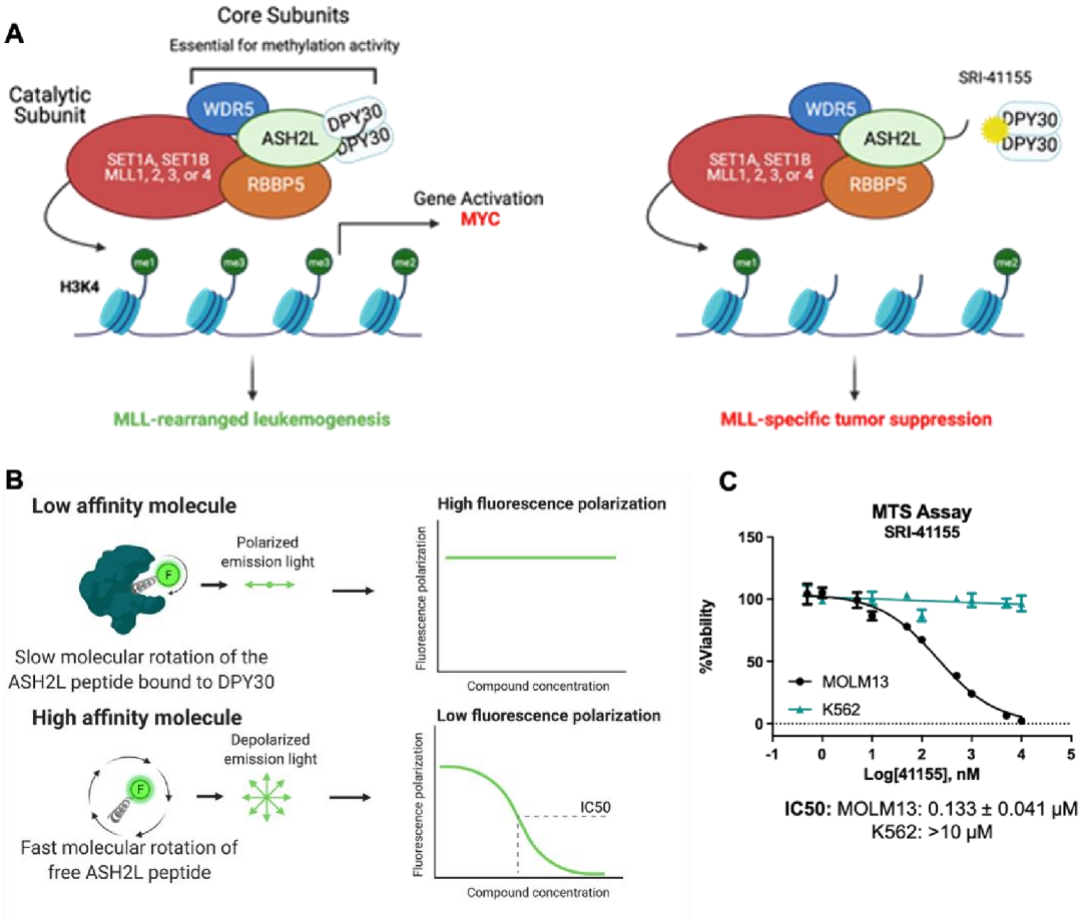

Figure 1. DPY30 as a target in MLL-rearranged leukemia. A. Overview of the targeting strategy in MLL-rearranged leukemia. **B.** Overview of the fluorescence polarization assay (FPA) used for biochemical screening and the initial identification of SRI-41155. **C.** MTS screening assay after SRI-41155 treatment for 72 hours in MOLM13 (black) vs. K562 (blue) cells. The IC50 is reported as the mean ± range in biological triplicate, with the graph showing one representative assay in technical triplicate. These assays have reproducibly been performed with four different lots of SRI-41155 with the above treatment from Lot04.

DPY30 and MYC Expression are Downregulated in Response to SRI-41155

Previous studies have shown that DPY30 directly modulates the growth of MLLrearranged leukemia cells, but it does not impact the oncogenic phenotype of the CML cell line K562, which is consistent with the screening data presented in Figure 1C[24,34,38]. To determine if SRI-41155 has an impact on DPY30 expression, we treated cells with 100

nM, 250 nM, and 500 nM compound for 48 hours. To our surprise, the DPY30 mRNA levels not only exhibited a statistically significant decrease, but they were downregulated close to non-detectable levels (Figure 2A). Furthermore, DPY30 protein expression was downregulated at concentrations as low as 100 nM, suggesting that SRI-41155 alters the regulation of DPY30 expression (Figure 2B).

DPY30 has previously been shown to regulate H3K4me3 over other histone modifications written by the SET/MLL HMT complex[19,24]. For instance oncogenes, such as c-MYC, are activated in MOLM13 cells due to aberrant H3K4me3 of the MYC promoter region[24]. Due to the decrease in DPY30 mRNA and protein expression, we sought to determine if SRI-41155 had an epigenetic impact on the H3K4 histone methylation status through western blot analysis. Similarly to the protein expression levels of DPY30, H3K4me3 was downregulated concurrently with the decrease in DPY30 (Figure 2B). Similarly to DPY30 and H3K4me3, c-MYC also exhibited decreased protein expression in a dose-dependent manner at concentrations starting as low as 500 nM (Figure 2B). Ultimately, similarly to DPY30, we observe a dose-dependent decrease in c-MYC expression at the mRNA level and a parallel decrease in the expression of two MYC target genes, CDCA7 and MCM3, which have previously been shown to be downregulated in response to DPY30 knockdown[38] (Figure 2C). These data demonstrate that SRI-41155 induces downregulation of DPY30 at the mRNA and protein levels. In addition to the decrease in DPY30, there is a decrease in H3K4me3 status, and inhibition of MYC and MYC target genes. SRI-41155 highlights a novel therapeutic avenue for epigenetic targets in cancer and an advancement in the quest to target the previously undruggable oncogene, MYC.

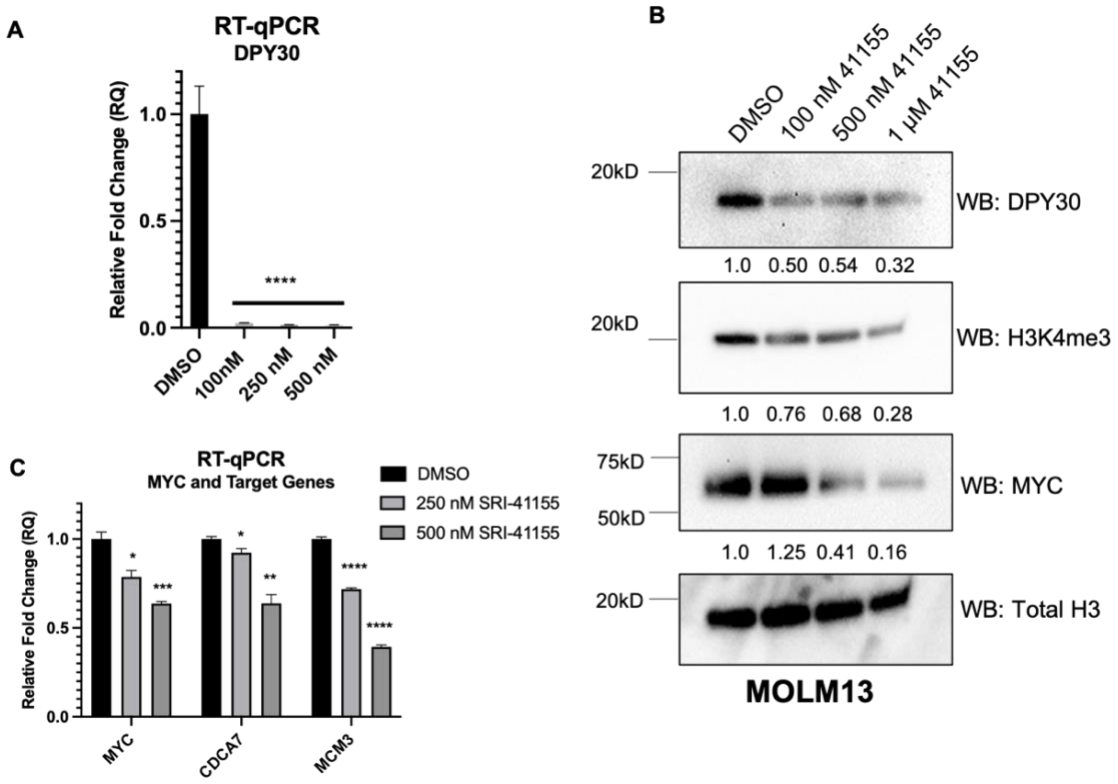

Figure 2. SRI-41155 downregulates DPY30, H3K4me3, and MYC. A. TaqMan RTqPCR analysis of DPY30 mRNA after treatment with SRI-41155 compared to a DMSOtreated control in MOLM13 cells. Cells were treated for 48 hours. **B.** Western Blot (WB) analysis of MOLM13 cells treated with an SRI-41155 dose-response. Targets include DPY30, H3K4me3, MYC and Total Histone H3 (loading control). The quantifications of band intensity are relative to the Total Histone H3 and the DMSO negative control. **C.** TaqMan RT-qPCR analysis of MYC and MYC target genes, CDCA7 and MCM3, after 48-hour treatment with SRI-41155. All RT-qPCR was performed in technical triplicate. Error represents the SD. P-values: * < 0.05, ** < 0.01, *** < 0.001, **** < 0.0001 using a Student's t-test comparing the DMSO control versus each experimental group.

MLL-Rearranged Leukemic Cell Growth is Selectively Inhibited by SRI-41155

Cell viability assays such as the MTS assay are valuable for high throughput screening but ultimately cannot differentiate between a change in cell number due to inhibition of proliferation or cell death. To begin investigating the mechanism of SRI41155 on MOLM13 cells, we analyzed cell growth curves over five days treated with 100 nM, 250 nM, and 500 nM SRI-41155 or DMSO as the vehicle control (Figure 3A). At all three concentrations of SRI-41155, we observed a significant decrease in MOLM13 cell number

over five days. 100 nM SRI-41155 had a significant decrease at 96 and 120 hours (data not shown), whereas 250 nM and 500 nM significantly impacted cell number as early as 48 hours (Figure 3A). Importantly, we observed only a mild decrease in Trypan Blue cell viability, suggesting that other mechanisms are contributing to the decreased cell growth following SRI-41155 treatment (Figure 3A and 3B).

Due to the impaired cell growth without a large induction of cell death, we tested the apoptotic-specific response to ensure the change in cell number was not due to an increase in apoptosis. Using Annexin V/PI staining and flow cytometry analysis, we confirmed that low-dose concentrations of SRI-41155 only mildly increases apoptosis (Figure 3C and 3D). Conversely micromolar concentrations, particularly 10μM SRI41155, significantly increased apoptotic induction in MOLM13 cells (Figure 3C and 3D). K562 exhibited no signs of cell death or apoptosis in the Trypan Blue or Annexin V/PI experiments, respectively (Figure 3E, Supplemental Figure 1).

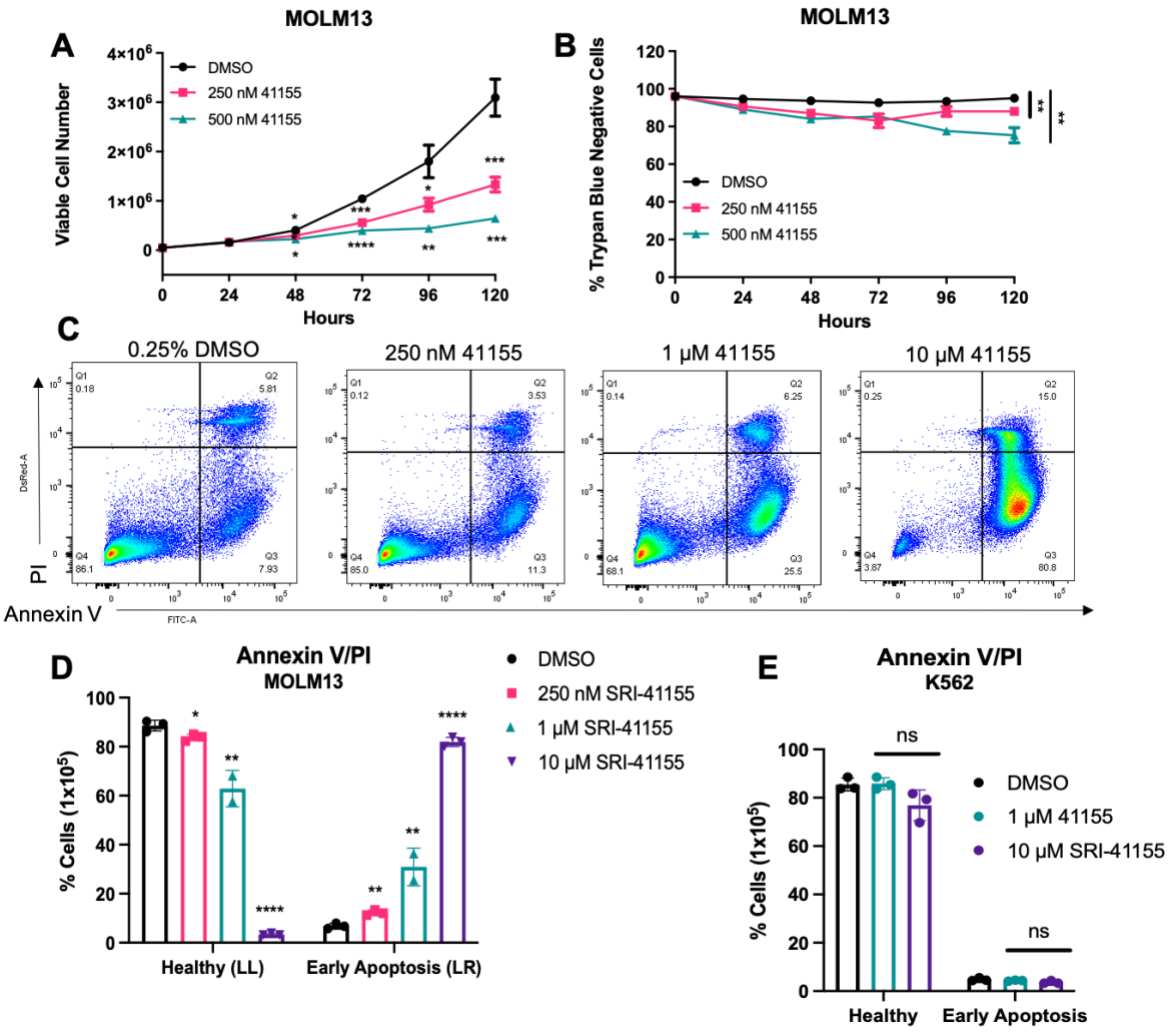

Figure 3. SRI-41155 inhibits MOLM13 cell growth without robust apoptotic induction. A. MOLM13 growth curves after 250 nM and 500 nM SRI-41155 treatment over five days. Plots are displayed in biological triplicate with the SD. Student's t-test at each time point was used for statistical analysis. **B.** At each timepoint from **A.**, cell viability was measured through Trypan Blue (TB) cell viability staining and plotted as a function of time with the SD (N=3). One-way ANOVA was used for statistical analysis. **C.** Annexin V/PI Staining followed by flow cytometry analysis. 100,000 cells were quantified per sample in a biological N=4. The four quadrants are as follows: Lower Left (LL): Healthy cells, Lower Right (LR): Early apoptosis, Upper Right: Late apoptosis/dead cells. Flow cytometry was performed after 96-hour treatment with SRI-41155. **D,E.** Quantification of the healthy and the early apoptosis cell populations as they show significant changes in MOLM13 cells. **E.** K562 do not show significant change as high as 10 µM SRI-41155. Bar graphs shown in biological triplicate with the SD plotted. P-values reported for statistical analysis, * < 0.05, ** < 0.01, *** < 0.001, **** < 0.0001.

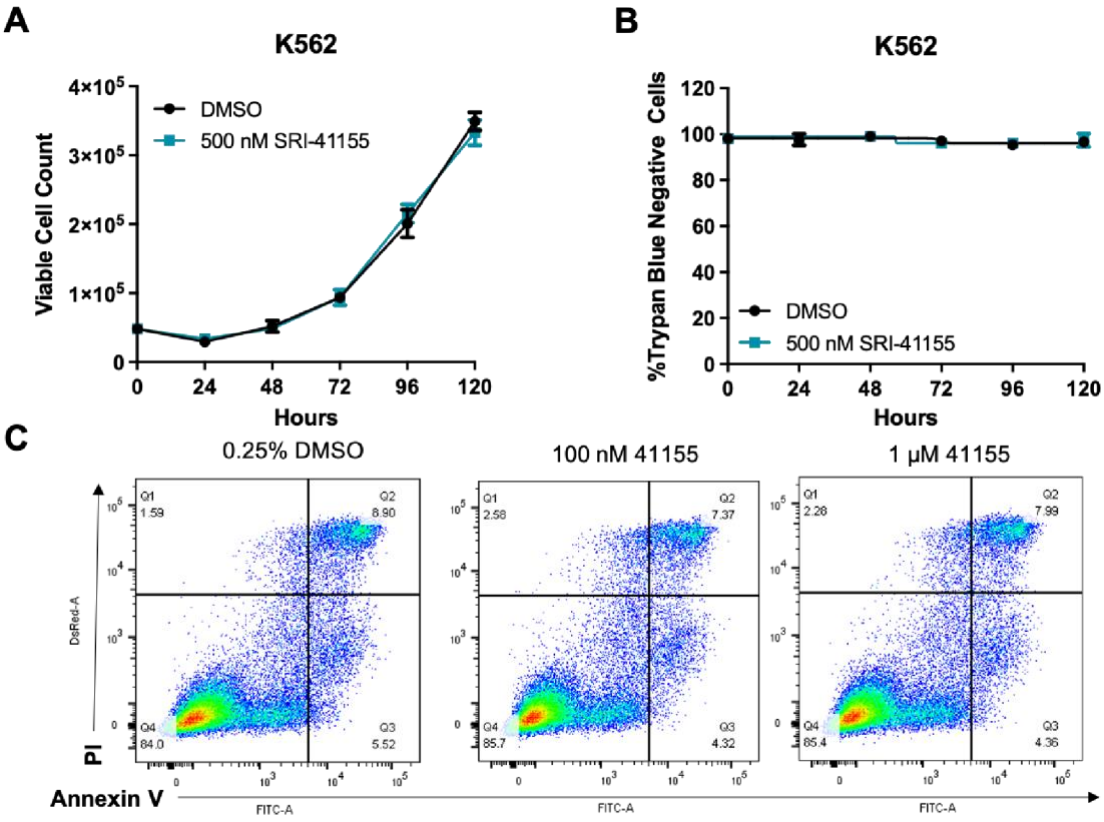

Supplemental Figure 1. 500 nM SRI-41155 has no impact on K562 cell viability or growth. A. K562 cell growth over 5 days after 500 nM SRI-41155 treatment compared to DMSO treated cells. **B.** At each time point from **A.**, cell viability was measured in biological triplicate through TB cell viability staining and plotted as a function of time with the SD. **C.** Annexin V/Propidium Iodide (PI) Staining followed by flow cytometry analysis. 100,000 cells were quantified per sample in biological triplicate. The negative data in this figure is not statistically significant.

One of the disadvantages of the MTS assay is that it measures the number of metabolically active mitochondria, which are highly variable between cell lines and does not always correlate with cell viability or cell death[41]. Furthermore, quantifying cell number over time does not delineate between cells undergoing apoptosis, senescence, or another non-canonical cell death pathway that could ultimately modulate cell growth. Cell growth curves are an inexpensive cell proliferation assay, but they also can be biased by the number of cells seeded or loss during harvesting[37,42]. The CellTrace Violet (CTV) flow cytometry

assay is a fluorescent-based method that is superior to both the MTS assay and cell counting over time as you do not have metabolic requirements or cell number bias that limit reproducibility of the other assays[43]. The CTV assay uses a non-toxic cell permeable dye that is stable in cell culture for more than 96 hours. This method can be multiplexed with other stains to gate out dead cells and debris that may otherwise impact the quantification of cell growth over time. Lastly, CTV is a single cell measurement, making it superior for quantification and data analysis over cell growth curves.

To complement the *in vitro* leukemic growth curves, we performed the CTV assay over 96 hours at 250 nM and 500 nM SRI-41155 treatment (Figure 4A and 4B). For this assay, we multiplexed the CTV cell permeable dye with a Live/Dead cell stain (*i.e.* Propidium Iodide or PI). Using these two stains, we can quantify the number of cell divisions a population of cells undergoes over 96 hours through single cell flow cytometry quantification[43]. Here, we show that post-SRI-41155 treatment, less MOLM13 cells are in the leading dividing cellular fraction compared with the DMSO control as early as 48 hours (Figure 4A). Additionally, the number of cells undergoing mitotic division correlates with the dose. For example, at 96 hours, there is minimal overlap between the DMSO control cells and 500 nM SRI-41155 (Figure 4A). At 500 nM treatment, cells predominantly are in the second or third cell division (2G, 3G) after four days. In contrast, the DMSO treated control cells are predominantly in the fourth or fifth cell division (4G, 5G) (Figure 4B). 250 nM SRI-41155 treatment seems to have a lesser impact, with significantly more cells remaining in the 2G and 3G fractions and less in the 5G fractions, compared to the DMSO control (Figure 4B). While this is a similar trend as observed with 500 nM treatment, there is no significant difference in the 4G fraction, whereas the 500 nM SRI-41155 has significantly less cells (Figure 4B). At every generation after the first cell division, the 250

nM and 500 nM treatments provide dose-dependent changes in cell proliferation (Figure 4B). Therefore, we can confidently conclude that there is a significant change in cell proliferation that occurs in a dose-dependent manner, irrespective of cell death or apoptosis. Importantly, there was no impact on proliferation or apoptosis in control K562 cells, highlighting the selectivity for the MLL-rearranged cell model (Figure 4A).

It has been previously reported that DPY30 coordinates senescence through the regulation of Inhibitors of Differentiation or ID proteins[39]. These proteins (*i.e.* ID1-4) are known negative regulators of the ETS family of transcription factors which activate cell cycle inhibitors such as CIP/KIP proteins, p16 and p21[44,45]. The knockdown of DPY30 induces senescence by the induction of ETS1/2 and the subsequent activation of p16 and p21[39]. Thus far, we have shown that SRI-41155 specifically inhibits cell proliferation in MLL-rearranged MOLM13 cells. Furthermore, at nanomolar concentrations, SRI-41155 does not induce a large increase in apoptosis or other cell death pathways, suggesting the senescent mechanism previously seen with DPY30 knockdown. In Figure 4C, we show that there is an increase CIP/KIP cell cycle inhibitor p21 at 100 nM SRI-41155 treatment at 48 hours. The elevated levels of p21 suggests that SRI-41155 inhibits cell proliferation through a senescent, non-apoptotic mechanism at nanomolar concentrations that shifts toward an apoptotic phenotype at increasing micromolar dosing. Importantly, there is no evidence of senescence or apoptosis in WT-MLL1 cell line, K562 (Supplemental Figure 1) .

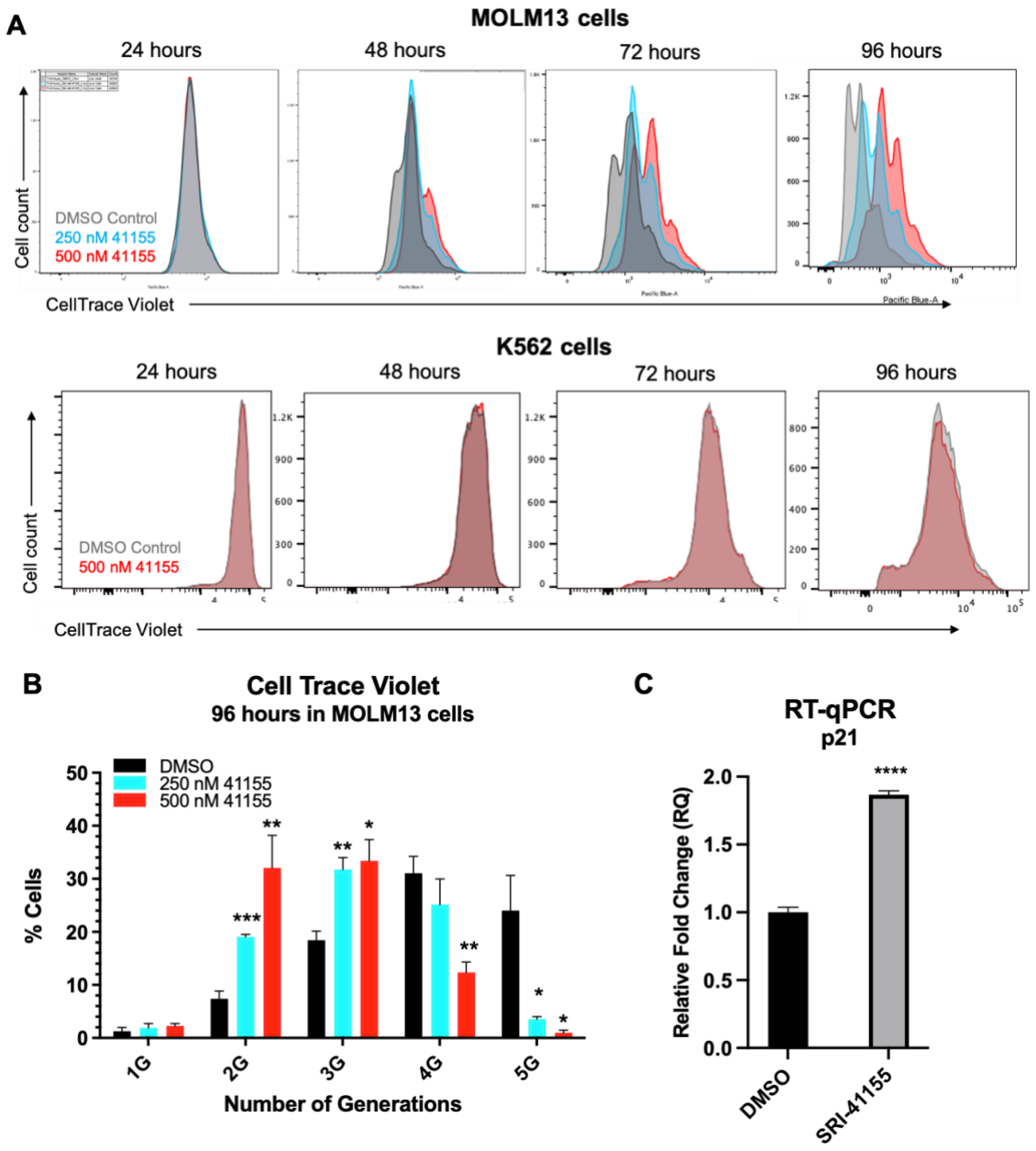

Figure 4. SRI-41155 inhibits cell proliferation through senescence. A. Histogram plots from the CellTrace Violot (CTV) flow cytometry cell proliferation assay over time. DMSO (gray), 250 nM (cyan), and 500 nM SRI-41155 (red) treated MOLM13 cells (top) and K562 (bottom) were analyzed every 24 hours and overlayed in FlowJo. **B.** MOLM13 CTV quantification at 96 hours. Each peak from **A**. represents one cell division or generation (G). **C.** TaqMan RT-qPCR analysis of p21 as a marker of senescence after treatment with 100 nM SRI-41155. P-values reported for statistical analysis, * < 0.05, ** < 0.01, *** < 0.001, **** <0.0001.

SRI-41155 Is Active In Three-Dimensional MOLM13 Models

Under normal cell culture conditions *in vitro* (*e.g.* RPMI 1640 Media supplemented 2.5% to 10% Fetal Bovine Serum or FBS), MOLM13 cells grow in suspension and form small 3D spheres during normal passaging. With very low concentrations of DMSO (*i.e.* 0.25%), the cells form large 3D clumps and display a spheroid-like morphology without any solid/gel matrix support (Figure 5A). At concentrations as low at 10 nM SRI-41155, the 3D spheroids grown in RPMI supplemented with 2.5% FBS are smaller in diameter compared to negative control-treated MOLM13 cells (Figure 5A). Furthermore, there is a dose-dependent decrease in the diameter of these 3D-spheroids with increasing concentrations of SRI-41155. For this experiment, an inactive analog called SRI-41154 was used for the dose-dependent negative control (Figure 5A). K562 cells do not display a similar 3D cell clumping phenotype that is seen with MOLM13 cells under normal *in vitro* culture conditions, prompting us to investigate pharmacokinetic parameters of SRI-41155 and exploration in other *in vitro* leukemic model systems.

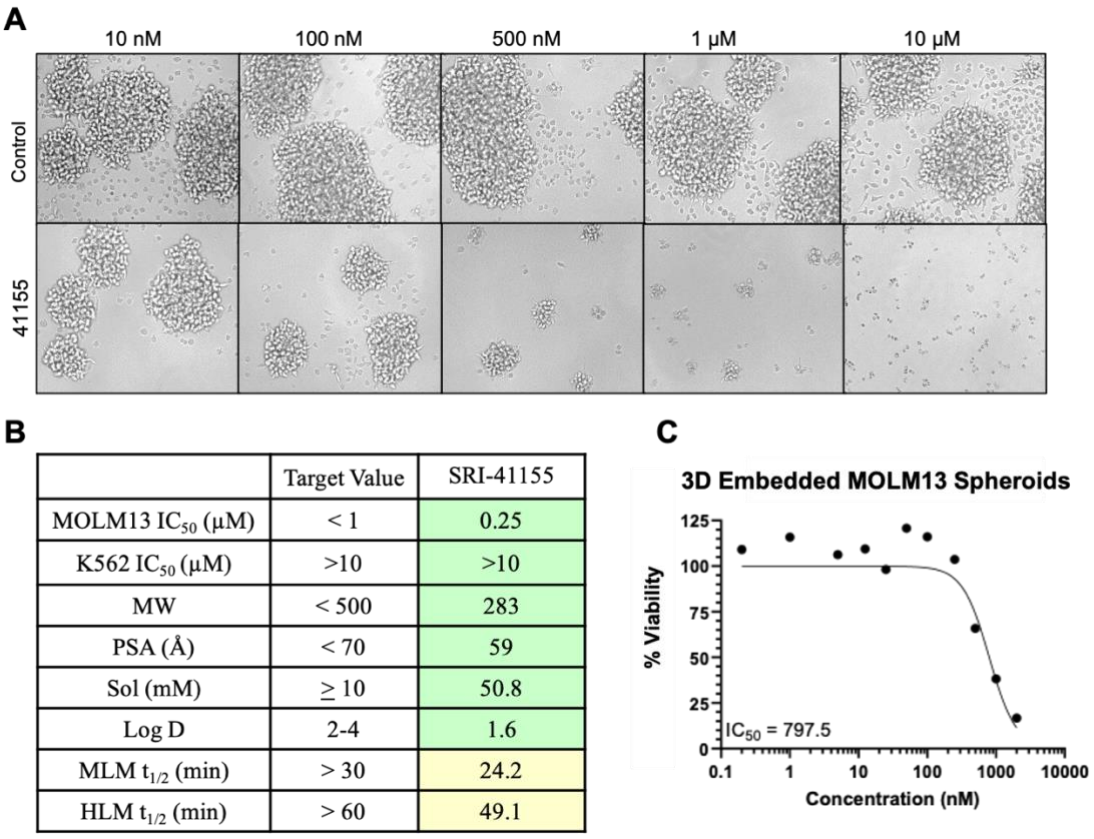

	Target Value	SRI-41155
MOLM13 IC_{50} (µM)	< 1	0.25
K562 IC_{50} (µM)	>10	>10
MW	< 500	283
PSA (Å)	< 70	59
Sol (mM)	≥ 10	50.8
Log D	2-4	1.6
MLM $t_{1/2}$ (min)	> 30	24.2
HLM $t_{1/2}$ (min)	> 60	49.1

Figure 5. SRI-41155 has suitable pharmacokinetic properties for translational modeling. A. Brightfield images of MOLM13 cells treated with SRI-41155 or negative control compound SRI-41154 (inactive analog). Images taken at 10X magnification on an EVOS FLoid Microscope. **B.** Summary table of PK results for SRI-41155 with target and experimental values. Experimental SRI-41155 results highlighted in green where values were within the target range; yellow indicate borderline values that are not out of the target range. **C.** Using a 3D-culture method that mimics the *in vivo* tumor microenvironment, SRI-41155 still retains MOLM13 cell killing with an IC50 = 797.5 nM.

MOLM13 and K562 are both suspension cell lines, but behave differently in culture media prompting us to investigate the use of SRI-41155 using an extracellular matrix to support 3D-spheroid formation. Three-dimensional culture systems have become increasingly popular in drug discovery efforts as they provide predictive indictors for small molecule efficacy *in vivo*[46]. Three dimensional *in vitro* culture methods better represent the spatial organization of a tumor and recapitulate the signaling network of the natural tumor microenvironment[47]. To determine if SRI-41155 would be suitable for translational model

system applications and ultimately an *in vivo* mouse study, we characterized the pharmacokinetic (PK) parameters listed in Figure 5B.

Pharmacokinetic studies of investigational compounds are vitally important to understand both how the compound is metabolized and if it will be stable enough to achieve a durable therapeutic response. The PK properties classically characterized are Absorption (A), Distribution (D), Metabolism (M), and Excretion (E). ADME properties essentially describe how the compound enters systemic circulation, how it moves about the body, how it changes and degrades over time, and how it leaves the body, respectively[48]. Using general lead optimization and drug discovery guidelines based on Lipinski's "rule of five[49]", cutoffs were generated for each parameter prior to the start of the SRI-41155 characterization study (Target, Borderline Target, and Out of the Target)[50]. Highlighted in green in Figure 5B, three out of the five PK parameters were within our target window and two out of the five were borderline (yellow). Importantly, none of the factors we characterized were outside of our target window and therefore would limit further investigation (red not indicated for SRI-41155). Amongst these, the Polar Surface Area (PSA), Drug Lipophilicity (LogD), and Solubility were all within the optimal range at 59Å, 1.6, and 50.8 mM, respectively (target range < 70Å, 2-4, and >10 mM). The PSA represents the polar portion of the compound that solvent-accessible and the LogD is a measure of how lipophilic the compound is[51,52]. Optimizing both PSA and LogD improves *in vivo* potency and can help avoid dose-limiting toxicities[52]. The two borderline values, Human and

Mouse Liver Microsome half-life (HLM and MLM $t_{1/2}$) were 49.1 minutes and 24.2 minutes, respectively (Figure 5B). While these values were not within the optimal target range of >60 minutes and >30 minutes, many therapeutics do not comply the "rule of five", including ~50% of orally bioavailable small molecule FDA-approved therapeutics[53].

With promising PK values that were largely within or near the target range, we sought to determine the potency of SRI-41155 in three-dimensional organoid modeling supported by an extracellular matrix containing factors at mimic the tumor microenvironment such as laminin and collagen IV *in vivo.* The organoids were seeded at $8x10^4$ cells/sphere and treated with an SRI-41155 dose-response for 96 hours. Using an MTS assay that was adapted from our original screening protocol, SRI-41155 had an IC50 in 3D culture of 797.5 nM (Figure 5C) with no efficacy in K562 cells (data not shown). This increase in IC50 from our original MTS assay is common amongst investigational and FDA-approved therapeutics as the 3D model fosters cell-to-cell interactions and recapitulates the complex environment that surrounds tumor tissue[54,55]. Efficacy in this model system was promising as it showed that SRI-41155 was able to penetrate an extracellular matrix-like environment and still elicit nanomolar potency on MOLM13 cells *in vitro*.

SRI-41155 Inhibits Tumor Burden In Vivo

Pharmacokinetic (PK) parameters specific for *in vivo* mouse models are important with experimental therapeutics to determine the dose, route of administration, and dosing schedule. To determine the *in vivo* PK profile for SRI-41155, three mice were dosed per cohort at 1 mg/kg intravenously (IV) or 10 mg/kg intraperitoneally (IP). SRI-41155 was optimally formulated in 20% NMP, 40% PEG, and 40% saline based on prior PK studies. The two routes of administration were characterized measuring the half-life ($T_{1/2}$), the maximum concentration (C_{max}), the time it takes to reach the maximum concentration (T_{max}), and the Area Under the Curve (AUC). Directly comparing the half-life of the two injections, the stability of SRI-41155 *in vivo* was far superior using IP injection at 10 mg/kg, improving the $T_{1/2}$ from 0.37 hours (IV) to 1.44 hours (IP). Furthermore, the C_{max}

with IP injection was 283 ng/mL (~1 μM) that was achieved at 0.08 hours or approximately five minutes after administration. Lastly, the amount of SRI-41155 that reaches systemic circulation with the 10 mg/kg IP injection is 77%. Given the bioavailability (%F) of this compound, we proceeded with a small proof-of-concept animal study. All *in vitro* and *in vivo* PK results are summarized in Figure 5B and Table 1.

Table 1. Overview of the pharmacokinetic parameters for *in vivo* studies of SRI-41155.

[a]$T_{1/2}$ (h) by IV	0.37
[b]$T_{1/2}$ (h) by IP	1.44
T_{max} (h)	0.08
C_{max} (ng/mL)	283 or 1 μM
AUC_{last} (h*mg/mL)	177
Bioavailability (%F)	77

[a] 1 mg/kg, N = 3
[b] 10 mg/kg, N = 3

MLL-rearranged leukemia animal models are highly controversial as they do not accurately recapitulate human acute leukemia due to the myriad to MLL-fusion proteins causing oncogenesis[11,56]. Furthermore, despite only a single genomic aberration, the MLL1-AF4 fusion protein, which is observed in MOLM13 cells, has been exceedingly difficult to model in mice, commonly leading to embryonic lethality or a non-acute malignant hematology phenotypes (*e.g.* B-cell lymphomas)[56]. Therefore, for our experimental proof-of-concept studies, we proceeded with a simpler model to determine if there was an efficacious response worth pursing more complex systems.

To determine if SRI-41155 has *in vivo* efficacy, immunodeficient Athymic Nude mice were injected subcutaneously with $1x10^6$ MOLM13 cells in Matrigel, the same

extracellular matrix used for the 3D-spheroid studies (Figure 6A and 5C). Once the MOLM13 tumor xenografts measured 75 mm^3 to 144 mm^3 (day 11), the mice were injected with SRI-41155 or a saline control through IP injection daily for two weeks (Figure 6A). The primary goal for this study was to determine if SRI-41155 would inhibit leukemic cell proliferation as seen *in vitro* and highlight any evidence of hematopoietic toxicity. At the start of this experiment, there were seven mice per experimental group. Initially, the proposed dosing schedule included a 10 mg/kg IP injection, twice daily based on the 77% bioavailability and the limited half-life and stability of this compound (Figure 5B and Table 1). After the first two days of SRI-41155 treatment, there were unexpected toxicities including lethargy and hypothermia prompting us to alter the dose schedule to once daily and euthanize three of the mice in our treatment group. Therefore, at the conclusion of this experiment, there are seven saline-treated control mice, but only four mice in the experimental SRI-41155 treatment group.

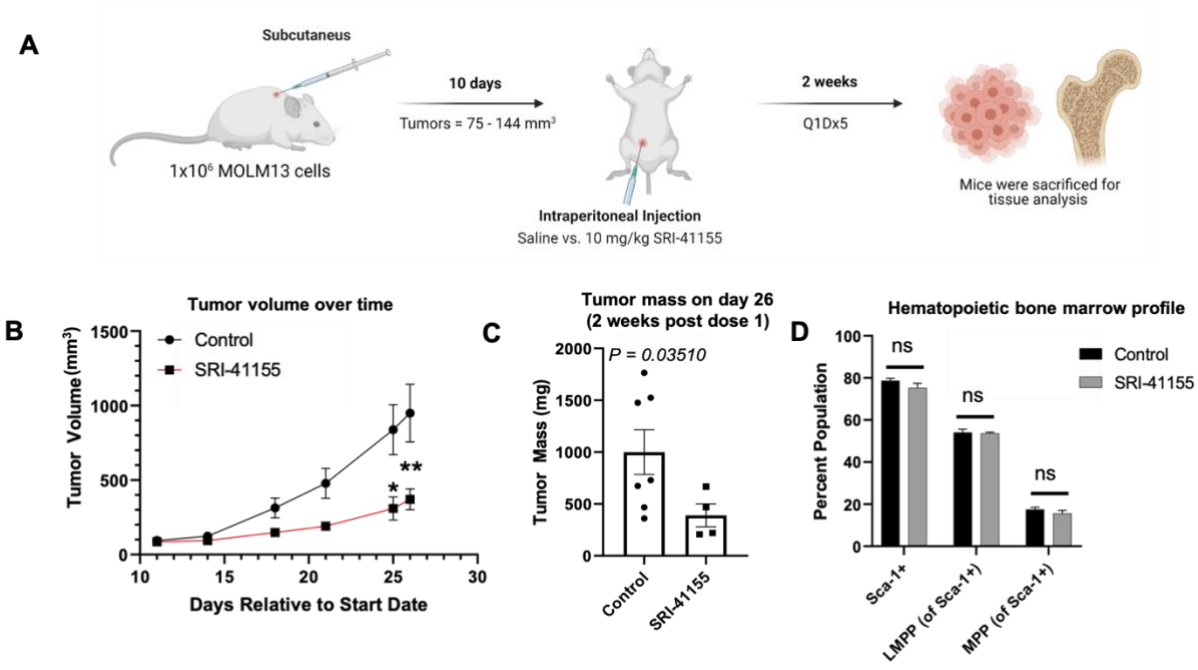

Figure 6. Treatment *in vivo* with SRI-41155 reduces tumor burden with no evidence of bone marrow toxicity. A. *In vivo* dosing schedule and protocol for the proof-of-concept animal study using SRI-41155 to treat subcutaneous MOLM13 tumors. **B.** Tumor volume measured over time through the course of the *in vivo* study over 26 days. **C.** Tumor mass (mg) quantified after the termination of the study. All points are individually plotted for clarity with a significant decrease in the treated group. **D.** Analysis of hematopoietic stem cells (*i.e.* Sca-1+) and progenitor populations (LMPPs, MPPs). There was no significant difference seen in saline versus SRI-41155 treated groups.

On day 26, which was two weeks after the first administered dose, all mice were sacrificed for tissue analysis. The metrics analyzed in this study include tumor volume over time, final tumor mass, and bone marrow for hematopoietic progenitor quantification. Significantly, prior to the end of the study on day 25, tumor volume was significantly decreased in the SRI-41155 treated group versus the control (Figure 6B). Furthermore, the final tumor mass was significantly higher in the saline treated group, highlighting the efficacy of SRI-41155 on bulk tumor burden (Figure 6C).

Independent of the tumor tissue analysis, bone marrow samples were collected and sorted from control and SRI-41155 treated mice. This analysis is critical for the future of

these studies as DPY30 knockout *in vivo* has previously been reported to induce pancytopenia due to a lack of hematopoietic progenitor cell (HPC) differentiation[19,38]. Importantly, SRI-41155 had no significant impact on hematopoietic stem cells (HSCs) or the two HPC populations, lympho-myeloid progenitors (LMPP) or multipotent progenitors (MPPs) (Figure 6D). This suggests that there is no evidence of bone marrow toxicity that was largely our biggest concern for the future of this target. Both the tumor analysis and the bone marrow studies provide an exciting proof-of-concept foundation to investigate future compounds targeting the core subunits of the MLL complex, highlighting DPY30 specifically as a candidate for further investigation.

Discussion

In summary, we have identified and characterized a first-in-class novel small molecule that inhibits the expression of DPY30, c-MYC, MYC target genes, and global H3K4me3. This work is highly important as MYC is one of the most dysregulated genes in human cancer and has been a therapeutic target for decades. Despite significant effort, MYC has largely remained 'undruggable' until the recent development of epigenetic inhibitors[25-27]. Thus, here we show that inhibition of DPY30 is a viable strategy to modulate MYC expression through inhibition of the gene activating pattern, H3K4me3.

Consistent with previous genetic manipulation studies, decreased DPY30 expression through SRI-41155 treatment inhibits the growth and proliferation of MLLrearranged leukemia cells through the induction of senescence[34,38,39]. While the pharmacokinetic parameters do not warrant the use of this compound in human studies, it is an important proof-of-concept foundation for the future of this target. Importantly, SRI41155 exhibits nanomolar potency in pre-clinical MLL-rearranged leukemia cell line

MOLM13 and has *in vivo* efficacy in mouse studies without significant bone marrow toxicity or evidence of pancytopenia.

Through this work, we have demonstrated the progression of a compound initially identified through a highly selective florescence polarization assay (FPA) optimized for high throughput screening (Figure 1B). Furthermore, we characterized its on-target efficacy through every phase of pre-clinical development including biochemical assays, *in vitro* cell culture experiments, three-dimensional modeling, and an *in vivo* mouse study. While this compound exhibits the characteristics of an inhibitor of DPY30, there are two possible mechanisms of how this compound elicits efficacy in MOLM13 cells. Initially, this compound was selected from a biochemical screen designed to identify compounds that directly inhibit the DPY30-ASH2L protein interaction[37]. While SRI-41155 may bind and inhibit the DPY30-ASH2L interaction *in vivo,* we have not been able to definitely test this in cells. Part of the reason we cannot perform endogenous co-immunoprecipitation experiments after dosing with SRI-41155 is due to the downregulation of DPY30 after treatment. This observation suggested a second possible mechanism where DPY30 is downregulated in response to SRI-41155 treatment but does not necessarily inhibit the interaction with ASH2L in cells. In this scenario, the transcriptional downregulation of DPY30 still translates to a dampened H3K4me3 pattern, ultimately downregulating oncogenic MYC expression through DPY30 manipulation.

The two mechanisms proposed above elicit the same impact on the highly undruggable oncogene, MYC[24,57]. If SRI-41155 inhibits the DPY30-ASH2L protein interaction as suggested by to the biochemical *in vitro* screening assay, c-MYC is downregulated through the inhibition of H3K4me3 secondary to the disruption of the

SET/MLL complex. Conversely, if SRI-41155 transcriptionally alters the expression of DPY30 through an alternative mechanism, this stimulates a domino effect where knockdown of DPY30 expression still disrupts the H3K4 methylation patterns and therefore, downregulates MYC expression through epigenetic modulation. Either mechanism is plausible, and they are not mutually exclusive. There is a scenario where SRI-41155 inhibits the DPY30-ASH2L interaction, creating a feedback mechanism to downregulate the expression of DPY30 at the mRNA and protein level. As there are chemical modifications and structure-activity-relationship (SAR) studies ongoing to optimize the chemical stability of SRI-41155 for further investigation, the mechanism of this first-in-class compound will continue to be examined. Ultimately for these studies, the goal of modulating MYC expression through a DPY30-dependent mechanism has been largely achieved.

While SRI-41155 has been an essential steppingstone to interrogate DPY30 as a therapeutic target in MLL-rearranged leukemia, there are current limitations of the compound structure that will require optimization for future *in vivo* studies and ultimately, for the filing of an Investigational New Drug (IND) application for human-use. Foremost, although the stability of SRI-41155 is borderline within range of the target values, it still remains out of the ideal therapeutic window in human and mouse liver microsome stability testing (Figure 5B). Microsomal stability is an indicator for *in vivo* stability and metabolism by cytochrome P450[58]. Sub-optimal mouse microsomal stability highlights the etiology of the compound's short half-life *in vivo* and the rapid C_{max} at approximately 5 minutes after administration. Continuous improvements of the PK will enhance the stability of the compound and therefore translate to better efficacy in future studies. Importantly, other characteristics of the metabolic stability like LogD and solubility are within the optimal

range, highlighting the promising nature of this compound as a prototype scaffold for improved pharmacokinetic and pharmacodynamic efficacy with further optimatization[58].

At the initiation of this project, we selected MLL-rearranged leukemia as our model system for several reasons. First, MLL-rearranged leukemia cell lines are highly sensitive to the knockdown of DPY30 and MYC[24,34,38]. Furthermore, MLL-rearranged leukemia is clinically highly aggressive and lacks the overall response rates of other hematologic cancers. Therefore, there is a need for new targeted therapeutics for this subtype of acute leukemias[1]. Importantly for our selection process, MLL-rearranged leukemias lack the genetic complexity of other solid tumor models that rely on MYC expression. For example, MYC expression is highly dysregulated in triple negative breast cancer (TNBC) but is commonly associated with the loss of other tumor suppressors such as p53, retinoblastoma protein, RB, and breast cancer susceptibility gene-1, BRCA1[59]. Outside of TNBC, MYC amplification has been identified as a common, but not exclusive, oncogene in gastric cancer[60], epithelial ovarian cancer[61,62], pancreatic ductal adenocarcinoma[63,64], and other cancer cell types[65]. Using MLL-rearranged leukemia as our model system allows us to easy track the on-target efficacy of our compound, but once the optimization is complete, it will be applicable across the entire oncology disease continuum as MYC dysregulation is frequently a prominent molecule feature of human malignancies[57,65].

In conclusion, we have identified a novel therapeutic target in DPY30 capable of modulating the highly dysregulated oncogene, MYC. While these studies were characterized in Mixed Lineage Leukemia, there are many other cancer cell types that will benefit from an optimized version of SRI-41155. This compound will be the prototype for a new class of targeted therapeutics modulating the SET/MLL histone methyltransferase

complex. Lastly, SRI-41155 can be utilized as a tool compound for pre-clinical studies to directly analyze the impact of DPY30 knockdown in other cancer cell types and diseases.

Materials and Methods

Cell Culture.

MOLM13 and K562 cells were maintained in humidified atmosphere with 5% CO_2 in RPMI-1640 Medium supplemented with 10% fetal bovine serum (FBS), 2.05 mM L-glutamine, 100 units/ml each of penicillin and streptomycin (Anti/Anti, Corning). All cells dosed with SRI-41155 were in RPMI-1640 supplemented with 2.5% FBS (No Anti/Anti during treatment incubations). Cell lines were regularly validated through STR profiling at the Heflin Center Genomics Core Facility at UAB.

MTS Cell Viability Assay.

Cells were seeded at $1x10^4$ cells per well in a flat-bottom clear 96-well plate in RPMI-1640 without phenol red supplemented with 2.5% FBS. Cells were equilibrated for four hours prior to dosing. Once the 4-hour incubation was complete, cells were dosed with SRI-41155 or 0.25% DMSO (negative control) for 72 hours and incubated in a humidified incubator with 5% CO_2. For the MTS Assay, 10 µL MTS reagent (Abcam) was added per well and incubated for 1 hour at 37°C. Plates were read at 490 nm on a Perkin Elmer Victor X5 Plate Reader.

RNA extraction and cDNA synthesis

RNA was purified from MOLM13 cells for RT- qPCR with the SurePrep Total RNA Purification Kit (Fisher BioReagents) by the manufacturer's protocol. The final concentration of purified RNA was measured using a Nanodrop 2000c spectrophotometer.

Once RNA concentration was determined, a single step cDNA synthesis reaction was made in TempAssure PCR 8-Tube Strips (USA Scientific) in technical duplicate as follows: 100ng RNA, 16µL nuclease-free water (Ambion, 1512103), and 4µL qScript cDNA SuperMix (Quanta BioSciences Inc., 84034). The cDNA synthesis reaction per the qScript cDNA SuperMix protocol is 25°C for 5 minutes, 42°C for 30 minutes, and 85°C for 5 minutes with a 4 °C hold. Concentration was determined after the cDNA synthesis on the Nanodrop 2000c spectrophotometer. cDNA was diluted to 25ng/µL into Molecular Biology Grade Water (Corning, 46-000-CM) and stored at −20 °C for future use. Remaining RNA was stored long-term at −80 °C.

RT-qPCR.

All RT-qPCR reactions were performed in technical triplicate. A master mix for each target was made with 15 µL RNAse-free water, 3 µL 20X TaqMan Primers (ThermoScientific), 12 µL 25 ng/µL cDNA and 30 µL TaqMan Universal Master Mix II, with UNG (Applied Biosystems). The mix was aliquoted 3X at 20 µL per well in a 96 well plate. RT-qPCR was performed on a BioRad CFX Opus 384 Real-Time PCR System for 40 cycles starting at 25°C. Each cycle is 50°C for 2 minutes, 95°C for 10 minutes, and 15 seconds, and 60 °C for 1 minute. Temperature shifts at 1.6 °C/s. All data are collected and analyzed using CFX Maestro Software. The primers used for TaqMan studies were predesigned by ThermoFisher with FAM-MGB probes. The Assay IDs are as follows: DPY30: (Hs00261491_m1), MYC (Hs00153408), CDCA7 (Hs00230589_m1), MCM3 (Hs00172459_m1), p21 (Hs00355782_m1).

Antibodies.

All antibodies were diluted in 5% BSA/PBST. Primary antibodies: *DPY30:* Rabbit Polyclonal antibody (Novus, NBP1-91848), *H3K4me3:* Rabbit Monoclonal antibody (Cell

Signaling, 9751S), *MYC:* Rabbit Monocloncal antibody (Cell Signaling, 13987T), *Total Histone H3:* Rabbit Monocloncal antibody (Cell Signaling, 9715S). Secondary antibodies: *Rabbit:* Goat anti-rabbit IgG-HRP, diluted 1:2000 (Cell Signaling).

Western Blots.

Western blots were performed using a histone extraction method to adequately visualize the global methylation expression. Cell pellets were lysed on ice in 50 mM Tris, 500 mM KCl, pH 7.4 supplemented with 100X Halt Protease Inhibitor for 15 minutes. After lysis, the lysates were sonicated for 15 cycles (30 seconds ON, 30 seconds OFF) in a 4°C rotating water bath with a Biorupter. Cell debris was collected at 16,000g x 15 minutes at 4°C and the supernatant was collected for protein quantification by BCA Assay.

An equal concentration of protein was loaded onto precast TGX 10- or 15-well gels (BioRad) and run at 150V for 45 minutes. The transfer was complete using the BioRad wet transfer system onto PVDF membranes activated with 100% Methanol at 100V for 1 hour.

Annexin V/PI Staining.

All Annexin V/PI experiments were performed at 96 hours after SRI-41155 or DMSO treatment. Cells were seeded in a six-well plate at $5x10^5$ cells/well in RPMI-1640 supplemented with 2.5% FBS. Cells and media were collected, and cell number was counted on a BioRad Automated Cell Counter. The final cell pellet was resuspended in 1X Annexin V binding buffer (BD Pharmingen) and $5x10^5$ cells were transferred to a FACS tube containing 5 µL propidium iodide (PI) staining solution (BD Pharmingen) and 5µL FITC-Annexin V (BD Pharmingen). Cells were incubated for 15 minutes and FACS was collected on a BD LSRFortessa at the UAB Flow Cytometry Core Facility. All data was analyzed using FlowJo v10. Compensation controls used for analysis include unstained cells and cells stained for each individual fluorophore (FITC-Annexin V and Cy5-PI).

Gating strategy eliminated cell debris and doublets through forward and side scatter plots.

Cell Trace Violet.

Cells were stained per the manufacturers staining protocol using 5μM CellTrace Violet dye (ThermoFisher, C34571) and seeded in a 6 well plates with $5x10^5$ cells/well. Cells were seeded in RPMI-1640 supplemented with 2.5% FBS and dosing was performed immediately following the staining protocol. Following dosing, cells were incubated in a humidified incubator for 24, 48, 72, or 96 hours. All cells for the CTV experiments were seeded, stained, and dosed on Day 0. Quantification of the results is a biological N=4 on separate days. At each time point, cells were collected and counted with Trypan Blue exclusion dye for comparison. Cells were stained with 5 μL propidium iodide (PI) staining solution (BD Pharmingen) and flow cytometry was collected using a BD LSRFortessa at the UAB Flow Cytometry Core Facility. All data was analyzed using FlowJo v10.

3D Spheroid Culture.

Cells were seeded at $8x10^4$ cells/sphere embedded in Matrigel. Three spheres were seeded/well and dosed with SRI-41155 or negative control compound SRI-44600 from 0.2 nM to 2 μM in an 11-point dose response curve for 72 hours. MTS protocol was performed to determine the IC50 of SRI-41155 in 3D culture.

In Vivo Mouse Study.

Fourteen athymic nude mice were injected subcutaneously with $1x10^6$ MOLM13 cells in a Matrigel suspension. On day 11 post-administration, tumors had grown to a size of 75-144 mm^3 . The mice were dosed with either 10 mg/kg SRI-41155 (N=7) or saline (N=7) through intraperitoneal inject daily for two weeks. The mice were sacrificed after the last dose for tissue and bone marrow analysis. On day two, the dosing schedule was decreased

from BID to once daily injections due to unforeseen toxicities. Mouse studies were performed by RGB through the Southern Research Drug Discovery Division.

Statistical Analysis.

All statistical analysis and representative figures for these experiments were completed in GraphPad Prism unless otherwise stated in the Figure or Methods. For all statistical analysis: ns – non-significant or p-value: * < 0.05, ** < 0.01, *** < 0.001, or **** < 0.0001. All schematic figures were created using templates from Biorender.com.

Acknowledgements

This work was funded by the Alabama Drug Discovery Alliance (ADDA) and the UAB Carmichael Scholarship (HW). MOLM13 and K562 cells were a generous gift from the laboratories of Hao Jiang and Xinyang Zhao.

Chapter 3 References

1 Winters, A. C. & Bernt, K. M. MLL-Rearranged Leukemias-An Update on Science and Clinical Approaches. *Front Pediatr* **5**, 4, doi:10.3389/fped.2017.00004 (2017).

2 Meyer, C. *et al.* The MLL recombinome of acute leukemias in 2013. *Leukemia* **27**, 2165-2176, doi:10.1038/leu.2013.135 (2013).

3 Britten, O., Ragusa, D., Tosi, S. & Kamel, Y. M. -Rearranged Acute Leukemia with t(4;11)(q21;q23)-Current Treatment Options. Is There a Role for CAR-T Cell Therapy? *Cells* **8**, doi:10.3390/cells8111341 (2019).

4 Ziemin-van der Poel, S. *et al.* Identification of a gene, MLL, that spans the breakpoint in 11q23 translocations associated with human leukemias. *Proc Natl Acad Sci U S A* **88**, 10735-10739, doi:10.1073/pnas.88.23.10735 (1991).

5 Hsieh, J. J., Ernst, P., Erdjument-Bromage, H., Tempst, P. & Korsmeyer, S. J. Proteolytic cleavage of MLL generates a complex of N- and C-terminal fragments that confers protein stability and subnuclear localization. *Mol Cell Biol* **23**, 186194, doi:10.1128/mcb.23.1.186-194.2003 (2003).

6 Hsieh, J. J., Cheng, E. H. & Korsmeyer, S. J. Taspase1: a threonine aspartase required for cleavage of MLL and proper HOX gene expression. *Cell* **115**, 293303, doi:10.1016/s0092-8674(03)00816-x (2003).

7 Meyer, C. *et al.* The MLL recombinome of acute leukemias in 2017. *Leukemia* **32**, 273-284, doi:10.1038/leu.2017.213 (2018).

8 Ferrando, A. A. *et al.* Gene expression signatures in MLL-rearranged T-lineage and B-precursor acute leukemias: dominance of HOX dysregulation. *Blood* **102**, 262-268, doi:10.1182/blood-2002-10-3221 (2003).

9 Armstrong, S. A. *et al.* MLL translocations specify a distinct gene expression profile that distinguishes a unique leukemia. *Nat Genet* **30**, 41-47, doi:10.1038/ng765 (2002).

10 Miyamoto, R. (ed Hiroshi Okuda Akinori Kanai , Satoshi Takahashi , Hirotaka Matsui , Toshiya Inaba , View ORCID Profile Akihiko Yokoyama) (BioRxiv, 2021).

11 Milne, T. A. Mouse models of MLL leukemia: recapitulating the human disease. *Blood* **129**, 2217-2223, doi:10.1182/blood-2016-10-691428 (2017).

12 Bates, S. E. Epigenetic Therapies for Cancer. *N Engl J Med* **383**, 650-663, doi:10.1056/NEJMra1805035 (2020).

13 Filippakopoulos, P. *et al.* Selective inhibition of BET bromodomains. *Nature* **468**, 1067-1073, doi:10.1038/nature09504 (2010).

14 Knutson, S. K. *et al.* Selective inhibition of EZH2 by EPZ-6438 leads to potent antitumor activity in EZH2-mutant non-Hodgkin lymphoma. *Mol Cancer Ther* **13**, 842-854, doi:10.1158/1535-7163.MCT-13-0773 (2014).

15 Darracq, A. *et al.* NPM and NPM-MLF1 interact with chromatin remodeling complexes and influence their recruitment to specific genes. *PLoS Genet* **15**, e1008463, doi:10.1371/journal.pgen.1008463 (2019).

16 Dou, Y. *et al.* Regulation of MLL1 H3K4 methyltransferase activity by its core components. *Nat Struct Mol Biol* **13**, 713-719, doi:10.1038/nsmb1128 (2006).

17 Li, Y. *et al.* Structural basis for activity regulation of MLL family methyltransferases. *Nature* **530**, 447-452, doi:10.1038/nature16952 (2016).

18 Tremblay, V. *et al.* Molecular basis for DPY-30 association to COMPASS-like and NURF complexes. *Structure* **22**, 1821-1830, doi:10.1016/j.str.2014.10.002 (2014).

19 Yang, Z., Shah, K., Khodadadi-Jamayran, A. & Jiang, H. Dpy30 is critical for maintaining the identity and function of adult hematopoietic stem cells. *J Exp Med* **213**, 2349-2364, doi:10.1084/jem.20160185 (2016).

20 Jiang, H. The complex activities of the SET1/MLL complex core subunits in development and disease. *Biochim Biophys Acta Gene Regul Mech* **1863**, 194560, doi:10.1016/j.bbagrm.2020.194560 (2020).

21 Vedadi, M. *et al.* Targeting human SET1/MLL family of proteins. *Protein Sci* **26**, 662-676, doi:10.1002/pro.3129 (2017).

22 Cao, F. *et al.* Targeting MLL1 H3K4 methyltransferase activity in mixed-lineage leukemia. *Mol Cell* **53**, 247-261, doi:10.1016/j.molcel.2013.12.001 (2014).

23 Aho, E. R., Weissmiller, A. M., Fesik, S. W. & Tansey, W. P. Targeting WDR5: A WINning Anti-Cancer Strategy? *Epigenet Insights* **12**, 2516865719865282, doi:10.1177/2516865719865282 (2019).

24 Yang, Z. *et al.* Hijacking a key chromatin modulator creates epigenetic vulnerability for MYC-driven cancer. *J Clin Invest* **128**, 3605-3618, doi:10.1172/JCI97072 (2018).

25 Mertz, J. A. *et al.* Targeting MYC dependence in cancer by inhibiting BET bromodomains. *Proc Natl Acad Sci U S A* **108**, 16669-16674, doi:10.1073/pnas.1108190108 (2011).

26 Wang, J. *et al.* Targeting c-Myc: JQ1 as a promising option for c-Myc-amplified esophageal squamous cell carcinoma. *Cancer Lett* **419**, 64-74, doi:10.1016/j.canlet.2018.01.051 (2018).

27 Li, N. *et al.* BET bromodomain inhibitor JQ1 preferentially suppresses EBVpositive nasopharyngeal carcinoma cells partially through repressing c-Myc. *Cell Death Dis* **9**, 761, doi:10.1038/s41419-018-0789-1 (2018).

28 Karatas, H. *et al.* High-affinity, small-molecule peptidomimetic inhibitors of MLL1/WDR5 protein-protein interaction. *J Am Chem Soc* **135**, 669-682, doi:10.1021/ja306028q (2013).

29 Karatas, H. *et al.* Discovery of a Highly Potent, Cell-Permeable Macrocyclic Peptidomimetic (MM-589) Targeting the WD Repeat Domain 5 Protein (WDR5)Mixed Lineage Leukemia (MLL) Protein-Protein Interaction. *J Med Chem* **60**, 4818-4839, doi:10.1021/acs.jmedchem.6b01796 (2017).

30 Getlik, M. *et al.* Structure-Based Optimization of a Small Molecule Antagonist of the Interaction Between WD Repeat-Containing Protein 5 (WDR5) and MixedLineage Leukemia 1 (MLL1). *J Med Chem* **59**, 2478-2496, doi:10.1021/acs.jmedchem.5b01630 (2016).

31 Chern, T. R. *et al.* Discovery of Potent Small-Molecule Inhibitors of MLL Methyltransferase. *ACS Med Chem Lett* **11**, 1348-1352, doi:10.1021/acsmedchemlett.0c00229 (2020).

32 Ye, X. *et al.* The Development of Inhibitors Targeting the Mixed Lineage Leukemia 1 (MLL1)-WD Repeat Domain 5 Protein (WDR5) Protein- Protein Interaction. *Curr Med Chem* **27**, 5530-5542, doi:10.2174/0929867326666190528080514 (2020).

33 Xu, S. *et al.* Discovery of M-808 as a Highly Potent, Covalent, Small-Molecule Inhibitor of the Menin-MLL Interaction with Strong. *J Med Chem* **63**, 4997-5010, doi:10.1021/acs.jmedchem.0c00547 (2020).

34 Shah, K. K. *et al.* Specific inhibition of DPY30 activity by ASH2L-derived peptides suppresses blood cancer cell growth. *Exp Cell Res* **382**, 111485, doi:10.1016/j.yexcr.2019.06.030 (2019).

35 Matsuo, Y. *et al.* Two acute monocytic leukemia (AML-M5a) cell lines (MOLM13 and MOLM-14) with interclonal phenotypic heterogeneity showing MLL-AF9 fusion resulting from an occult chromosome insertion, ins(11;9)(q23;p22p23).
Leukemia **11**, 1469-1477, doi:10.1038/sj.leu.2400768 (1997).

36 Klein, E. *et al.* Properties of the K562 cell line, derived from a patient with chronic myeloid leukemia. *Int J Cancer* **18**, 421-431, doi:10.1002/ijc.2910180405 (1976).

37 Whitaker, R. H. (ProQuest, 2019).

38 Yang, Z. *et al.* The DPY30 subunit in SET1/MLL complexes regulates the proliferation and differentiation of hematopoietic progenitor cells. *Blood* **124**, 2025-2033, doi:10.1182/blood-2014-01-549220 (2014).

39 Simboeck, E. *et al.* DPY30 regulates pathways in cellular senescence through ID protein expression. *EMBO J* **32**, 2217-2230, doi:10.1038/emboj.2013.159 (2013).

40 Hong, Z. F. *et al.* Upregulation of DPY30 promotes cell proliferation and predicts a poor prognosis in cholangiocarcinoma. *Biomed Pharmacother* **123**, 109766, doi:10.1016/j.biopha.2019.109766 (2020).

41 Wang, P., Henning, S. M. & Heber, D. Limitations of MTT and MTS-based assays for measurement of antiproliferative activity of green tea polyphenols. *PLoS One* **5**, e10202, doi:10.1371/journal.pone.0010202 (2010).

42 Pereira, T. F. *et al.* Fluorescence-based method is more accurate than countingbased methods for plotting growth curves of adherent cells. *BMC Res Notes* **13**, 57, doi:10.1186/s13104-020-4914-8 (2020).

43 Tario, J. D., Conway, A. N., Muirhead, K. A. & Wallace, P. K. Monitoring Cell Proliferation by Dye Dilution: Considerations for Probe Selection. *Methods Mol Biol* **1678**, 249-299, doi:10.1007/978-1-4939-7346-0_12 (2018).

44 Ohtani, N. *et al.* Opposing effects of Ets and Id proteins on p16INK4a expression during cellular senescence. *Nature* **409**, 1067-1070, doi:10.1038/35059131 (2001).

45 Shin, S. Y., Kim, C. G., Lim, Y. & Lee, Y. H. The ETS family transcription factor ELK-1 regulates induction of the cell cycle-regulatory gene p21(Waf1/Cip1) and

the BAX gene in sodium arsenite-exposed human keratinocyte HaCaT cells. *J Biol Chem* **286**, 26860-26872, doi:10.1074/jbc.M110.216721 (2011).

46 Edmondson, R., Broglie, J. J., Adcock, A. F. & Yang, L. Three-dimensional cell culture systems and their applications in drug discovery and cell-based biosensors. *Assay Drug Dev Technol* **12**, 207-218, doi:10.1089/adt.2014.573 (2014).

47 Lee, J., Cuddihy, M. J. & Kotov, N. A. Three-dimensional cell culture matrices: state of the art. *Tissue Eng Part B Rev* **14**, 61-86, doi:10.1089/teb.2007.0150 (2008).

48 Doogue, M. P. & Polasek, T. M. The ABCD of clinical pharmacokinetics. *Ther Adv Drug Saf* **4**, 5-7, doi:10.1177/2042098612469335 (2013).

49 Lipinski, C. A., Lombardo, F., Dominy, B. W. & Feeney, P. J. Experimental and computational approaches to estimate solubility and permeability in drug discovery and development settings. *Adv Drug Deliv Rev* **46**, 3-26, doi:10.1016/s0169-409x(00)00129-0 (2001).

50 Doak, B. C., Over, B., Giordanetto, F. & Kihlberg, J. Oral druggable space beyond the rule of 5: insights from drugs and clinical candidates. *Chem Biol* **21**, 1115-1142, doi:10.1016/j.chembiol.2014.08.013 (2014).

51 Barret, R. 89-95 (Elsevier, Therapeutical Chemistry, 2018).

52 Edwards, M. P. Vol. 45 (ed David A. Price) 380-391 (Elsevier, Annual Reports in Medicinal Chemistry, 2010).

53 Zhang, M. Q. & Wilkinson, B. Drug discovery beyond the 'rule-of-five'. *Curr Opin Biotechnol* **18**, 478-488, doi:10.1016/j.copbio.2007.10.005 (2007).

54 Eglen, R. M. & Klein, J. L. Three-Dimensional Cell Culture: A Rapidly Emerging Approach to Cellular Science and Drug Discovery. *SLAS Discov* **22**, 453-455, doi:10.1177/2472555217702448 (2017).

55 Koch, J. *et al.* Three dimensional cultivation increases chemo- and radioresistance of colorectal cancer cell lines. *PLoS One* **16**, e0244513, doi:10.1371/journal.pone.0244513 (2021).

56 Ottersbach, K. *et al.* The "Never-Ending" Mouse Models for MLL-Rearranged Acute Leukemia Are Still Teaching Us. *Hemasphere* **2**, e57, doi:10.1097/HS9.0000000000000057 (2018).

57 Allen-Petersen, B. L. & Sears, R. C. Mission Possible: Advances in MYC Therapeutic Targeting in Cancer. *BioDrugs* **33**, 539-553, doi:10.1007/s40259019-00370-5 (2019).

58 Di, L., Kerns, E. H., Ma, X. J., Huang, Y. & Carter, G. T. Applications of high throughput microsomal stability assay in drug discovery. *Comb Chem High Throughput Screen* **11**, 469-476, doi:10.2174/138620708784911429 (2008).

59 Fallah, Y., Brundage, J., Allegakoen, P. & Shajahan-Haq, A. N. MYC-Driven Pathways in Breast Cancer Subtypes. *Biomolecules* **7**, doi:10.3390/biom7030053 (2017).

60 Calcagno, D. Q. *et al.* MYC, FBXW7 and TP53 copy number variation and expression in gastric cancer. *BMC Gastroenterol* **13**, 141, doi:10.1186/1471230X-13-141 (2013).

61 Jung, M. *et al.* Clinical Importance of Myc Family Oncogene Aberrations in Epithelial Ovarian Cancer. *JNCI Cancer Spectr* **2**, pky047, doi:10.1093/jncics/pky047 (2018).

62 Konecny, G. E. Combining PARP and CDK4/6 inhibitors in MYC driven ovarian cancer. *EBioMedicine* **43**, 9-10, doi:10.1016/j.ebiom.2019.04.009 (2019).

63 Korc, M. Beyond Kras: MYC Rules in Pancreatic Cancer. *Cell Mol Gastroenterol Hepatol* **6**, 223-224, doi:10.1016/j.jcmgh.2018.04.009 (2018).

64 Sodir, N. M. *et al.* MYC Instructs and Maintains Pancreatic Adenocarcinoma Phenotype. *Cancer Discov* **10**, 588-607, doi:10.1158/2159-8290.CD-19-0435 (2020).

65 Schaub, F. X. *et al.* Pan-cancer Alterations of the MYC Oncogene and Its Proximal Network across the Cancer Genome Atlas. *Cell Syst* **6**, 282-300.e282, doi:10.1016/j.cels.2018.03.003 (2018).

DISCUSSION

Overall, this dissertation brings new perspective to two complex intracellular signaling circuits that are currently in the spotlight for targeted therapeutic development for cancer treatment. The Bcl-2 family is currently a therapeutic target for BH3-mimetics, a class of small molecule inhibitors of the anti-apoptotic proteins: BCL2, MCL1, and BCLxL. Currently, there is one FDA-approved BH3-mimetic called Venetoclax targeting BCL2, but other BH3-mimetics targeting anti-apoptotic proteins like MCL1 remain under clinical investigation in Phase I/II trials[21]. In addition to BH3-mimetics, another cuttingedge field within targeted therapy includes epigenetic regulation in cancer. Here, we developed a novel first-in-class small molecule tool compound targeting the SET/MLL H3K4 histone methyltransferase complex that will provide future insight into the specific epigenetic regulation by the complex core subunit, DPY30.

According to the National Cancer Institute (cancer.gov), there are four main types of cancer treatment outside of surgical resection and radiation therapy: Chemotherapy, Immunotherapy, Hormone Therapy, and Targeted Therapy. Targeted Therapy includes two main classes: Small Molecule Drugs or Monoclonal Antibodies. Currently, we are in an era of multi -omics strategies to fully elucidate any targetable candidates for specific tumor types[51,52]. This approach is called Personalized Medicine or Precision Oncology and has allowed the individualization of cancer treatment, improving both quality of life and duration of response[53]. Targeted therapeutic small molecule drugs like BH3-mimetics or novel epigenetic inhibitors are cutting-edge treatments as Targeted Therapy is the foundation of Precision Oncology and the way of future cancer treatment[53,54].

Through the first two chapters, we describe a myriad of non-canonical protein interactions between MCL1 and other cell regulatory proteins, notably binding partners through cell cycle regulation and DNA damage response. In targeted therapeutic drug discovery efforts, it is easy to focus on the anticipated outcome and overlook the other impacts the substrate may have on the cell. Chapter 1 provides an up-to-date synopsis of MCL1 regulation across diverse cell signaling pathways outside of intrinsic apoptosis, which has not been reviewed in over eight years[55]. While some of this information has been reviewed elsewhere, this is the first time MCL1's role in DNA damage response has been synthesized into a formal review.

This publication is timely as there are numerous MCL1 inhibitors currently in clinical trials for multiple indications across hematologic malignancies. As adverse events are encountered, this review will be referenced to identify the possible etiology of adverse reactions or 'off-target' side effects as a result of MCL1 inhibition. For example, AMG397 (sponsored by Amgen), an MCL1 inhibitor under investigation in acute myeloid leukemia (AML), was temporarily suspended during the first-in-human Phase I doseescalation study. According to an Amgen Press Release, this suspension was placed after a safety signal of cardiac toxicity. Based on our work in Chapter 1, these side effects should not be unanticipated as MCL1 conditional knockout in murine cardiomyocytes promotes rapid death secondary to heart failure[56,57]. Furthermore, we show that MCL1 elicits strict control on mitochondrial dynamics, highlighting another pathway that may impact cardiac tissue over other cell types.

While this review may seem like it suggests that MCL1 inhibitors will fail in clinical trials, that is not our objective. This review will provide a framework for clinical trial monitoring and provide an in-depth pathway analysis for future combination studies with

MCL1 inhibitors. Due to the diverse regulatory role MCL1 plays across the cellular milieu, it can be exploited to sensitize cells to cancer therapy, which has been seen in preclinical studies with cytotoxic agents, radiation therapy, and other targeted therapeutics[19,58-60]. Furthermore, for the first time in a single review, we highlight multiple new therapeutic areas that may benefit from MCL1 inhibitors such as reactive airway disease[61,62] and neurodegenerative disorders like Alzheimer's Disease[63].

One of the protein interactions highlighted in Chapter 1 and extensively detailed in Chapter 2 is the direct protein-protein interaction between MCL1 and p73[64]. p73 is a member of the p53 family of transcription factors that includes p53, p63, and p73. The protein interaction between MCL1 and p73 is mediated through a putative rBH3-motif in the first of two alpha-helices in the p73 tetramerization domain[64]. Like p73, p63 retains a putative rBH3 motif and two alpha-helices in the homologous tetramerization domain, but unlike the other two members, p53 does not contain an rBH3-motif[65]. Likewise, the p53 tetramerization domain only retains one alpha helix, making the interaction between MCL1 and p53 highly unlikely and was used as a negative control in preliminary experiments[66]. Nevertheless, given the sequence and structural homology between p63 and p73, future directions of the rBH3-mediated protein interactions should include investigation of MCL1 interacting with p63. While it is probable the binding interaction is redundant between p63 and p73, p63 has its own unique cellular implications during development that should be explored[67-69].

p73 is a member of the p53 family, but it has many divergent functions and unique regulatory mechanisms from the established tumor suppressive role. Unlike p53, global p73 knockout mice lack a spontaneous tumor phenotype[70]. Instead, they display a hydrocephalus phenotype with severe abnormalities in brain development and other

multiorgan defects that have now been identified as ciliopathies[70-73]. Furthermore, the transcriptionally active form of p73 (*i.e.* TAp73) uniquely regulates gene expression to promote glucose metabolism through the pentose phosphate pathway (PPP)[74,75], serineglycine biosynthesis[76], and anti-oxidant defense[74,77]. The interplay between the N-terminal isoforms of p73, TAp73 verses ΔNp73, continues to emerge as knockout mouse studies and *in vitro* techniques become more advanced[78,79]. Future work from our laboratory includes this dynamic interplay, elucidating both structural, functional, and biological impacts of these two isoforms on the cell and how the interaction with MCL1 impacts both cancerous and normal cell types.

Although p73 has unique target gene specificity and overall protein functionality, there is still significant evidence of crosstalk amongst the p73 family. All p53 members share a highly conserved DNA binding domain (DBD) that that promotes significant overlap of target genes, especially between p53 and p73[80,81]. At the regulatory level, all members of the p53 family are regulated by the ring finger ubiquitin ligase MDM2, albeit through different mechanisms of negative feedback. The levels of p53 are modulated by MDM2 through prosteosomal degradation and subsequent transcriptional suppression[82]. While MDM2 still negatively regulates p73 through a protein-interaction, MDM2 stabilizes the p73 protein stability in the cell[83]. Both p53 and p73 exhibit a feedback regulatory loop by upregulating and relying on MDM2 levels for steady-state expression.

Importantly for the transcriptional activity for p73, MDM2 binds to the N-terminal region of p73 and competitively interacts with transcriptional co-activators like p300 and CREBbinding protein, CBP[84]. Therefore, the expression and interactions with these opposing binding partners directly determines the activity of p73.

Other post-translational modifications of p73 including phosphorylation, acetylation, SUMOlation, and neddylation modulate the stability, localization, and protein activity of p73[85-87]. While the bulk of the post-translational modifications occur in the Nterminal transactivation domain, the DNA binding domain, and the C-terminus, there are few sites that are potentially influenced by the binding of MCL1[66]. For example, Serine 388 in the p73-TD is phosphorylated by protein kinase C[88]. Although this does not alter the structure or kinetics of the tetramer formation, it has been hypothesized that this modification could recruit other factors that impact the oligomeric state[66,88]. The status of post-translational modifications in the presence and absence of MCL1 binding remains to be determined in future studies.

At the structural level, p73 elicits transcriptional activity by tetramerizing onto DNA response elements. p63 and mutant p53 have both been suggested to heterotetramerize with p73, highlighting a common mechanism of the p53 family to regulate cell fate[79,89,90]. Interestingly, heterotetramers between p63 and p73 are more stable than a homotetramer, suggesting a level of functional overlap between the two proteins[89]. Using immunostaining techniques and ChIP-sequencing experiments, heterotetramers have been suggested to occur *in vivo*[77,89]. As discussed in Chapter 2, MCL1 was suggested to disrupt the tetramer formation of p73 on DNA, subsequently decreasing the target gene expression of p73 transcriptional targets[64]. As part of the future directions of this project, optimized techniques for studying the oligomeric state of p73 should be designed. It should be noted that the lack of definitive evidence showing this mechanism was not an oversight. Methods including analytical size exclusion chromatography (AnSEC) and numerous Native Gel conditions were attempted and unsuccessful in visualizing the monomer, dimer,

and tetramer fractions conclusively. Other techniques such as analytical ultracentrifugation may improve the limit of detection to characterize this interaction.

One of the therapeutic combinations that previously has been characterized in detail in cancer cell models is MCL1 inhibitors with Cisplatin. Knockdown or inhibition of MCL1 sensitizes Cisplatin-resistant cancer cells or improves the efficacy of platinumbased therapeutics[19,91,92]. Generally, this sensitization to Cisplatin in combination with MCL1 knockdown has been contributed to the anti-apoptotic activity of MCL1 at the outer mitochondrial membrane. Although briefly highlighted in the DNA damage response section in Chapter 1, Chapter 2 describes a novel protein-protein interaction between MCL1 and p73 that could further contribute to MCL1-mediated chemoresistance to platinum-based chemotherapeutics outside of MOMP regulation and intrinsic apoptosis[64].

In cells that harbor a p53 mutation or null-p53 expression, p73 potentiates the activity of Cisplatin-induced apoptosis across cancer cell types[92-94]. In summary, Chapter 2 describes a novel mechanism of MCL1 eliciting transcriptional inhibition on p73 through a direct protein interaction with MCL1s canonical BH3-binding cleft[64]. Thus, instead of MCL1 inhibitors having a synergistic impact on Cisplatin response through sensitizing cells to apoptosis, we show that MCL1 inhibition promotes p73 transcriptional activation, comparable to that elicited with low-dose Cisplatin treatment alone. Importantly for these studies, the concentrations of MCL1 inhibitor and Cisplatin treatment alone did not induce apoptosis and therefore, the effects are not secondary to the induction of early cell death[64].

While both Cisplatin and MCL1 inhibition activate p73 target gene expression, combining an MCL1-specific BH3-mimetic, A-1210477, with Cisplatin enhanced the induction of critical target genes associated p73-mediated Cisplatin response[64]. It should be noted that for this manuscript, which was prepared in 2019, the MCL1 inhibitors that

were available were far less potent and lacked the solubility to work in high concentrations compared to the current commercially available MCL1 inhibitors. For comparison, A1210477 has a binding affinity to MCL1 of 0.45 nM versus AMG-176, which is currently in clinical trials, has a binding affinity of 0.06 nM[95]. Therefore, combination studies that are more clinically relevant with therapeutics that can directly translate into patient care are now feasible, which is an exciting new avenue our lab is investigating. There are currently 13 ongoing clinical trials where MCL1 inhibition is the primary objective (clinicaltrials.gov – April 2021). All trials are currently in malignant hematology and include MCL1-specific BH3-mimetics MIK665 (Novartis), S64315 (Servier), ABBV-467 (AbbVie), AMG176 (Amgen), and PRT1419 (Prelude). The number of MCL1 inhibitors currently under clinical investigation with more in pre-clinical development highlights the excitement and anticipation around the success of these therapeutics. As Precision Oncology becomes more accessible to patients and more targeted therapeutics become available in the anti-cancer arsenal, these combination studies as well as their mechanism become highly important for translation into clinical practice.

In addition to combination studies being explored by numerous labs across the cancer biology field, there are future directions of the MCL1-p73 interaction that are important general biology questions. As MCL1 has never been described as a transcriptional regulator, we are now exploring various sequencing avenues to determine the precise impact MCL1 regulation has on direct transcription of target genes. Using potent MCL1 inhibitors and genetic knockdown studies, RNA-sequencing is being utilized by new members of the Placzek lab to determine the general transcriptional changes with MCL1 manipulation. Furthermore, we are deploying ChIP-sequencing methods to determine the p73-specific changes in DNA binding on a genome-wide scale. The EMSA

studies and RT-qPCR analysis of p73 target genes p21, NOXA, PUMA, and GADD45 suggest MCL1 will have an impact on p73 through inhibiting the tetramerization which subsequently decreases the DNA binding affinity for canonical response elements (Chapter 2, Figure 5 and 6). While this data provides a rationale hypothesis for this mechanism, there is no direct evidence that MCL1 directly impacts the oligomerization of p73. Future followup of this interaction should also include experiments characterizing the modulation of oligomerization of p73 by MCL1, determining if it does indeed limit the p73 tetramerization. p73 also binds to DNA as a dimer of dimers mediated by the DNA binding domain, so it should be determined if MCL1 inhibits tetramerization and dimerization or if the dimerization of p73 can still occur, promoting the same response elements, only with lower potency. Optimizing methods of characterizing p73 oligomerization will be highly valuable for these studies, as well for advancing the p73 field in overall.

From 2016-2021, which is the time this work was completed, I have had the opportunity to observe MCL1 inhibitors truly go from bench-to-bedside. The rise of BH3mimetics piqued my interest in Drug Discovery and initiated my involvement with the project described in Chapter 3, the development of a novel small molecule targeting the DPY30-ASH2L interaction. Like the Bcl-2 family, DPY30 and ASH2L are involved in a complex cellular network that regulates diverse target genes required for both normal cellular functions and can contribute to tumorigenesis and cancer cell maintenance[96,97].

Importantly for the culmination of my time on this project, I have learned a tremendous amount about the Research and Development (R&D) phases of drug discovery and working with a cross-functional team between multiple institutions. While we have not yet identified a compound with Pharmacokinetic parameters ready for the filing of an Investigational New Drug (IND) application, SRI-41155 can be used as a novel tool

compound for pre-clinical studies in order to characterize the impact of DPY30 downregulation in cancer. This compound is a first-in-class DPY30 inhibitor and likely will be the prototype for other small molecule inhibitors targeting this interaction. At this point in time, we are working with the technology transfer office to file a New Patent Application for SRI-41155 and its indication specifically in MLL-rearranged leukemia.

Like the status of most BH3-mimetics five years ago upon the start of my graduate career, the current work in targeting the SET/MLL histone methyltransferase complex remains largely preliminary in pre-clinical development. Interestingly, we are not the only group interested in both the Bcl-2 family and H3K4 methylation as therapeutic targets. One of the pioneers in the development of NMR-based fragment screening used to identify MCL1-specific inhibitors recently developed a WRD5 inhibitor, which targets another core subunit of the MLL-complex[98,99]. Furthermore, inhibitors of the catalytic subunit, MLL1, and other binding partners of the MLL-fusion proteins like Menin also have of interest of many cancer researchers[100,101]. Therefore, I anticipate over the next five years to see our work showcased like many of the early BH3-mimetic studies to tease out the mechanistic roles DPY30 plays in the cell, as more potent and druggable chemical scaffolds are designed. Comparably to the explosion of BH3-mimetic findings in the literature over the past five years ubiquitously across cancer cell types, I anticipate that the application of the SET/MLL complex inhibitors will translate across the oncology disease continuum, extending into other hematologic malignancies and MYC-dependent solid tumors.

In conclusion, this dissertation has summarized and explored new avenues of complex cell signaling pathways that are prime protein targets for targeted therapy and the future Precision Oncology. The insights gained from this work will provide a framework to explore novel therapeutic indications for existing drugs such as BH3-mimietics and lay

the foundation for new inhibitors targeting epigenetic regulatory complexes. Lastly, all three chapters will ultimately provide detailed information on how to deploy investigational therapeutics targeting these complex and intertwined pathways into combination therapy to enhance a patient's response to cytotoxic and targeted cancer therapy as the War on Cancer continues.

REFERENCES

1 Vaux, D. L. & Korsmeyer, S. J. Cell death in development. *Cell* **96**, 245-254, doi:10.1016/s0092-8674(00)80564-4 (1999).

2 Galluzzi, L. *et al.* Molecular mechanisms of cell death: recommendations of the Nomenclature Committee on Cell Death 2018. *Cell Death Differ* **25**, 486-541, doi:10.1038/s41418-017-0012-4 (2018).

3 Hanahan, D. & Weinberg, R. A. Hallmarks of cancer: the next generation. *Cell* **144**, 646-674, doi:10.1016/j.cell.2011.02.013 (2011).

4 Hanahan, D. & Weinberg, R. A. The hallmarks of cancer. *Cell* **100**, 57-70, doi:10.1016/s0092-8674(00)81683-9 (2000).

5 Kale, J., Osterlund, E. J. & Andrews, D. W. BCL-2 family proteins: changing partners in the dance towards death. *Cell Death Differ* **25**, 65-80, doi:10.1038/cdd.2017.186 (2018).

6 Naseri, M. H. *et al.* Up regulation of Bax and down regulation of Bcl2 during 3NC mediated apoptosis in human cancer cells. *Cancer Cell Int* **15**, 55, doi:10.1186/s12935-015-0204-2 (2015).

7 Andersson, Y., Juell, S. & Fodstad, Ø. Downregulation of the antiapoptotic MCL1 protein and apoptosis in MA-11 breast cancer cells induced by an anti-epidermal growth factor receptor-Pseudomonas exotoxin a immunotoxin. *Int J Cancer* **112**, 475-483, doi:10.1002/ijc.20371 (2004).

8 Wei, M. C. *et al.* Proapoptotic BAX and BAK: a requisite gateway to mitochondrial dysfunction and death. *Science* **292**, 727-730, doi:10.1126/science.1059108 (2001).

9 Dorstyn, L., Akey, C. W. & Kumar, S. New insights into apoptosome structure and function. *Cell Death Differ* **25**, 1194-1208, doi:10.1038/s41418-017-0025-z (2018).

10 Chinnaiyan, A. M. The apoptosome: heart and soul of the cell death machine. *Neoplasia* **1**, 5-15, doi:10.1038/sj.neo.7900003 (1999).

11 Brentnall, M., Rodriguez-Menocal, L., De Guevara, R. L., Cepero, E. & Boise, L. H. Caspase-9, caspase-3 and caspase-7 have distinct roles during intrinsic apoptosis. *BMC Cell Biol* **14**, 32, doi:10.1186/1471-2121-14-32 (2013).

12 Aouacheria, A., Combet, C., Tompa, P. & Hardwick, J. M. Redefining the BH3 Death Domain as a 'Short Linear Motif'. *Trends Biochem Sci* **40**, 736-748, doi:10.1016/j.tibs.2015.09.007 (2015).

13 Chipuk, J. E. & Green, D. R. How do BCL-2 proteins induce mitochondrial outer membrane permeabilization? *Trends Cell Biol* **18**, 157-164, doi:10.1016/j.tcb.2008.01.007 (2008).

14 Nickells, R. W. Variations in the rheostat model of apoptosis: what studies of retinal ganglion cell death tell us about the functions of the Bcl2 family proteins. *Exp Eye Res* **91**, 2-8, doi:10.1016/j.exer.2010.03.004 (2010).

15 Placzek, W. J. *et al.* A survey of the anti-apoptotic Bcl-2 subfamily expression in cancer types provides a platform to predict the efficacy of Bcl-2 antagonists in cancer therapy. *Cell Death Dis* **1**, e40, doi:10.1038/cddis.2010.18 (2010).

16 Tessoulin, B. *et al.* BCL2-Family Dysregulation in B-Cell Malignancies: From Gene Expression Regulation to a Targeted Therapy Biomarker. *Front Oncol* **8**, 645, doi:10.3389/fonc.2018.00645 (2018).

17 D'Aguanno, S. & Del Bufalo, D. Inhibition of Anti-Apoptotic Bcl-2 Proteins in Preclinical and Clinical Studies: Current Overview in Cancer. *Cells* **9**, doi:10.3390/cells9051287 (2020).

18 Wen, Q. *et al.* Elevated expression of mcl-1 inhibits apoptosis and predicts poor prognosis in patients with surgically resected non-small cell lung cancer. *Diagn Pathol* **14**, 108, doi:10.1186/s13000-019-0884-3 (2019).

19 Michels, J. *et al.* MCL-1 dependency of cisplatin-resistant cancer cells. *Biochem Pharmacol* **92**, 55-61, doi:10.1016/j.bcp.2014.07.029 (2014).

20 Skvara, H. *et al.* Mcl-1 blocks radiation-induced apoptosis and inhibits clonogenic cell death. *Anticancer Res* **25**, 2697-2703 (2005).

21 Bolomsky, A. *et al.* MCL-1 inhibitors, fast-lane development of a new class of anticancer agents. *J Hematol Oncol* **13**, 173, doi:10.1186/s13045-020-01007-9 (2020).

22 Letai, A. *et al.* Distinct BH3 domains either sensitize or activate mitochondrial apoptosis, serving as prototype cancer therapeutics. *Cancer Cell* **2**, 183-192, doi:10.1016/s1535-6108(02)00127-7 (2002).

23 Chen, L. *et al.* Differential targeting of prosurvival Bcl-2 proteins by their BH3only ligands allows complementary apoptotic function. *Mol Cell* **17**, 393-403, doi:10.1016/j.molcel.2004.12.030 (2005).

24 Kuwana, T. *et al.* BH3 domains of BH3-only proteins differentially regulate Baxmediated mitochondrial membrane permeabilization both directly and indirectly. *Mol Cell* **17**, 525-535, doi:10.1016/j.molcel.2005.02.003 (2005).

25 Oltersdorf, T. *et al.* An inhibitor of Bcl-2 family proteins induces regression of solid tumours. *Nature* **435**, 677-681, doi:10.1038/nature03579 (2005).

26 Croce, C. M. & Reed, J. C. Finally, An Apoptosis-Targeting Therapeutic for Cancer. *Cancer Res* **76**, 5914-5920, doi:10.1158/0008-5472.CAN-16-1248 (2009).

27 Wilson, W. H. *et al.* Navitoclax, a targeted high-affinity inhibitor of BCL-2, in lymphoid malignancies: a phase 1 dose-escalation study of safety, pharmacokinetics, pharmacodynamics, and antitumour activity. *Lancet Oncol* **11**, 1149-1159, doi:10.1016/S1470-2045(10)70261-8 (2010).

28 Kipps, T. J. *et al.* A phase 2 study of the BH3 mimetic BCL2 inhibitor navitoclax (ABT-263) with or without rituximab, in previously untreated B-cell chronic lymphocytic leukemia. *Leuk Lymphoma* **56**, 2826-2833, doi:10.3109/10428194.2015.1030638 (2015).

29 Roberts, A. W. *et al.* Substantial susceptibility of chronic lymphocytic leukemia to BCL2 inhibition: results of a phase I study of navitoclax in patients with relapsed or refractory disease. *J Clin Oncol* **30**, 488-496, doi:10.1200/JCO.2011.34.7898 (2012).

30 Debrincat, M. A. *et al.* BCL-2 is dispensable for thrombopoiesis and platelet survival. *Cell Death Dis* **6**, e1721, doi:10.1038/cddis.2015.97 (2015).

31 Souers, A. J. *et al.* ABT-199, a potent and selective BCL-2 inhibitor, achieves antitumor activity while sparing platelets. *Nat Med* **19**, 202-208, doi:10.1038/nm.3048 (2013).

32 Cang, S., Iragavarapu, C., Savooji, J., Song, Y. & Liu, D. ABT-199 (venetoclax) and BCL-2 inhibitors in clinical development. *J Hematol Oncol* **8**, 129, doi:10.1186/s13045-015-0224-3 (2015).

33 Kehr, S. & Vogler, M. It's time to die: BH3 mimetics in solid tumors. *Biochim Biophys Acta Mol Cell Res* **1868**, 118987, doi:10.1016/j.bbamcr.2021.118987 (2021).

34 Roberts, A. W. & Huang, D. Targeting BCL2 With BH3 Mimetics: Basic Science and Clinical Application of Venetoclax in Chronic Lymphocytic Leukemia and Related B Cell Malignancies. *Clin Pharmacol Ther* **101**, 89-98, doi:10.1002/cpt.553 (2017).

35 Kantarjian, H. M., Kadia, T. M., DiNardo, C. D., Welch, M. A. & Ravandi, F. Acute myeloid leukemia: Treatment and research outlook for 2021 and the MD Anderson approach. *Cancer* **127**, 1186-1207, doi:10.1002/cncr.33477 (2021).

36 Zhu, H. & Almasan, A. Development of venetoclax for therapy of lymphoid malignancies. *Drug Des Devel Ther* **11**, 685-694, doi:10.2147/DDDT.S109325 (2017).

37 Ramsey, H. E. *et al.* A Novel MCL1 Inhibitor Combined with Venetoclax Rescues Venetoclax-Resistant Acute Myelogenous Leukemia. *Cancer Discov* **8**, 1566-1581, doi:10.1158/2159-8290.CD-18-0140 (2018).

38 Hormi, M. *et al.* Pairing MCL-1 inhibition with venetoclax improves therapeutic efficiency of BH3-mimetics in AML. *Eur J Haematol* **105**, 588-596, doi:10.1111/ejh.13492 (2020).

39 Wyatt, P. G., Gilbert, I. H., Read, K. D. & Fairlamb, A. H. Target validation: linking target and chemical properties to desired product profile. *Curr Top Med Chem* **11**, 1275-1283, doi:10.2174/156802611795429185 (2011).

40 Hughes, J. P., Rees, S., Kalindjian, S. B. & Philpott, K. L. Principles of early drug discovery. *Br J Pharmacol* **162**, 1239-1249, doi:10.1111/j.1476-5381.2010.01127.x (2011).

41 Carroll, P. M., Dougherty, B., Ross-Macdonald, P., Browman, K. & FitzGerald, K. Model systems in drug discovery: chemical genetics meets genomics. *Pharmacol Ther* **99**, 183-220, doi:10.1016/s0163-7258(03)00059-7 (2003).

42 Cagan, R. Drug screening using model systems: some basics. *Dis Model Mech* **9**, 1241-1244, doi:10.1242/dmm.028159 (2016).

43 Nadeau, J. H. & Auwerx, J. The virtuous cycle of human genetics and mouse models in drug discovery. *Nat Rev Drug Discov* **18**, 255-272, doi:10.1038/s41573018-0009-9 (2019).

44 Uhl, E. W. & Warner, N. J. Mouse Models as Predictors of Human Responses: Evolutionary Medicine. *Curr Pathobiol Rep* **3**, 219-223, doi:10.1007/s40139-0150086-y (2015).

45 Holbein, M. E. Understanding FDA regulatory requirements for investigational new drug applications for sponsor-investigators. *J Investig Med* **57**, 688-694, doi:10.2310/JIM.0b013e3181afdb26 (2009).

46 Thind, M. & Kowey, P. R. The Role of the Food and Drug Administration in Drug Development: On the Subject of Proarrhythmia Risk. *J Innov Card Rhythm Manag* **11**, 3958-3967, doi:10.19102/icrm.2020.110103 (2020).

47 Abedtash, H. & Duke, J. D. An Interactive User Interface for Drug Labeling to Improve Readability and Decision-Making. *AMIA Annu Symp Proc* **2015**, 278-286 (2015).

48 Kircik, L., Sung, J. C., Stein-Gold, L. & Goldenberg, G. United States Food and Drug Administration Product Label Changes. *J Clin Aesthet Dermatol* **9**, 39-48 (2016).

49 Starr, P. Venetoclax Shows Strong Activity in CLL. *Am Health Drug Benefits* **9**, 21 (2016).

50 Parry, N., Wheadon, H. & Copland, M. The application of BH3 mimetics in myeloid leukemias. *Cell Death Dis* **12**, 222, doi:10.1038/s41419-021-03500-6 (2021).

51 Melisi, D. *et al.* Role of next-generation genomic sequencing in targeted agents repositioning for pancreaticoduodenal cancer patients. *Pancreatology*, doi:10.1016/j.pan.2021.04.004 (2021).

52 Belizário, J. E., Sangiuliano, B. A., Perez-Sosa, M., Neyra, J. M. & Moreira, D. F. Using Pharmacogenomic Databases for Discovering Patient-Target Genes and Small Molecule Candidates to Cancer Therapy. *Front Pharmacol* **7**, 312, doi:10.3389/fphar.2016.00312 (2016).

53 Soldatos, T. G., Kaduthanam, S. & Jackson, D. B. Precision Oncology-The Quest for Evidence. *J Pers Med* **9**, doi:10.3390/jpm9030043 (2019).

54 Greenwalt, I., Zaza, N., Das, S. & Li, B. D. Precision Medicine and Targeted Therapies in Breast Cancer. *Surg Oncol Clin N Am* **29**, 51-62, doi:10.1016/j.soc.2019.08.004 (2020).

55 Perciavalle, R. M. & Opferman, J. T. Delving deeper: MCL-1's contributions to normal and cancer biology. *Trends Cell Biol* **23**, 22-29, doi:10.1016/j.tcb.2012.08.011 (2013).

56 Thomas, R. L. *et al.* Loss of MCL-1 leads to impaired autophagy and rapid development of heart failure. *Genes Dev* **27**, 1365-1377, doi:10.1101/gad.215871.113 (2013).

57 Wang, X. *et al.* Deletion of MCL-1 causes lethal cardiac failure and mitochondrial dysfunction. *Genes Dev* **27**, 1351-1364, doi:10.1101/gad.215855.113 (2013).

58 Lestini, B. J. *et al.* Mcl1 downregulation sensitizes neuroblastoma to cytotoxic chemotherapy and small molecule Bcl2-family antagonists. *Cancer Biol Ther* **8**, 1587-1595, doi:10.4161/cbt.8.16.8964 (2009).

59 Wei, D. *et al.* Targeting mcl-1 for radiosensitization of pancreatic cancers. *Transl Oncol* **8**, 47-54, doi:10.1016/j.tranon.2014.12.004 (2015).

60 Zhang, Y. *et al.* Mcl-1 downregulation sensitizes glioma to bortezomib-induced apoptosis. *Oncol Rep* **33**, 2277-2284, doi:10.3892/or.2015.3875 (2015).

61 Felton, J. M. *et al.* Mcl-1 protects eosinophils from apoptosis and exacerbates allergic airway inflammation. *Thorax* **75**, 600-605, doi:10.1136/thoraxjnl-2019213204 (2020).

62 Lucas, C. D. *et al.* Downregulation of Mcl-1 has anti-inflammatory pro-resolution effects and enhances bacterial clearance from the lung. *Mucosal Immunol* **7**, 857868, doi:10.1038/mi.2013.102 (2014).

63 Cen, X. *et al.* Pharmacological targeting of MCL-1 promotes mitophagy and improves disease pathologies in an Alzheimer's disease mouse model. *Nat Commun* **11**, 5731, doi:10.1038/s41467-020-19547-6 (2020).

64 Widden, H., Kaczmarczyk, A., Subedi, A., Whitaker, R. H. & Placzek, W. J. MCL1 binds and negatively regulates the transcriptional function of tumor suppressor p73. *Cell Death Dis* **11**, 946, doi:10.1038/s41419-020-03068-7 (2020).

65 Placzek, W. J. *et al.* Identification of a novel Mcl-1 protein binding motif. *J Biol Chem* **286**, 39829-39835, doi:10.1074/jbc.M111.305326 (2011).

66 Coutandin, D. *et al.* Conformational stability and activity of p73 require a second helix in the tetramerization domain. *Cell Death Differ* **16**, 1582-1589, doi:10.1038/cdd.2009.139 (2009).

67 Soares, E. & Zhou, H. Master regulatory role of p63 in epidermal development and disease. *Cell Mol Life Sci* **75**, 1179-1190, doi:10.1007/s00018-017-2701-z (2018).

68 King, K. E. *et al.* Unique domain functions of p63 isotypes that differentially regulate distinct aspects of epidermal homeostasis. *Carcinogenesis* **27**, 53-63, doi:10.1093/carcin/bgi200 (2006).

69 Lu, Y. *et al.* Distinct function of P63 isoforms during embryonic skeletal development. *Gene* **519**, 251-259, doi:10.1016/j.gene.2013.02.021 (2013).

70 Yang, A. *et al.* p73-deficient mice have neurological, pheromonal and inflammatory defects but lack spontaneous tumours. *Nature* **404**, 99-103, doi:10.1038/35003607 (2000).

71 Agostini, M. *et al.* p73 regulates maintenance of neural stem cell. *Biochem Biophys Res Commun* **403**, 13-17, doi:10.1016/j.bbrc.2010.10.087 (2010).

72 Marshall, C. B. *et al.* p73 Is Required for Multiciliogenesis and Regulates the Foxj1-Associated Gene Network. *Cell Rep* **14**, 2289-2300, doi:10.1016/j.celrep.2016.02.035 (2016).

73 Nemajerova, A. *et al.* TAp73 is a central transcriptional regulator of airway multiciliogenesis. *Genes Dev* **30**, 1300-1312, doi:10.1101/gad.279836.116 (2016).

74 Du, W. *et al.* TAp73 enhances the pentose phosphate pathway and supports cell proliferation. *Nat Cell Biol* **15**, 991-1000, doi:10.1038/ncb2789 (2013).

75 Agostini, M. *et al.* TAp73 promotes anti-senescence-anabolism not proliferation. *Aging (Albany NY)* **6**, 921-930, doi:10.18632/aging.100701 (2014).

76 Amelio, I. *et al.* p73 regulates serine biosynthesis in cancer. *Oncogene* **33**, 50395046, doi:10.1038/onc.2013.456 (2014).

77 Nemajerova, A. *et al.* Non-oncogenic roles of TAp73: from multiciliogenesis to metabolism. *Cell Death Differ* **25**, 144-153, doi:10.1038/cdd.2017.178 (2018).

78 Engelmann, D., Meier, C., Alla, V. & Pützer, B. M. A balancing act: orchestrating amino-truncated and full-length p73 variants as decisive factors in cancer progression. *Oncogene* **34**, 4287-4299, doi:10.1038/onc.2014.365 (2015).

79 Billant, O. *et al.* The dominant-negative interplay between p53, p63 and p73: A family affair. *Oncotarget* **7**, 69549-69564, doi:10.18632/oncotarget.11774 (2016).

80 Dötsch, V., Bernassola, F., Coutandin, D., Candi, E. & Melino, G. p63 and p73, the ancestors of p53. *Cold Spring Harb Perspect Biol* **2**, a004887, doi:10.1101/cshperspect.a004887 (2010).

81 Fontemaggi, G. *et al.* Identification of direct p73 target genes combining DNA microarray and chromatin immunoprecipitation analyses. *J Biol Chem* **277**, 4335943368, doi:10.1074/jbc.M205573200 (2002).

82 Haupt, Y., Maya, R., Kazaz, A. & Oren, M. Mdm2 promotes the rapid degradation of p53. *Nature* **387**, 296-299, doi:10.1038/387296a0 (1997).

83 Ongkeko, W. M. *et al.* MDM2 and MDMX bind and stabilize the p53-related protein p73. *Curr Biol* **9**, 829-832, doi:10.1016/s0960-9822(99)80367-4 (1999).

84 Zeng, X. *et al.* The N-terminal domain of p73 interacts with the CH1 domain of p300/CREB binding protein and mediates transcriptional activation and apoptosis. *Mol Cell Biol* **20**, 1299-1310, doi:10.1128/MCB.20.4.1299-1310.2000 (2000).

85 Conforti, F., Sayan, A. E., Sreekumar, R. & Sayan, B. S. Regulation of p73 activity by post-translational modifications. *Cell Death Dis* **3**, e285, doi:10.1038/cddis.2012.27 (2012).

86 Watson, I. R. & Irwin, M. S. Ubiquitin and ubiquitin-like modifications of the p53 family. *Neoplasia* **8**, 655-666, doi:10.1593/neo.06439 (2006).

87 Omran, Z. *et al.* Targeting Post-Translational Modifications of the p73 Protein: A Promising Therapeutic Strategy for Tumors. *Cancers (Basel)* **13**, doi:10.3390/cancers13081916 (2021).

88 Nyman, U. *et al.* Protein kinase C-dependent phosphorylation regulates the cell cycle-inhibitory function of the p73 carboxy terminus transactivation domain. *Mol Cell Biol* **29**, 1814-1825, doi:10.1128/MCB.00585-08 (2009).

89 Gebel, J. *et al.* Mechanism of TAp73 inhibition by ΔNp63 and structural basis of p63/p73 hetero-tetramerization. *Cell Death Differ* **23**, 1930-1940, doi:10.1038/cdd.2016.83 (2016).

90 Di Como, C. J., Gaiddon, C. & Prives, C. p73 function is inhibited by tumor-derived p53 mutants in mammalian cells. *Mol Cell Biol* **19**, 1438-1449, doi:10.1128/MCB.19.2.1438 (1999).

91 Yu, X. *et al.* Targeting MCL-1 sensitizes human esophageal squamous cell carcinoma cells to cisplatin-induced apoptosis. *BMC Cancer* **17**, 449, doi:10.1186/s12885-017-3442-y (2017).

92 You, L., Wang, Y., Jin, Y. & Qian, W. Downregulation of Mcl-1 synergizes the apoptotic response to combined treatment with cisplatin and a novel fiber chimeric oncolytic adenovirus. *Oncol Rep* **27**, 971-978, doi:10.3892/or.2012.1636 (2012).

93 Ma, Y. *et al.* 1alpha,25-Dihydroxyvitamin D3 potentiates cisplatin antitumor activity by p73 induction in a squamous cell carcinoma model. *Mol Cancer Ther* **7**, 3047-3055, doi:10.1158/1535-7163.MCT-08-0243 (2008).

94 Leong, C. O., Vidnovic, N., DeYoung, M. P., Sgroi, D. & Ellisen, L. W. The p63/p73 network mediates chemosensitivity to cisplatin in a biologically defined subset of primary breast cancers. *J Clin Invest* **117**, 1370-1380, doi:10.1172/JCI30866 (2007).

95 Hird, A. W. & Tron, A. E. Recent advances in the development of Mcl-1 inhibitors for cancer therapy. *Pharmacol Ther* **198**, 59-67, doi:10.1016/j.pharmthera.2019.02.007 (2019).

96 Vedadi, M. *et al.* Targeting human SET1/MLL family of proteins. *Protein Sci* **26**, 662-676, doi:10.1002/pro.3129 (2017).

97 Jiang, H. The complex activities of the SET1/MLL complex core subunits in development and disease. *Biochim Biophys Acta Gene Regul Mech* **1863**, 194560, doi:10.1016/j.bbagrm.2020.194560 (2020).

98 Aho, E. R., Weissmiller, A. M., Fesik, S. W. & Tansey, W. P. Targeting WDR5: A WINning Anti-Cancer Strategy? *Epigenet Insights* **12**, 2516865719865282, doi:10.1177/2516865719865282 (2019).

99 Friberg, A. *et al.* Discovery of potent myeloid cell leukemia 1 (Mcl-1) inhibitors using fragment-based methods and structure-based design. *J Med Chem* **56**, 15-30, doi:10.1021/jm301448p (2013).

100 Xu, S. *et al.* Discovery of M-808 as a Highly Potent, Covalent, Small-Molecule Inhibitor of the Menin-MLL Interaction with Strong. *J Med Chem* **63**, 4997-5010, doi:10.1021/acs.jmedchem.0c00547 (2020).

101 Ye, X. *et al.* The Development of Inhibitors Targeting the Mixed Lineage Leukemia 1 (MLL1)-WD Repeat Domain 5 Protein (WDR5) Protein- Protein Interaction. *Curr Med Chem* **27**, 5530-5542, doi:10.2174/0929867326666190528080514 (2020).